Distribution
Category UC-126

SAND89-0821
UNLIMITED RELEASE
July 1989

CALCULATION OF NATURAL CONVECTION BOUNDARY LAYER PROFILES USING THE LOCAL SIMILARITY APPROACH INCLUDING TURBULENCE AND MIXED CONVECTION

Stephen W. Webb
SPR Geotechnical Division 6257
Sandia National Laboratories
Albuquerque, New Mexico 87185

Abstract

The Strategic Petroleum Reserve (SPR) cavern fluid velocity model for natural convection uses the Modified Local Similarity (MLS) method to analyze the boundary layer behavior. In order to use the MLS approach, boundary layer velocity and temperature profiles are calculated in terms of local similarity variables based on the natural convection equations. Modifications were made to the local similarity equations enabling consideration of turbulent flow and mixed convection conditions. The details of these changes are addressed in thisreport.

For turbulent flow, an existing model was modified for application to local similarity conditions. For mixed convection, the natural convection local similarity equation set was modified to meet the appropriate boundary conditions. This model is the first application of the natural convection local similarity equation set to mixed convection. In addition, the traditional shooting method used to solve the local similarity equations was unreliable so an alternate method was developed.

The local similarity models developed in this report for turbulent flow and mixed convection are compared to the available experimental data. The models perform reasonably well when compared to the limited data, and the numerical method was found to be much more reliable and robust than the traditional method. With these modifications to the local similarity approach, the full range of conditions needed for the MLS method in the SPR velocity model can be calculated.

Table of Contents

List of Figures

List of Tables

I. Introduction

The Strategic Petroleum Reserve (SPR) cavern fluid velocity model for natural convection developed by Webb (1988a) uses the Modified Local Similarity (MLS) method to analyze the boundary layer behavior. The MLS method is based on the traditional local similarity methodology with modifications to ensure conservation of energy as the boundary layer develops (Webb (1988b)). In order to use the MLS approach in the cavern fluid velocity model, boundary layer velocity and temperature profiles must be calculated in terms of similarity variables considering the conditions encountered in SPR caverns.

Typical features of an SPR cavern are depicted in Figure 1 with reference to Bryan Mound Cavern 105. The approximate cavern dimensions are a radius of 100-150 feet and an overall height of 2000 feet; the top of the cavern is about 2000 feet underground in a large salt dome. Most of the cavern is filled with crude oil, which overlies a shallow brine layer. At the top of the cavern, the temperature of the salt is about 120°F. The geothermal temperature gradient is approximately .014°F/ft of depth, and the salt at the bottom of the cavern is 30°F hotter than that at the top, or about 150°F. The oil is introduced to the cavern piping system at approximately 70°F.

The fluid velocity in the caverns is caused by the geothermal temperature gradient in the surrounding salt and the large fluids-to-salt temperature difference. Since the salt is hotter than the oil or brine, heat is added to the fluids near the walls causing the fluid to rise due to buoyancy. With this upward flow near the walls, the flow is downward in the center of the cavern, and the center fluid temperature is stratified with the higher temperature fluid on top. This natural convection flow pattern will continue for 30 years or more due to the large extent of the salt region. Highly turbulent conditions with Rayleigh numbers up to 10^{16} are expected due to the large height of the caverns (Webb (1988a)).

For application to SPR caverns, boundary layer conditions which must be considered for the MLS method include laminar and turbulent flow, environmental fluid temperature stratification, and mixed convection with opposing boundary layer and center region velocities. Laminar flow and environmental fluid temperature stratification can be handled directly by the local similarity approach if the similarity parameters can be defined as done by the MLS method. However, local similarity has not generally been

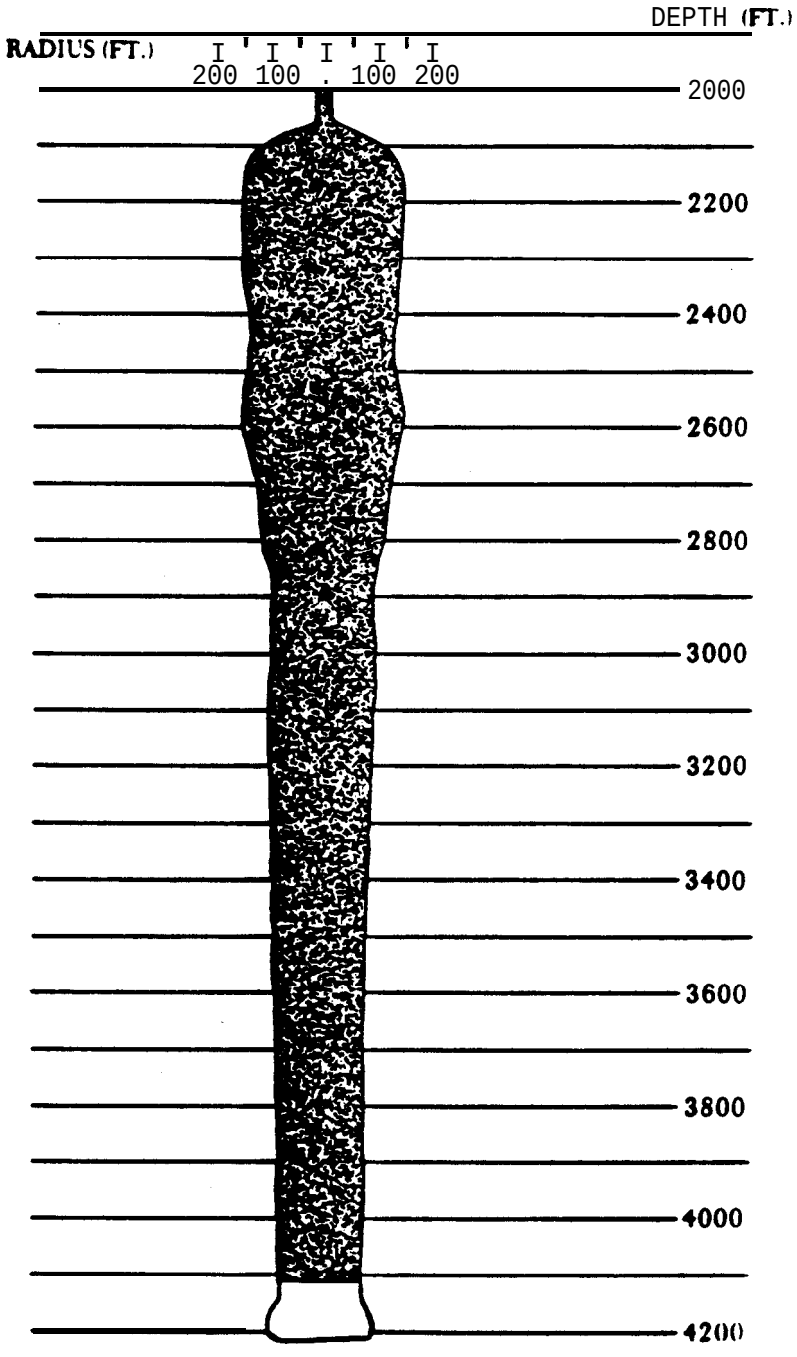

Figure 1. Typical features of an SPR cavern.

extended to turbulent conditions. The only application of the approach to turbulent flow has been performed by Noto and Matsumoto (1975). For mixed convection conditions, local similarity based on the natural convection equations has never been done since the traditional form is incompatible with the applicable boundary conditions.

In order to apply the local similarity approach to SPR caverns, modifications have been made to the appropriate equation set to accommodate turbulence and mixed convection conditions. This report addresses the changes that were made to calculate the necessary boundary layer profiles. In addition, the traditional numerical method used to solve the local similarity equations was found to be unreliable for the modified equation set and another approach was found as detailed in this report. Details of the fluid velocity model and of the MLS approach are given elsewhere (Webb (1988a,1988b)) and are not discussed in this report.

Local Similarity Approach

In order to understand the changes described in this report, the traditional local similarity method will be presented and discussed. The local similarity method is the basis of the MLS approach developed by Webb (1988b) and used in the SPR velocity model (Webb (1988a)). To illustrate the local similarity approach, the similarity equations for natural convection along a vertical surface will be derived, and the local similarity assumptions will be imposed.

Consider a boundary layer as depicted in Figure 2. The steady-state natural convection boundary layer mass, momentum, and energy conservation equations for a constant temperature environment are (Jaluria (1980))

mass

$$\frac{\partial u}{\partial x} + \frac{\partial v}{\partial y} = 0 \qquad (1)$$

x-momentum

$$u \frac{\partial u}{\partial x} + v \frac{\partial u}{\partial y} = g \beta (T - T_f(x)) + \nu \frac{\partial^2 u}{\partial y^2} \qquad (2)$$

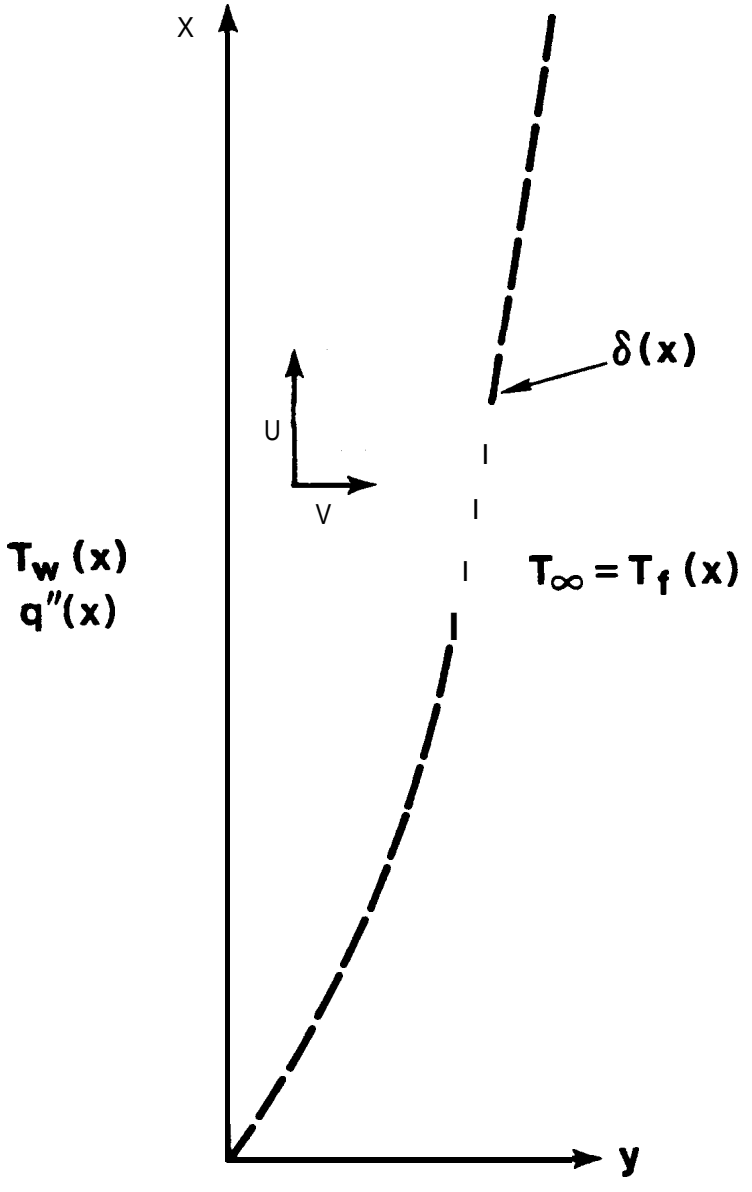

Figure 2. Boundary layer coordinates.

energy

(3)

where the Boussinesq approximations for natural convection have been used.

The natural convection boundary layer conservation equations for mass, momentum, and energy given above are coupled partial differential equations for the boundary layer behavior and are time-consuming to solve. However, for appropriate boundary conditions, these partial differential equations (PDEs) can be transformed into ordinary differential equations (ODEs) through the local similarity approach. The resulting ODEs are much easier to solve than the original PDEs.

According to Sparrow and Gregg (1958) and Yang (1960), similarity only exists for two specific distributions of the temperature difference between the wall and the fluid: the power-law and the exponential distributions. As evaluated by Gebhart and Mollendorf (1969) and by Webb (1988b), the exponential distribution has significant non-physical behavior and is therefore not often used. The more useful power-law distribution is employed in the following example.

For the power-law similarity distribution, the wall-to-fluid temperature difference must be of the form

$$\Delta T(x) = T_w(x) - T_f(x) = N\, x^n \tag{4}$$

where two common values of n are 0.0 for uniform wall temperature and 0.2 for uniform wall heat flux.

If the fluid temperature is nonuniform, the variation must be of the form

$$T_f(x) - T_r = \frac{JN}{4\,n}\, x^n = \frac{J}{4\,n}\, \Delta T(x) \tag{5}$$

where the reference temperature, T_r, is the fluid temperature at x-0. If the fluid temperature is constant, J is equal to 0.

For a vertical flat plate in a uniform temperature fluid (J-O.), application of the similarity approach with the power-law distribution reduces the boundary layer PDEs to the following set of equations:

$$f''' + (n+3)\, f\, f'' - 2\,(n+1)\, f'^{2} + \theta = 4X \left[f' \frac{\partial f'}{\partial x} - f'' \frac{\partial f}{\partial x} \right]_{I} \qquad (6)$$

$$\frac{\theta''}{Pr} + (n+3)\, f\, \theta' - 4\, n\, f'\, B = 4X \left[f' \frac{\partial \theta}{\partial x} - \theta' \frac{\partial f}{\partial x} \right] \qquad (7)$$

where the stream function and other variables are

$$\psi = 4 \left(\frac{Gr_x}{4} \right)^{1/4} \nu\, f(x,\eta) \qquad (8)$$

$$u = \frac{\partial \psi}{\partial y} = \frac{2\,\nu}{x}\, Gr_x^{1/2}\, f' \qquad (9)$$

$$\eta = \frac{y}{x} \left(\frac{Gr_x}{4} \right)^{1/4} \qquad (10)$$

$$\theta(\eta) = \frac{T(\eta) - T_f(x)}{T_w(x) - T_f(x)} \qquad (11)$$

$$Gr_x = \frac{g\, \beta\, x^3\, (T_w(x) - T_f(x))}{\nu^2} \qquad (12)$$

$'$ denotes $d/d\eta$.

The above equations are subject to the following boundary conditions

$f(0) = 0.$ (equivalent to zero mass flow at the wall) (13)

$f'(0) = 0.$ (equivalent to $u = 0.$ at the wall) (14)

$f'(\infty) = 0.$ (equivalent to $u = 0.$ at ∞) (15)

$\theta(0) = 1.$ (equivalent to $T(0) = T_w$) (16)

$\theta(\infty) = 0.$ (equivalent to $T(\infty) = T_f$) (17)

The preceding similarity equations for the natural convection boundary layer are still partial differential equations due to the RHS of both equations. In order to greatly simplify the equation set, the RHS of each equation is often assumed to be equal to zero. In this case, f and θ are only a function of η, and the equations become

$$f''' + (n+3)\, f\, f'' - 2\,(n+1)\, f'^{2} + \theta = 0 \qquad (18)$$

$$\frac{\theta''}{Pr} + (n+3)\, f\, \theta' - 4\, n\, f'\, \theta = 0 \qquad (19)$$

This assumption will be approximated for small x values or if the partial derivatives of f, f', and θ are small with respect to x. This procedure is referred to as the local similarity approach since the resulting equations are independent of x and are therefore local. Under this assumption, the natural convection equations reduce to two ODEs instead of the three PDEs given earlier.

The local similarity technique was first applied to natural convection by Pohlhausen as a supplement to the experiments of Schmidt and Beckmann (1930) who gave approximate solutions to the equations. Numerical solution of the equations was first provided by Ostrach (1953) with the use of a digital computer. Since then, local similarity solutions have emerged as an important analytical tool for analyzing natural convection under certain conditions. Examples of situations which are often analyzed by the local similarity approach include vertical surfaces with constant temperature or constant heat flux wall conditions, and buoyant jets and plumes (Jaluria (1980)).

The traditional similarity approach, while being powerful, has limited applicability due to the restrictions on the forms of the temperature variation. In the above example, the solution is only applicable if the temperature difference is of the power-law form. The Modified Local Similarity (MLS) approach developed by Webb (1988b) has significantly improved the usefulness of the similarity approach by providing a reasonable definition of the similarity parameters for non-similar boundary conditions.

The local similarity approach (and MLS extension) is an approximate technique that is extremely attractive since only two coupled ODEs have to be solved for the boundary layer solution. In addition, the solution at any x location is independent of the solution at other x locations. A problem with the method, however, is that the uncertainty of the approach in unknown. This concern led to the development of the local nonsimilarity approach (Sparrow, et al. (1970,1971) and Minkowycz and Sparrow (1974)) in which the partial derivatives are retained. Additional differential equations are used to evaluate the partial derivatives in the basic conservation equations while keeping the equations independent of solutions at other x locations like the local similarity method. By keeping the partial derivatives, the error is much smaller in the local nonsimilarity approach than for the local similarity method.

While the local similarity method is not as accurate as the local nonsimilarity method, the local similarity method has a feature that is critical for application to SPR in that the results can be easily tabulated. The boundary layer results are just a function of the fluid properties and the similarity parameters n and J. Thus, for a known fluid, if the local values of n and J can be determined, the boundary layer results can be evaluated. Evaluation of n and J is done in the present case through the MLS method developed by Webb (1988b). In contrast, the local nonsimilarity approach is dependent on the fluid properties, the similarity parameters n and J, and the location x. Tabulation of the results for the local nonsimilarity approach is much more complex than for the local similarity method due to the additional x parameter. The development of the MLS approach, which imposes conservation of energy as the boundary layer develops, has also significantly reduced the error of the local similarity procedure as shown by Webb (1988b). In addition, no method comparable to the MLS approach is available for the local nonsimilarity method to evaluate the n and J values for nonsimilar boundary conditions. Therefore, in the present application for SPR caverns, the local similarity approach as modified by the MLS method is employed.

II. Numerical Method

As discussed in the Introduction, the local similarity approach reduces the natural convection boundary layer conservation equations from a set of three coupled partial differential equations (PDEs) to two coupled ordinary differential equations (ODEs), or

$$f''' + (n+3)\, f\, f'' - 2\,(n+1)\, f'^{2} + \theta - 0 \qquad (18)$$

$$\frac{\theta''}{Pr} + (n+3)\, f\, 19' - 4\, n\, f'\, \theta = 0 \qquad (19)$$

which are considerably easier to solve than the PDE set.

The standard procedure to solve this set of coupled ODEs is to break the equation set down into five first order ODEs. The shooting method is then employed to simultaneously solve the ODE equation set using, for example, the Runge-Kutta ODE equation solver (Jaluria (1980)). The values of f"(0) and $\theta'(0)$ are guessed and iterated upon until the boundary conditions f'(m) and $\theta(\infty)$ are met within the desired tolerances. The iteration process is schematically depicted in Figure 3 for the velocity profile. The process continues until the solution hits the target at ∞.

Application of the shooting method to solve the above equations leads to a number of problems. The end point, η_∞, has to be specified. Common practice is to initially set the end point to a small value. Once the shooting method converges for this end point, the value is increased. If the results do not change significantly with a larger end point, the process is assumed to have converged. However, if the results are substantially different, further increase in η_∞ is required. Convergence is typically judged from the changes in the guessed values of f"(0) and $\theta'(0)$ with an increase in η_∞.

A number of problems can occur when the above procedure is used. First, the simultaneous numerical integration of five ODEs can "blow up" if the initial guesses are significantly different than the correct answers. In this case, the initial guesses have to be changed and/or the value of the end point, η_∞, decreased. Therefore, it is wise to start out with a known solution and proceed from there. For example, if the laminar velocity profile for a Prandtl number of 80 were needed, the results for a

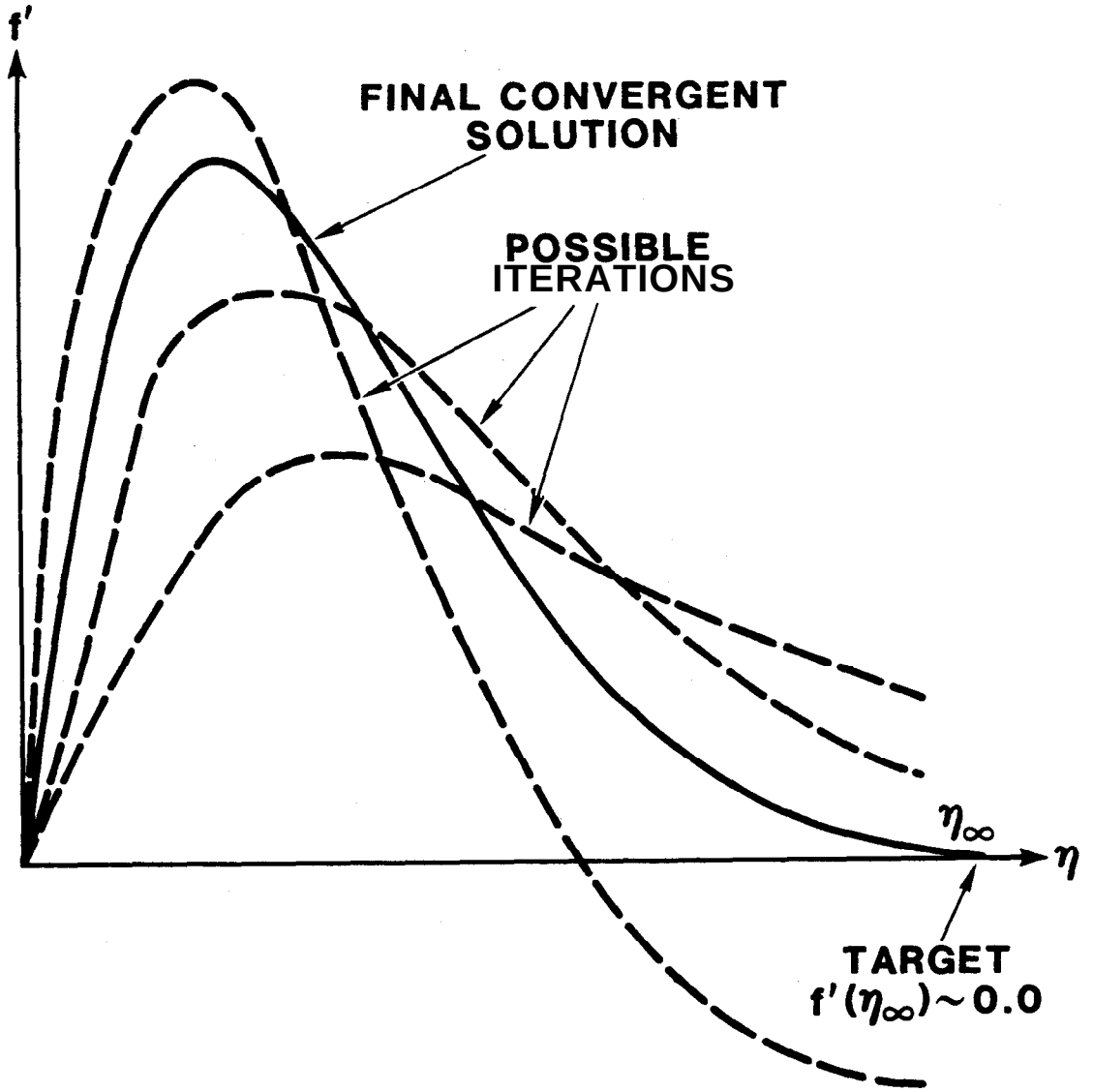

Figure 3. Typical iterations for the shooting method (after Jaluria (1980)).

Prandtl number of 100 could be used as a starting guess. Laminar local similarity results for a variety of Prandtl numbers for constant heat flux and constant wall temperature conditions are tabulated by a number of authors such as Jaluria (1980) and Gebhart (1985).

Second, even if the initial guesses are reasonably close to the correct answers, the change in the values of $f''(0)$ and $\theta'(0)$ for the next iteration needs to be determined. An excellent procedure for this problem is given by Nachtsheim and Swigert (1965) who use a least squares procedure to minimize the error in order to determine the change in $f''(0)$ and $\theta'(0)$. For laminar natural convection conditions, convergence is usually rapid for this approach with reasonable initial guesses.

Third, the need for asymptotic values of f' and θ at η_∞ leads to the two additional restrictions on the solution of $f''(\infty) = \theta'(\infty) = 0$. which are needed to obtain a unique solution to the problem. These restrictions have been incorporated into the scheme for choosing the updated values of f"(0) and $\theta'(0)$ by Nachtsheim and Swigert (1965). Their method also provides an alternate way of choosing η_∞ through their definition of the error term. This approach is vastly superior to monitoring changes in f"(0) and $\theta'(0)$ as discussed earlier.

Finally, when the value of the end point is large, the shooting method can be susceptible to small errors which can build up through the multiple integration processes, and the whole procedure can diverge. Thus, determination of an appropriate end value can be difficult. While this problem can often be alleviated by a more accurate ODE solver, this is not always the case. Laminar conditions do not usually encounter this problem. However, turbulent calculations often result in very large values of the end point, and the shooting method often fails as encountered in this study and in the work of Gominho and White (1984) as discussed by White (1988).

In order to overcome the problems with the shooting method, especially for turbulent flow and mixed convection conditions, the Box finite difference method developed by Keller (1971) has been employed in this study. This method is most often used to solve PDEs, especially for boundary layer calculations, and has been extensively tested by Cebeci and Smith (1974) and Cebeci and Bradshaw (1977,1984). The use of a finite difference approach instead of the shooting method has been suggested in Bejan (1984) in the discussion of the shooting method for natural convection, although the idea was not developed further. Blottner (1975) and Keller and Cebeci

(1972) mention the procedure for solution of the similarity equations for forced convection but not for natural convection.

The Box method consists of writing the higher order equations as a set of first order equations similar to the shooting method procedure. The equations are then written in terms of central differences at m specified mesh point locations. After linearization of the equations, if needed, a linear system of m-l equations with m-l unknowns must be solved. The distinguishing feature of the Box method as opposed to other numerical methods is the form of the central difference which readily allows for nonuniform mesh point spacing.

As an example, consider the first order equation

$$f' = g \tag{20}$$

where g is a known function. For the mesh points n and n+1, the Box method representation is simply

$$\frac{f^{n+1} - f^{n}}{\Delta\eta} = g^{n+1/2} = \frac{g^{n} + g^{n+1}}{2}. \tag{21}$$

Thus, the expression is centered about the middle of the "box" between the two mesh points instead of being centered at a mesh point. By using this approach, variable mesh point spacing is easily accomplished.

The Box method has been used in the present investigation to solve the local similarity boundary layer equations. The ODE equation set is broken down into five first order ODEs, and the finite difference approximations are done using the Box method. Newton's method is employed to solve the equations for the correction terms, and the resulting matrix is solved by a matrix inversion routine. The variables are updated by the calculated correction terms and the procedure continues until convergence. Keller (1978) outlines the above approach for PDEs.

The Box method automatically imposes the five boundary conditions listed earlier. Thus, when the method converges for a given set of conditions, the boundary conditions are automatically satisfied. The only problem is determination of the end point, a problem that is also faced with the shooting method.

In the present approach, the end point is reached when the error for the calculated profile is acceptably low. The error definition is that given by Nachtsheim and Swigert (1965) which is

$$E = (f'(\infty) - f'_{\infty})^2 + f''^2(\infty) + \theta^2(\infty) + \theta'^2(\infty). \tag{22}$$

However, since the first and third terms are automatically satisfied by the Box method (note that they are <u>not</u> automatically satisfied in the shooting method), the error term reduces to the square of the slopes at η_∞, or

$$E - f''^2(\infty) + \theta'^2(\infty). \tag{23}$$

The above error definition is used to determine the location of the end point, η_∞; the end point is increased until the error is acceptably low. For laminar natural convection calculations, the error is deemed acceptable when the value is less than $1. \times 10^{-10}$. For turbulent and mixed convection conditions, errors less than $1. \times 10^{-10}$ were desired but often only values of $1. \times 10^{-8}$ were obtainable due to the sensitivity of the model to certain parameters and the large end points encountered. However, when combined with the conservation checks discussed next, the results are satisfactory.

As an additional check on the results, conservation of energy and momentum is evaluated. From Webb (1988b), assuming $f''(\infty) = 0.$, the integrated natural convection local similarity boundary layer equations are

Momentum

$$(5 + 3n) \int_0^{\eta_\infty} f'^2 \, d\eta = \int_0^{\eta_\infty} \theta \, d\eta - f''_w \tag{24}$$

Energy

$$(5n + 3) \int_0^{\eta_\infty} f' \theta \, d\eta = -\frac{\theta'_w}{Pr} - J \int_0^{\eta_\infty} f' \, d\eta. \tag{25}$$

The use of the above integrated conservation equations can point out programming errors for either the shooting method or the Box approach. For example, if momentum is not conserved even for large values of the end point or for conditions such as laminar flow where the answers are known, the programmed equations are probably incorrect. If convergence of $f''(0)$ were used, programming errors may not be found. While this criterion has some problems of its own, such as accurate evaluation of the integrals, convergence has typically been to within 1.0% or less including turbulent flow conditions.

An example using this criterion is a very high Rayleigh number (10^{16}) turbulent flow case employing the standard shooting method. The end point was assumed to have been reached when the f"(0) and $\theta'(0)$ values did not change by more than 1% for a significant increase in η_∞. However, application of the conservation equations revealed that conservation of energy was in error by a factor of 5 and that, in fact, the end point had not been reached. Further use of the shooting method for larger end points was not practical since the shooting method "blew up" or diverged. The above Box method was subsequently developed and successfully applied to the problem.

In contrast to the shooting method, the Box method procedure is extremely stable, even when the initial guesses are poor. Turbulence also poses no problem to the method, and very large values of the end point are handled without difficulty. On the average, about 50 mesh points are used in the Box scheme to calculate the boundary layer profile compared with about 100-200 intervals for the shooting method with a fifth order Runge-Kutta method. Computer times for one iteration with each technique are comparable. However, the number of iterations required with the Box method are much smaller than for the shooting method since the zero velocity and temperature boundary conditions are automatically satisfied and larger changes in the end point values can be used, Differences between the results of the two methods are indistinguishable on a plot when the shooting method converged; the values of f"(0) and $\theta'(0)$ generally differ by less than 0.1 percent. Some typical results for laminar flow are shown in Table 1 along with tabulated results from Gebhart (1985). All the results in this table for the Box method had errors less than $1. \times 10^{-10}$.

The above integrated conservation equations apply to laminar and turbulent natural convection conditions but not to mixed convection flows. The appropriate integrated equations can only be developed after the local similarity equation modifications are completed. The integrated equations are presented in Section IV.

Table 1

Comparison of Results of Shooting Method and Box Method
for Laminar Flow Similarity Profiles

Pr	$f''(0)$		$f'(max)$		$-\theta'(0)$	
	Shooting*	Box	Shooting*	Box	Shooting*	Box
			Uniform Wall Temperature (UWT)			
0.72	0.6760	0.6761	0.2762	0.2762	0.5046	0.5048
1.0	0.6422	0.6423	0.2513	0.2515	0.5671	0.5673
5.0	0.4818	0.4818	0.1484	0.1485	0.9540	0.9546
10.	0.4192	0.4192	0.1149	0.1151	1.1693	1.1702
100.	0.2517	0.2517	0.0442	0.0443	2.1913	2.1946
			Uniform Heat Flux (UHF)			
0.72	0.6389	0.6394	0.2514	0.2520	0.5756	0.5759
1.0	0.6069	0.6071	0.2288	0.2292	0.6453	0.6456
5.0	0.4543	0.4545	0.1345	0.1347	1.0759	1.0768
10.	0.3951	0.3951	0.1042	0.1043	1.3164	1.3173
100.	0.2367	0.2367	0.040	0.0400	2.4584	2.4616

* - from Gebhart (1985)

At the time of the development of the Box finite difference method discussed above, no other application of the finite difference approach to the local similarity natural convection equations was known. During the final preparation of this report, a finite difference approach for solving the local similarity equations was published by Henkes and Hoogendoorn (1989a). Their reason for developing an alternative method was the same as encountered in the present investigation and that of Gominho and White (1984); the traditional shooting method was unreliable. However, their numerical approach assumes constant mesh point spacing. While this assumption is adequate for laminar flow conditions, uniform spacing is not appropriate for turbulent conditions. Although the approach given in the present report and that of Henkes and Hoogendoorn (1989a) are related since they are both finite difference methods, the present scheme is the more versatile of the two methods since it allows for variable mesh point spacing, a must for turbulent flow.

III. Turbulence

Data and models for turbulent natural convection are limited compared to forced convection conditions. Only a few investigations have obtained turbulent natural convection mean (average) velocity and temperature profile data for the simple configuration of a vertical flat plate. Most of the natural convection turbulence models are based on forced convection applications with little or no modification. Much more experimental and analytical work remains to be done for turbulent natural convection conditions.

For the present evaluation, only turbulent natural convection data and models applicable to vertical flat plates will be considered since this configuration is the most often studied. Note, however, that turbulent natural convection data in enclosures have been briefly discussed by Webb (1988a) in his report on the SPR velocity model.

The state of the fluid in natural convection is generally referred to in terms of a Grashof or Rayleigh number. Two variations exist depending on the type of experiment or analysis performed. For the constant wall temperature case, the normal Grashof and Rayleigh numbers are employed which are

$$Gr_x = \frac{g \beta x^3 \Delta T}{\nu^2} \tag{26}$$

$$Ra_x = Gr_x Pr \tag{27}$$

where AT is the temperature difference between the wall and the fluid. For the constant heat flux case, however, an alternate definition is used. The two forms are differentiated by a superscript * on the constant heat flux value, and the definitions are

$$Gr_x^* = \frac{g \beta x^4 \quad "}{k \nu^2} = Gr_x Nu_x \tag{28}$$

$$Ra_x^* = Gr_x^* Pr = Ra_x Nu_x . \tag{29}$$

The two forms are simply related through the local Nusselt number.

Some other parameters are used in data presentations. The velocity is often normalized with respect to u^*, which is a velocity characteristic of natural convection. Two definitions are commonly used which differ by a factor of two. In this report, the following definition is used

$$u^* = 2 (g \beta x \Delta T)^{1/2} \tag{30}$$

This definition is particularly convenient since the actual velocity divided by u^* is exactly equal to the velocity similarity variable f'

$$f' = \frac{x}{2 \nu Gr_x^{1/2}} u = \frac{u}{2 (g \beta x \Delta T)^{1/2}} = \frac{u}{u^*}. \tag{31}$$

The other definition of u^* is simply without the factor of 2.

Transition between laminar and turbulent flow is generally considered to be at a Grashof number of approximately 10^9 for a vertical flat plate. The exact location of the end of laminar flow and the start of turbulent conditions is difficult to determine and depends on parameters other than just the Grashof number (Jaluria and Gebhart (1974)). However, a value of 10^9 for the Grashof number for the start of turbulence is often used. For SPR caverns, the Grashof number is expected to be considerably higher ($\sim 10^{14}$) (Webb (1988a)), so the boundary layer will be highly turbulent.

A. Natural Convection Data

Early investigations into turbulent natural convection focused primarily on the influence of turbulence on the mean fluid velocity and temperature profiles. Later on, additional turbulence quantities have been measured during the studies such as the fluctuation of the velocities and the temperature. The presentation given here will show mostly mean fluid velocity and temperature profiles due to the ultimate decision to use a mixing length turbulence model as discussed later on in this report.

The data presentations have been given in a variety of coordinates. Some investigators use physical quantities such as velocity and distance, but most data are reported in transformed variables similar to f' and η in the local similarity approach. The definition of the coordinates used in the data presentations will be included in each figure as appropriate.

The first measurements of turbulent mean velocity and temperature profiles were made by Griffiths and Davis (1922) in air. These data were the basis of the turbulent velocity and temperature profiles shapes assumed in the integral analysis of turbulent natural convection flow performed by Eckert and Jackson (1951). However, Eckert and Jackson (1951) were not able to reproduce the magnitude of the measured velocities and concluded that the measurements were inaccurate.

Cheesewright (1968) was the next investigator to measure mean velocity and temperature profiles in turbulent flow. Data for air on a constant temperature vertical plate were obtained for a variety of different Grashof numbers and are shown in Figures 4 and 5. A comparison of the data with those of Griffiths and Davis (1922) shows that the two sets of data are in reasonable agreement. Poor agreement between the assumed profiles used by Eckert and Jackson (1951) and the data was noted. Even use of the experimental data for the maximum velocity and boundary layer thickness did not bring the profiles into reasonable agreement with the data. Thus, the turbulent profiles of Eckert and Jackson (1951) do not fit the data.

For many years, the Cheesewright data were the primary target of the developers of turbulence models for natural convection as will be seen in the next section. However, Hoogendoorn and Euser (1978) noted some heat balance inconsistencies in the data that led them to believe that the velocity values were too small. They obtained some limited data which indicate that the velocity data of Cheesewright are low as shown in Figure 6. This figure also shows predictions made by the model of Mason and Seban (1974) which is discussed briefly later. In response, Cheesewright and Ierokiopitis (1982) investigated the velocity data problems by using a different measurement technique (Laser Doppler Anemometer (LDA) versus hot-wire anemometer) and provided new velocity data that are indeed higher than the earlier information. The new data of Cheesewright and Ierokiopitis are given in Figure 7 with a comparison to the earlier Cheesewright (1968) data. Note that this figure is adapted from To and Humphrey (1986). These data are not contained in the acknowledged reference but are probably from a more detailed report by Cheesewright and Ierokiopitis. Additional data are given in Figure 8 from Cheesewright and Ierokiopitis (1982).

Other investigations of turbulent mean profiles performed about the time of the first Cheesewright study were performed by Warner and Arpaci (1968) and by Lock and Trotter (1968). Warner and Arpaci (1968) measured temperature profiles and heat transfer coefficients; velocity data were not obtained. Lock and Trotter (1968) present mean velocity and temperature

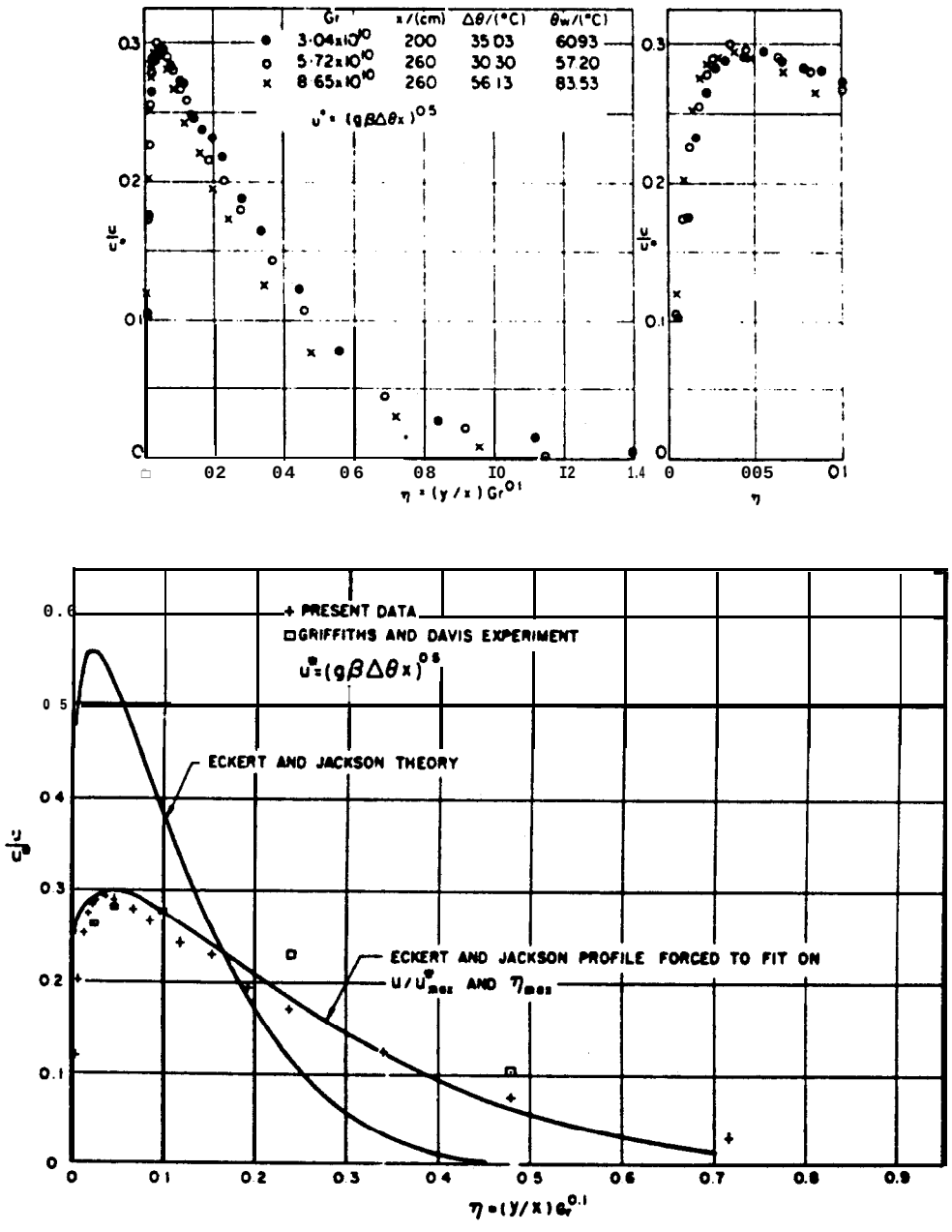

Figure 4. Cheesewright (1968) velocity data (Cheesewright (1968)). velocity units = 2f' (note use of alternate u* definition).

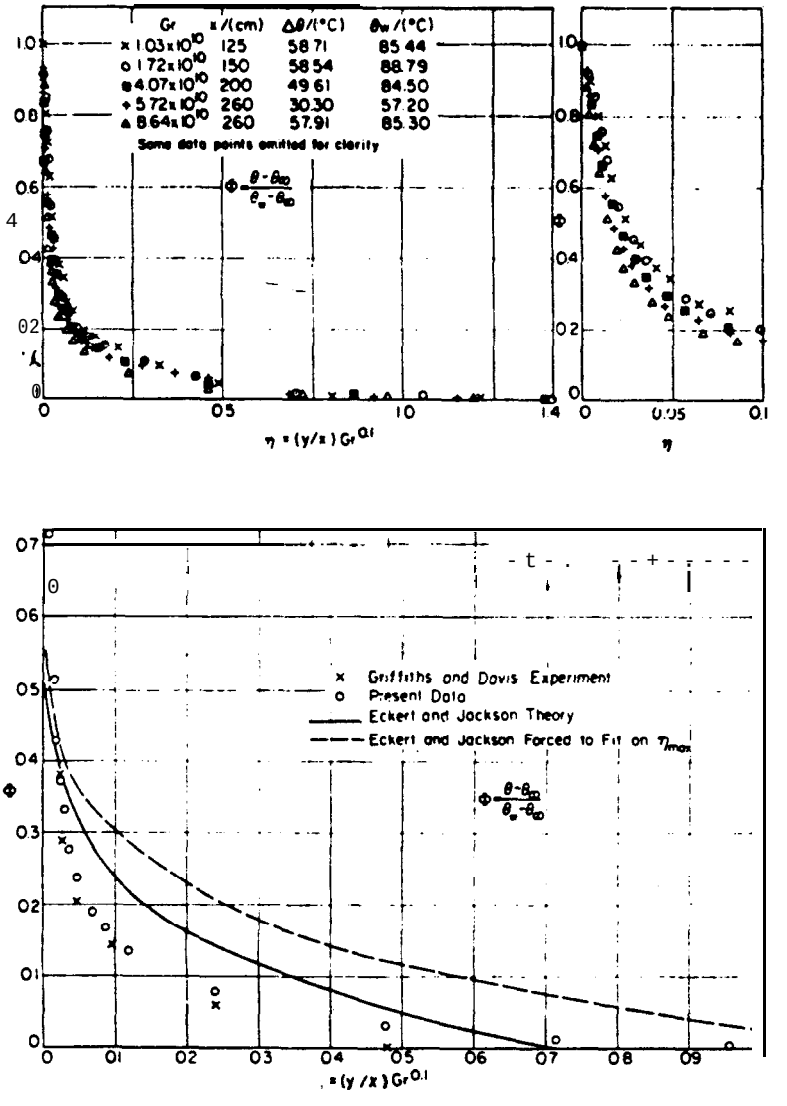

Figure 5. Cheesewright (1968) temperature data (Cheesewright (1968)). temperature units = θ.

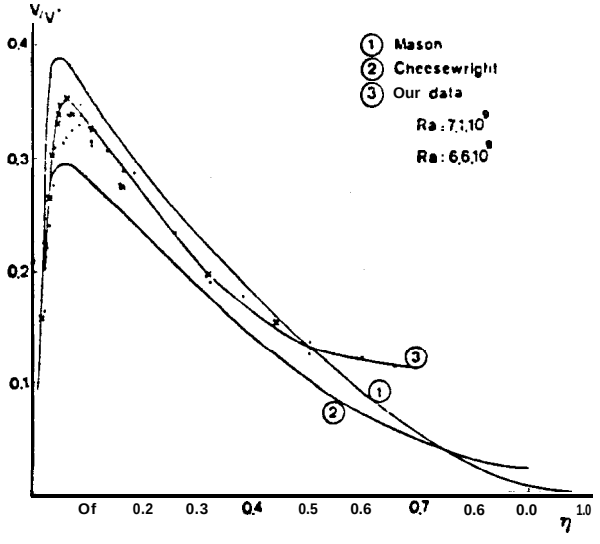

Figure 6. Hoogendoorn and Euser (1978) data compared to Mason (1974) predictions and Cheesewright (1968) data.
(Hoogendoorn and Euser (1978))
velocity units = $2f'$
distance units = (y/x) $Gr^{0.1}$
(Same coordinates as Cheesewright (1968) in Figure 4)

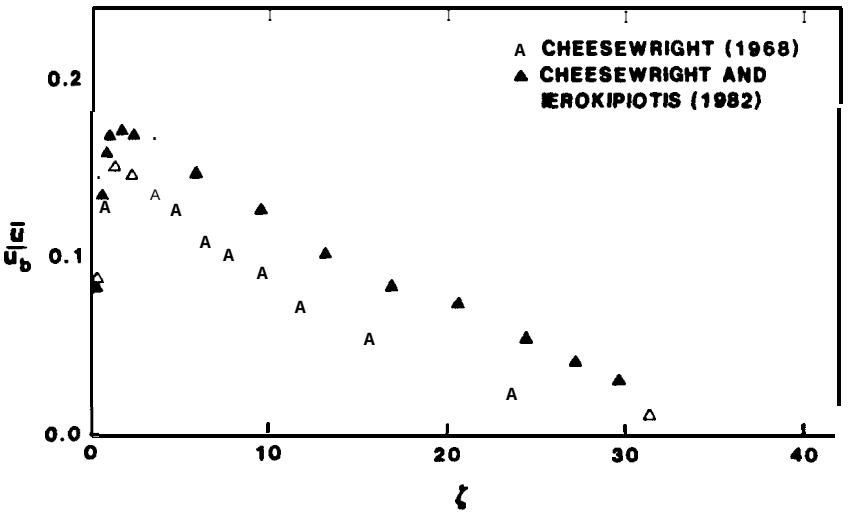

Figure 7. Comparison of early Cheesewright (1968) and later Cheesewright and Ierokiopitis (1978) velocity data (after To and Humphrey (1986)).
velocity units = f'.

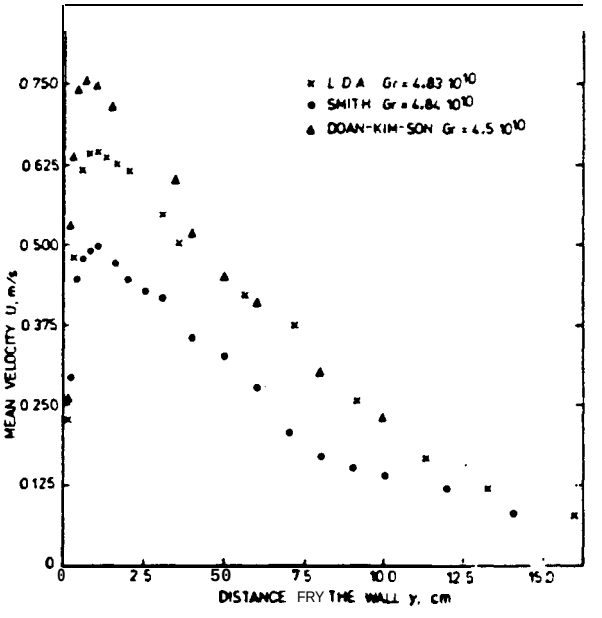

Figure 8. Cheesewright and Ierokiopitis (1978) velocity profile data (labelled L.D.A.) (Cheesewright and Ierokiopitis (1978)).

profiles as well as temperature fluctuation data for water on a constant heat flux vertical plate. Some of the mean velocity data are shown in Figure 9. As indicated in the paper, the boundary layer is not completely turbulent even at the highest value of Grashof number reported. The velocity data seem high, since the peak f' value for the data is 0.32 compared to a peak f' value for laminar flow of about 0.11 for water with a Prandtl number of 10.25 (see Table 1). These data are discussed in more detail in Section III.C.

Shortly thereafter, Vliet and Liu (1969) published mean velocity and temperature data for water on a vertical plate with constant heat flux including Nusselt number and velocity fluctuation data. The velocity and temperature profile data, which are shown in Figure 10, have shapes similar to the air data of Cheesewright (1968). Fujii, et al. (1970) measured Nusselt numbers and mean and fluctuating temperatures for a vertical cylinder in water, spindle oil, and Mobiltherm oil. Unfortunately, no velocity data were obtained. However, these temperature data, which are given in Figure 11, are valuable due to the wide range of Prandtl numbers involved. Kutateladze, et al. (1972) reported some mean and fluctuating velocity data for ethyl alcohol as the working fluid as shown in Figure 12.

More recently, Miyamoto, et al. (1982) published mean velocity data as well as other turbulence parameters for air on a constant heat flux vertical plate. The mean velocity profile data are shown in Figure 13a. To and Humphrey (1986) calculated some turbulent Prandtl number information for the Miyamoto, et al. (1982) data which is shown in Figure 13b. Also shown are turbulent Prandtl number predictions by To and Humphrey (1986) using their stress models.

Finally, Tsuji and Nagano (1988) present some mean and fluctuating data for air on an isothermal vertical plate. According to the authors, problems have been noticed in most of the other investigations due to environmental fluid temperature stratification. Tsuji and Nagano (1988) took care to minimize this effect in their experiments. Comparison of their mean velocity and temperature data with others is consistent with a smaller ambient temperature stratification. The mean velocity profile data given in Figure 14a show a larger boundary layer for Tsuji and Nagano than for other investigators. Velocity data for a variety of Grashof numbers are shown in Figure 14b. The mean temperature profile data also indicate the larger boundary layer trend as shown in Figure 14c.

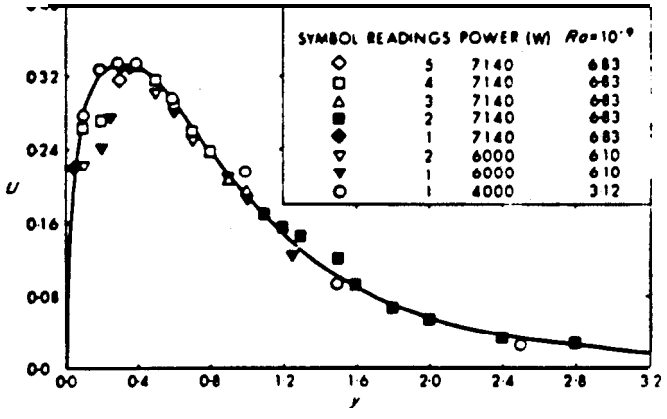

Figure 9. Lock and Trotter (1968) water velocity data (Lock and Trotter (1968)).
velocity units = f'
distance units = 0.1 inches.

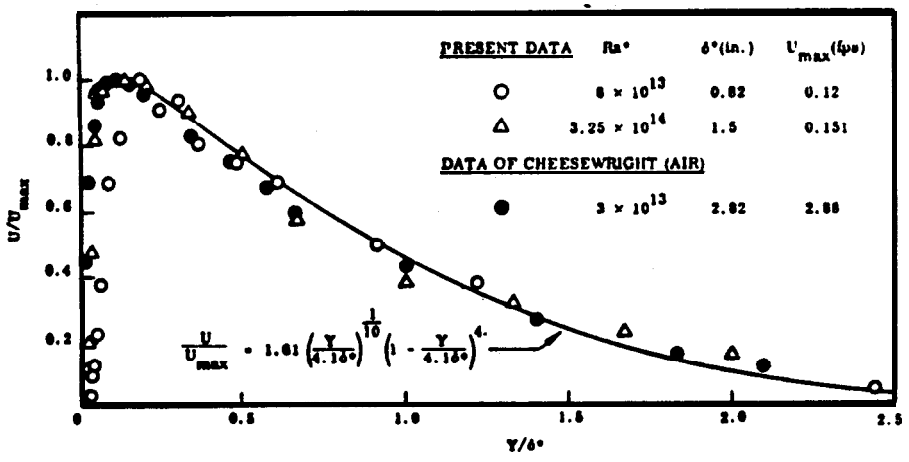

Figure 10a. Comparison of Vliet and Liu (1968) water velocity data with Cheesewright (1968) air data (Vliet and Liu (1968)).

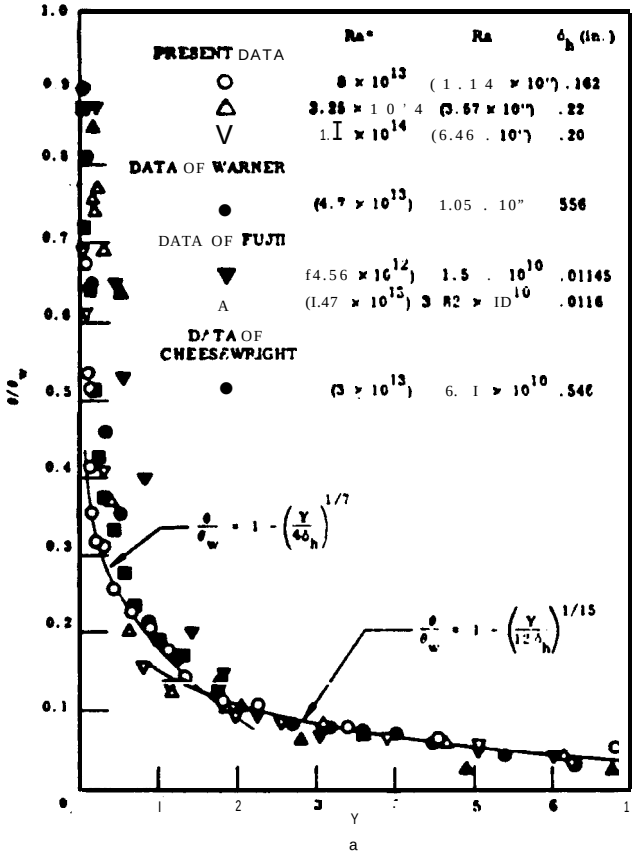

Figure 10b. Comparison of Vliet and Liu (1968) temperature data with others temperature units = 8.

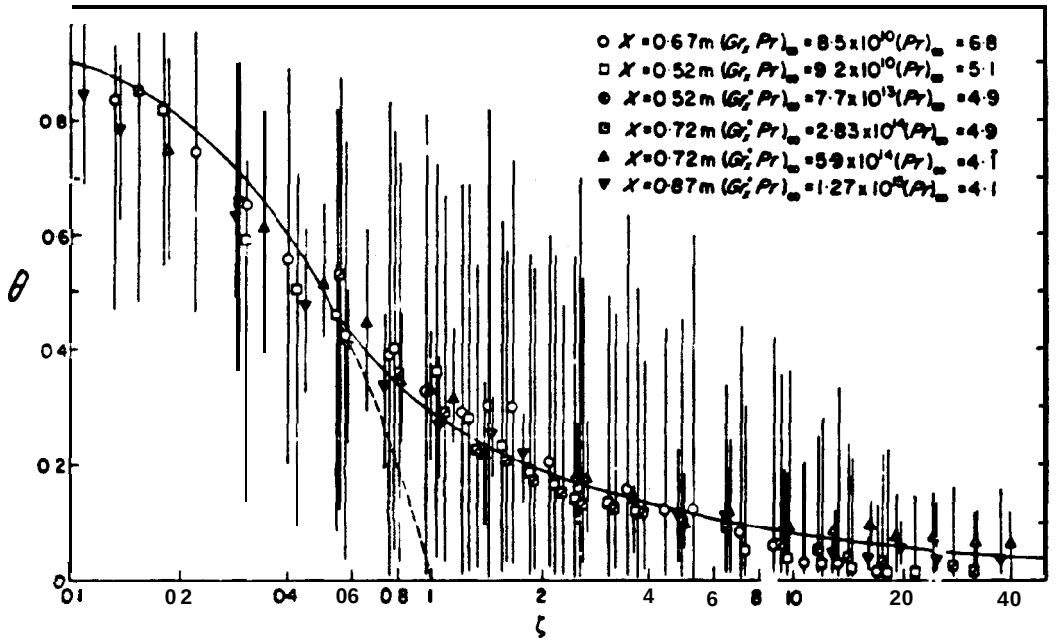

Figure lla. Fujii, et al. (1970) temperature data for water (Fujii, et al. (1970)).

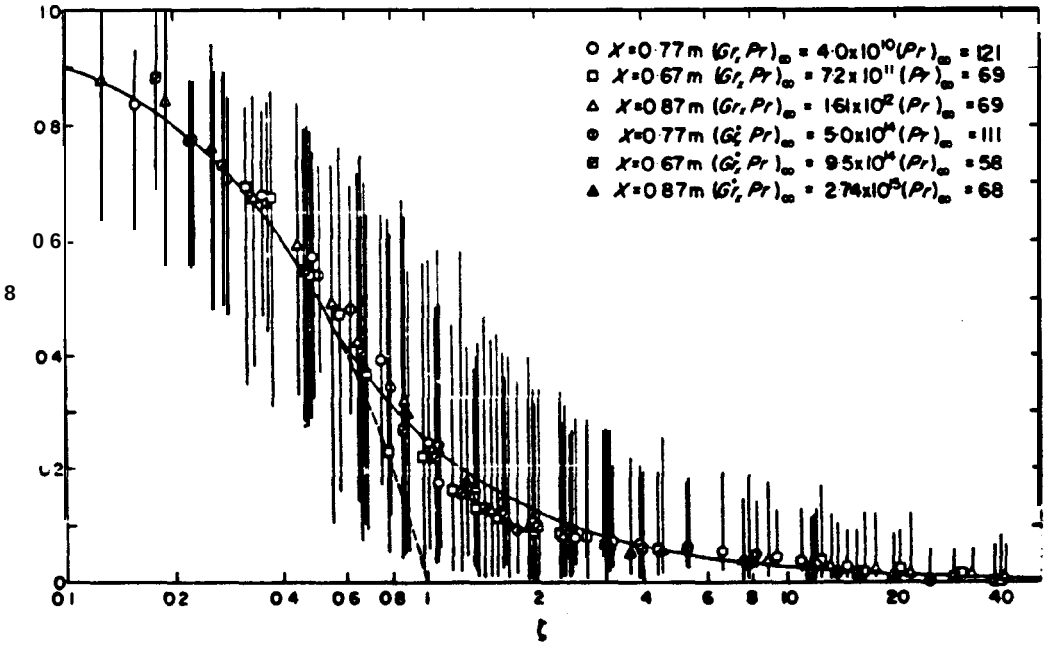

Figure llb. Fujii, et al. (1970) temperature data for spindle oil (Fujii, et al. (1970)).

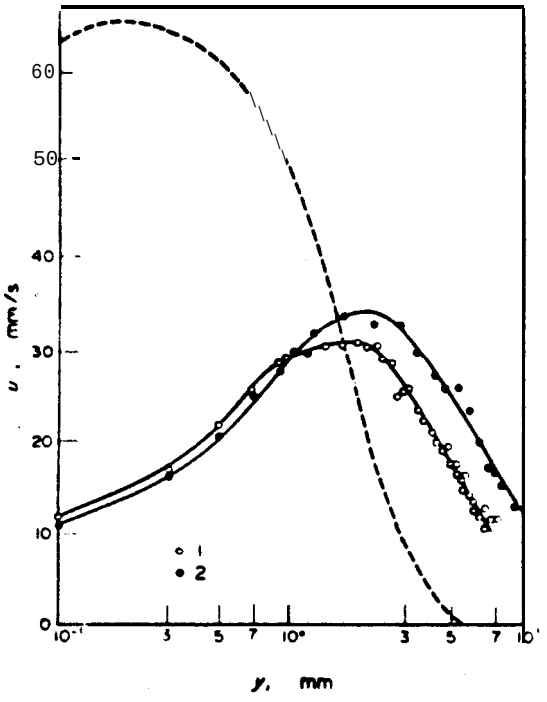

Figure 12. Kutateladze, et al. (1972) velocity data for ethyl alcohol.
1. Ra = 2.15×10^{10}; x = 275 mm; AT = 11.8°C; T_o = 29.2°C.
2. Ra = 4.83×10^{10}; x = 363 mm; AT = 11.6°C; T_o = 29.4°C.
--- Integral Theory for Pr = 13.2; x = 360 mm; AT = 11.6°C.
(Kutateladze, et al. (1972))

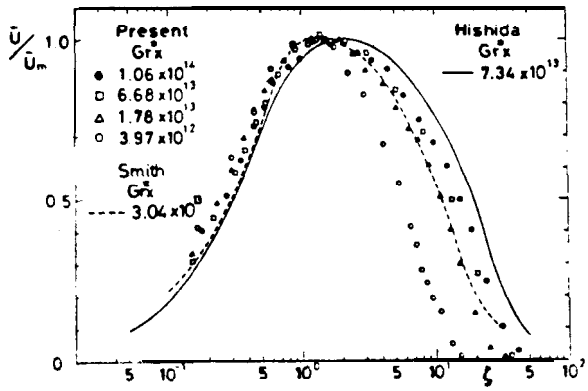

Figure 13a. Miyamoto, et al. (1982) air velocity data (Miyamoto, et al. (1982)).

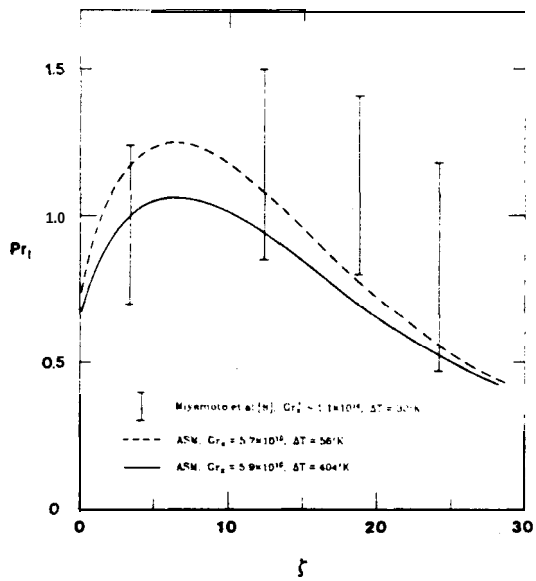

Figure 13b. Miyamoto, et al. (1982) Pr, variation and To and Humphrey (1986) model predictions. (To and Humphrey (1986)).

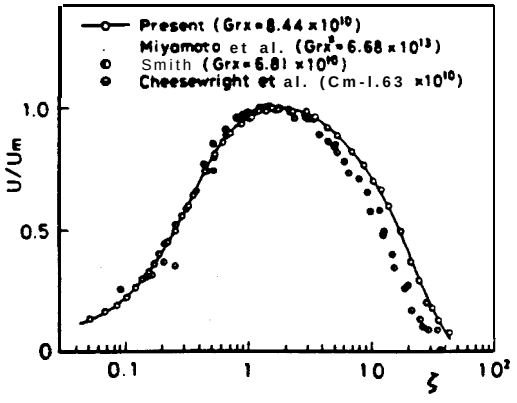

Figure 14a. Tsuji and Nagano (1988) air velocity data comparison (Tsuji and Nagano (1988)).

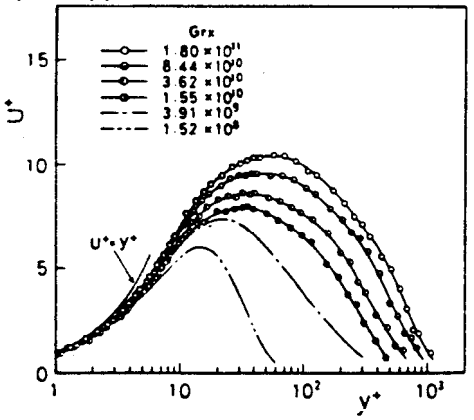

Figure 14b. Tsuji and Nagano (1988) air velocity data (Tsuji and Nagano (1988)).

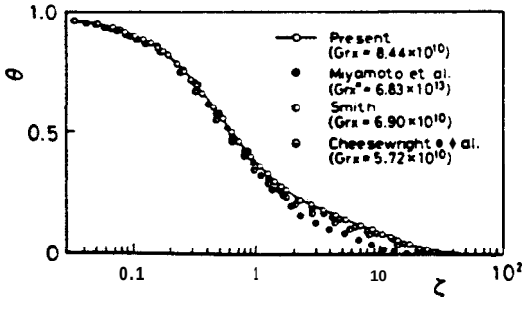

Figure 14c. Tsuji and Nagano (1988) air temperature data (Tsuji and Nagano (1988)).

B. Natural Convection Models

Yang and Aung (1985) summarize a number of approaches to turbulent natural convection including eddy viscosity models, stress models, large eddy simulation, and the vortex method. Based on computer time restraints in the present application, the only acceptable approach is the eddy viscosity method. From Appendix A, the applicable conservation equations for an eddy viscosity turbulence model are:

mass

$$\frac{\partial u}{\partial x} + \frac{\partial v}{\partial y} = 0 \qquad \text{(A-12)}$$

x-momentum

$$u \frac{\partial u}{\partial x} + v \frac{\partial u}{\partial y} = g \beta (T - T_f(x)) + \frac{\partial}{\partial y} \left[(\nu + \nu_t) \frac{\partial u}{\partial y} \right] \qquad \text{(A-13)}$$

energy

$$u \frac{\partial T}{\partial x} + v \frac{\partial T}{\partial y} = \frac{a}{\partial y} \left[(a + \alpha_t) \frac{\partial T}{\partial y_1} \right. \qquad \text{(A-14)}$$

where closure equations for ν_t and α_t have to be defined.

A variety of eddy viscosity models for ν_t exist ranging from the simple to the complex. The various categories are generally referred to as zero-, one-, and two-equation models. The number of equations in the category designation is the number of turbulent parameter PDEs involved in the eddy viscosity model. Thus, in the zero-equation category, the eddy viscosity is specified by an algebraic relationship, not by solution of PDEs in conjunction with the conservation equations. Similarly, a two-equation model uses two PDEs to define the eddy viscosity which are solved simultaneously with the conservation equations.

Models for the eddy thermal diffusivity, α_t, are generally expressed in terms of a turbulent Prandtl number, which is defined as

$$Pr_t = \frac{\nu_t}{\alpha_t} \qquad (32)$$

in analogy with the molecular Prandtl number

$$Pr = \frac{\nu}{\alpha}. \tag{33}$$

Only a few models for the turbulent Prandtl number exist, and these models are of the zero-equation or algebraic type; the subject is reviewed in detail by Reynolds (1975). The most notable model is that by Cebeci (1973) which will be discussed later. However, in many practical applications, a constant turbulent Prandtl number of 0.9 is sufficient, at least for forced flow situations.

The one- and two-equation eddy viscosity models are too complicated for use with the local similarity approach since they require simultaneous solution of the boundary layer and turbulent parameter PDEs. Therefore, in the present study, a zero-equation eddy viscosity model will be used. Zero-equation eddy viscosity models have been successfully applied in forced convection for years as exemplified by work summarized by Cebeci and Smith (1974) and by Cebeci and Bradshaw (1977,1984). While it is recognized that one- and two-equation models provide results superior to zero-equation approaches, the computer time and similarity equation restraints imposed on SPR calculations necessitate the use of a zero-equation model.

The appropriate local similarity form of the above conservation equations for a uniform fluid temperature (J-O) is

$$(1 + \frac{\nu_t}{\nu} f'')' + (n+3)\, f\, f'' - 2\,(n+1)\, f'^2 + \theta = 0 \tag{34}$$

$$\left(\left(\frac{1}{Pr} + \frac{\nu_t}{\nu}\frac{1}{Pr_t}\right) \theta' \right)' + (n+3)\, f\, \theta' - 4\, n\, f'\, \theta = 0 \tag{35}$$

which reduce to the laminar form of the local similarity equations given earlier (equations (18) and (19)) for zero eddy viscosity. The different eddy viscosity models are discussed next.

1. Zero-Eauation Models

Two types of zero-equation models have been extensively used - the original eddy viscosity form in which the variation of ν_t is prescribed, i.e., $\nu_t = f(y)$, and the Prandtl mixing length hypothesis which relates the eddy viscosity to the absolute value of the local velocity gradient, or

$$\nu_t = l^2 \left| \frac{\partial u}{\partial y} \right| . \tag{36}$$

For the mixing length case, the turbulent shear stress becomes

$$-\overline{u'v'} = \nu_t \frac{\partial u}{\partial y} = l^2 \left| \frac{\partial u}{\partial y} \right| \frac{\partial u}{\partial y} . \tag{37}$$

Problems with mixing length eddy viscosity models exist since the model predicts that the eddy viscosity is proportional to $\partial u/\partial y$. Thus, at velocity maximums or minimums, the eddy viscosity is zero. In contrast, the more accurate one- and two- equation eddy viscosity models predict an increasing eddy viscosity at the velocity maximum in natural convection as shown by Henkes and Hoogendoorn (1989b) in Appendix B, although the turbulent shear stress is zero at the velocity maximum for all eddy viscosity models. This shortcoming of the mixing length approach was also recognized by Prandtl in his original work according to Schlichting (1969).

The mixing length eddy viscosity problem has been investigated by Doshi and Gill (1970,1971) for forced convection. Their reformulation of the mixing length significantly improved the model predictions compared to data for forced convection in a duct with two different wall temperatures. However, this reformulation will not be used in the present investigation at this time. This problem is discussed further in Appendix B.

Four applications of a zero-equation eddy viscosity model have been performed for natural convection. Cebeci and Khattab (1975) and Noto and Matsumoto (1975) used forced convection models without modifications for buoyancy effects. Yang and Lloyd (1985) present a zero-equation model for enclosures, while the Popov and Yan'kov (1985) approach is similar to that of Cebeci and Khattab (1975) and Noto and Matsumoto (1975) in that existing forced convection models are used. However, these last two models have explicit modifications to account the effect of buoyancy. Each model is discussed in detail below.

a. Cebeci and Khattab

Cebeci and Khattab (1975) and Khattab (1975) investigated use of the Cebeci and Smith (1974) forced convection turbulence mixing length model for natural convection conditions. Inner and outer regions are used in the approach in accordance with the Cebeci and Smith (1974) model. The eddy viscosity in the inner region is the same as that used by Cebeci and Smith (1974). In the outer region, the original model is in terms of the free stream velocity. While this definition is satisfactory for forced convection, application to free convection caused a change from an eddy viscosity concept to a mixing length approach in the outer region. The equations used by Cebeci and Khattab (1975) are

$$\nu_t = l^2 \left|\frac{\partial u}{\partial y}\right| \tag{36}$$

$$l_i = 0.4y\ (1 - \exp(-y/A)) \quad \text{(inner region)} \tag{38}$$

$$l_0 = 0.075\ 6 \quad \text{(outer region)} \tag{39}$$

$$l = \min(l_i, l_o) \tag{40}$$

$$A = 26\ \nu\ (\tau_w/\rho)^{-1/2} \tag{41}$$

$$\tau_w = \mu \left.\frac{\partial u}{\partial y}\right|_{wall} \tag{42}$$

where Khattab (1975) defines 6, the boundary layer thickness, as the location where $f' = 0.01$ and $f'' < 0$.

The minimum mixing length from both regions is used. For the present set of equations, this operation means that the eddy viscosity will increase from zero at the wall to a maximum value dependent on the boundary layer thickness, 6. The eddy viscosity will remain constant further out in the boundary layer. This behavior is consistent with forced convection experimental data as shown in Figure 15.

For forced convection, the boundary layer thickness, 6, is typically calculated as the location where the boundary layer velocity is within 0.5% of the free stream value (Cebeci and Bradshaw (1984)). However, in natural convection, the free stream velocity is zero, so Khattab (1975) used the

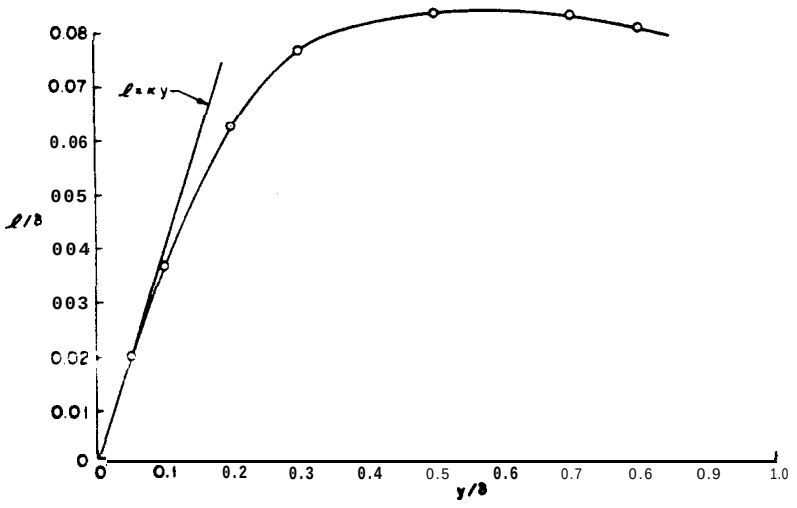

Figure 15. Distribution of mixing length in forced convection (Cebeci and Bradshaw) (1977)).

alternate definition given above. A ratio of the velocity at the edge of the boundary layer to the peak value may be more appropriate due to the variation in peak f' values as given earlier in Table 1.

The turbulent Prandtl number used by Cebeci and Khattab (1975) is based on the model of Cebeci (1973). However, when a constant turbulent Prandtl number of 0.9 is used, very little difference was noted. A variable turbulent Prandtl number is only important for low Prandtl number fluids according to Cebeci and Khattab (1975). The turbulent Prandtl number equations based on the Cebeci (1973) model as given by Cebeci and Smith (1974) are

$$Pr_t = \frac{\nu_t}{\alpha_t} = \frac{0.4\ (1 - \exp(-y/A))}{0.44\ (1 - \exp(-y/B))} \tag{43}$$

$$B = B^* \nu\ (\tau_w/\rho)^{-1/2}\ ,\ Pr^{1/2} \tag{44}$$

$$B^* = \sum_{i-1}^{5} C_i\ (\log_{10} Pr)^{i-1} \tag{45}$$

$$C_i = 34.96,\ 28.79,\ 33.95,\ 6.33,\ -1.186\ (i\text{-}1 \text{ to } 5) \tag{46}$$

The results presented by Cebeci and Khattab (1975) are based on solution of the PDE equation set for natural convection with the above turbulence model. The equations were integrated up the wall from the leading edge to determine the local velocity and temperature profiles.

Figure 16 compares the turbulent velocity profile predictions by Khattab (1975) with turbulent data for air (Cheesewright (1968)) and for water (Vliet and Liu (1969)). Reasonable agreement between the predictions and the data is shown for the velocity normalized to the peak value. No comparison of the actual velocities are presented by Cebeci and Khattab (1975) or by Khattab (1975); only normalized values are given.

Figure 17 presents the temperature profile data-model comparisons. Figure 17a shows adequate agreement although the data have a considerable amount of scatter. The results given in Figure 17b show excellent agreement between the data and the model for air (Cheesewright (1968)), water (Fujii, et al. (1970)), and spindle oil (Fujii, et al. (1970)). Also shown are the predictions made by Mason and Seban (1974) which will be discussed briefly later on.

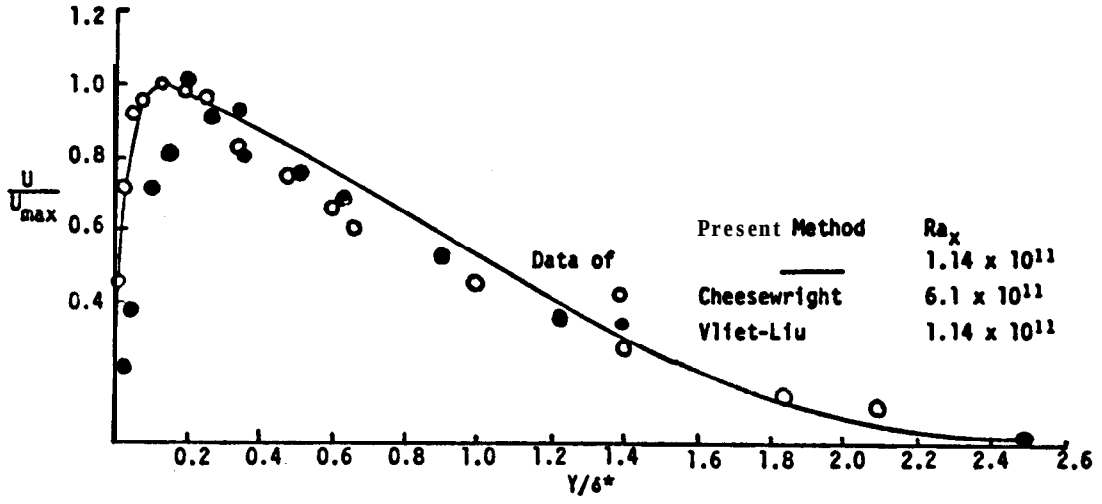

Figure 16. Cebeci and Khattab (1975) velocity profile data-model comparison (Khattab (1975)).

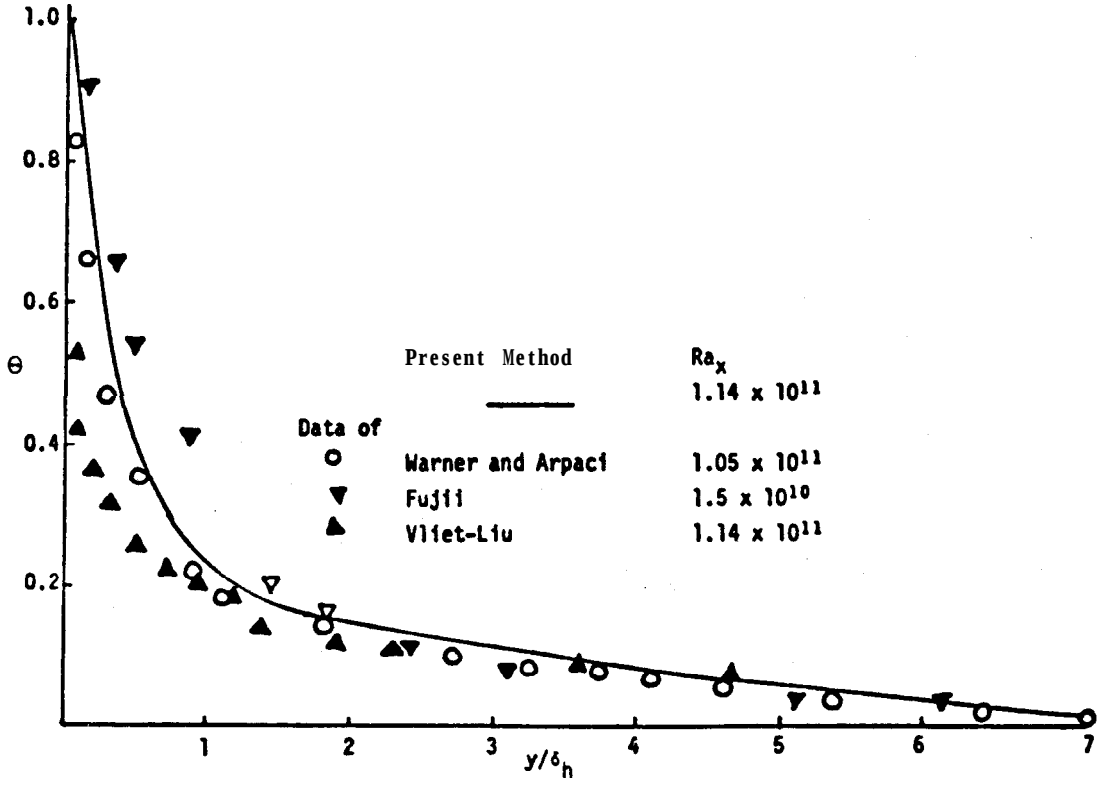

Figure 17a. Cebeci and Khattab (1975) temperature data-model comparison for air (Khattab (1975)).

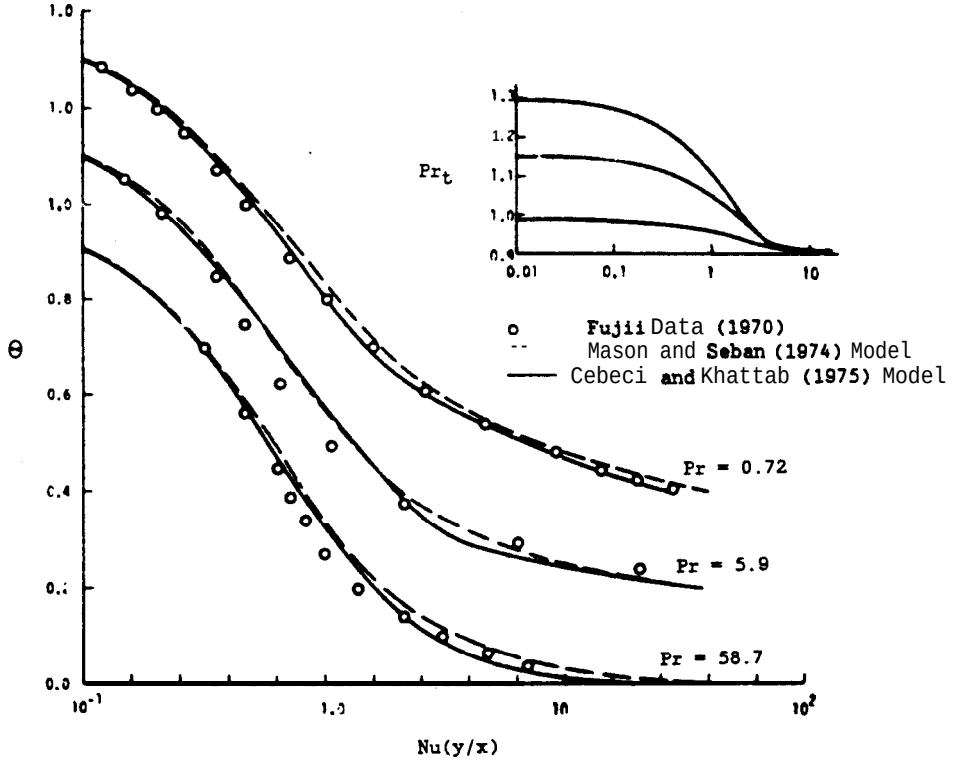

Figure 17b. Cebeci and Khattab (1975) temperature data-model comparison for air, water, and oil (Cebeci and Khattab (1975)).

In addition, Figure 17b shows the variation of the turbulent Prandtl number calculated by the model. Note that for air, the value approaches 1.3 at the wall and goes to 0.9 further out. This behavior is not inconsistent with the turbulent Prandtl number experimental data shown in Figure 13b, although the large scatter in the data prevents any firm conclusion of the applicability, and a constant value of 0.9 or 1.0 also seems reasonable based on the data.

Figures 18a-c show the Nusselt number, or heat transfer coefficient, predictions for the Cebeci and Khattab (1975) model with data for air, water, and spindle oil. In all cases, the agreement between the model and data is reasonable, although the good comparison may be a little misleading for the last two cases. For the first prediction, transition at a Ra, number of 6. x 10^8 was used in the computations. However, for the last two plots, the calculations by Cebeci and Khattab were made by matching the experimental results for a Ra, number of 5.5 x 10^{10}. Therefore, for the last two cases, only the slope of the predictions should be compared with the data. Figure 18d is the spindle oil Nusselt number variation for the Cebeci and Khattab (1975) model as presented by Cebeci and Bradshaw (1984). Note that the Nusselt number predictions are lower than those presented earlier by Cebeci and Khattab (1975). Apparently, the values in Figure 18d are those predicted by the Cebeci and Khattab model without being modified to match certain experimental results as was done for Figures 18b and 18c.

b. Noto and Matsurnoto

Noto and Matsumoto (1975) applied the forced convection eddy viscosity expression given by Kato, et al. (1968) to natural convection conditions assuming a turbulent Prandtl number of 1.0. Noto and Matsumoto (1975) used the model in a local similarity set of equations to predict the natural convection boundary layer velocity and temperature profiles. The eddy viscosity expression is

$$\nu_t/\nu = 0.4\, y^+ \left(1 - \exp(-0.0017\, y^{+2})\right) \tag{47}$$

where

$$y^+ = \frac{(\tau_w/\rho)^{1/2}}{\nu}\, Y \tag{48}$$

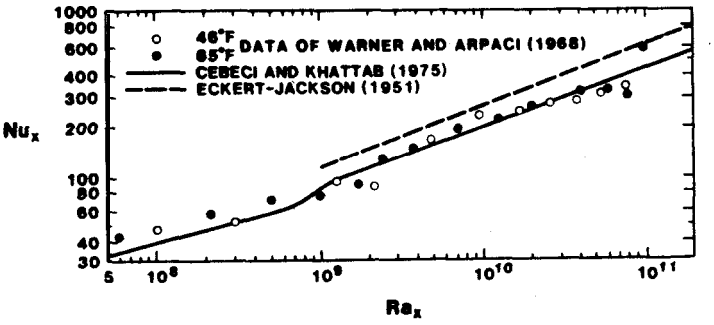

a) Air (Cebeci and Khattab (1975)).

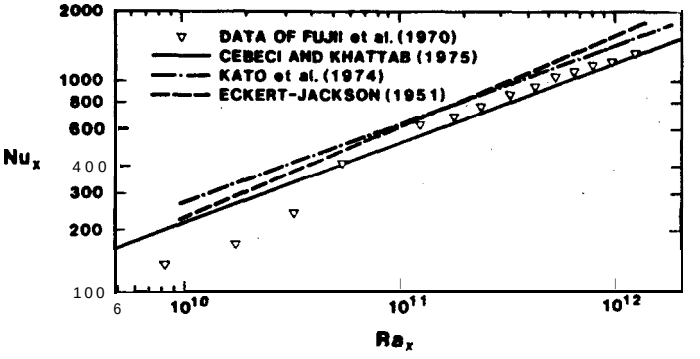

b) Water (Cebeci and Khattab (1975)).

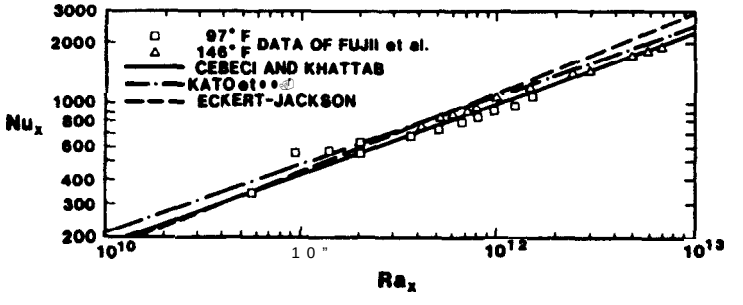

c) Spindle oil (Cebeci and Khattab (1975)).

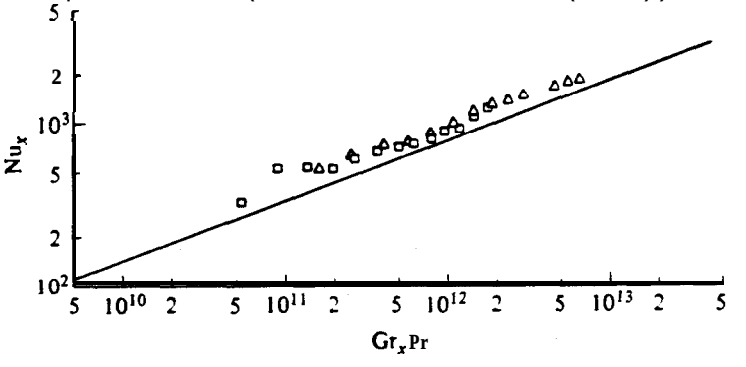

d) Spindle oil (unmodified) (Cebeci and Bradshaw (1984)).

Figure 18. Cebeci and Khattab data-model comparisons.

In contrast to the data shown earlier in Figure 15, the eddy viscosity and mixing length increases indefinitely as y increases. The implication of this behavior will be discussed in more detail later.

A velocity profile data-model comparison for the Noto and Matsumoto (1975) results is shown in Figure 19a including the peak velocity. This figure gives results for the air data of Cheesewright (1968) which indicates that the predicted shape is similar to experimental data. The peak velocity predicted by the model is about 30% too high in this figure. However, as discussed in detail earlier in this report, the velocity data reported by Cheesewright (1968) are low. The results of Mason and Seban (1974) are also shown on this figure; their prediction virtually lies on top of that by Noto and Matsumoto. Figure 19b gives the temperature profile data-model comparison which shows good agreement although the scale is too compressed for an accurate evaluation. Figure 20 shows the predicted Nusselt numbers for air and for oil. The results compare well to the data.

c. Yang and Llovd

Yang and Lloyd (1985) present a zero-equation turbulence model designed for modelling the behavior of vented enclosures. The application of the model is primarily in the area of room fires to predict the behavior of the fire and the resulting smoke. The model considers shear stresses in all directions as exemplified by the equations presented by Yang and Lloyd (1985) for the two-dimensional case as given below

$$\tau_{xx} = \frac{2}{Re_t}\frac{\partial u}{\partial x}\ , \quad \tau_{xy} = \frac{1}{Re_t}\left(\frac{\partial u}{\partial y} + \frac{\partial v}{\partial x}\right)\ , \quad \tau_{yy} = \frac{2}{Re_t}\frac{\partial v}{\partial y} \tag{49}$$

where

$$Re_t = \frac{\bar{\rho}_o \bar{U}_o H}{\mu_{eff}} \tag{50}$$

and

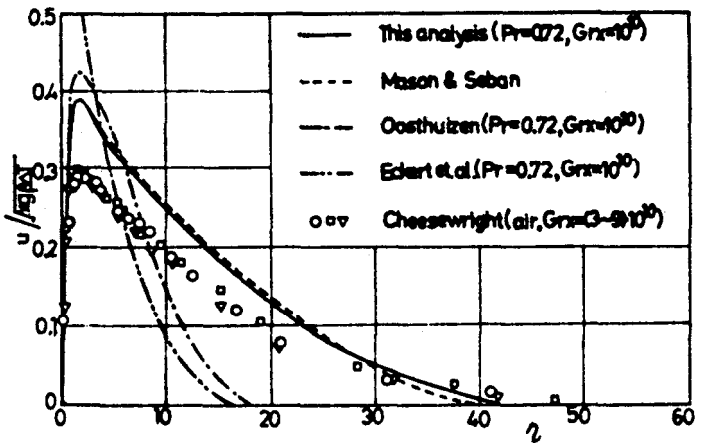

Figure 19a. Noto and Matsumoto (1975) velocity data-model comparison (Noto and Matsumoto (1975)).
velocity units = 2f'
distance units = y/x $Gr_x^{1/4}$.

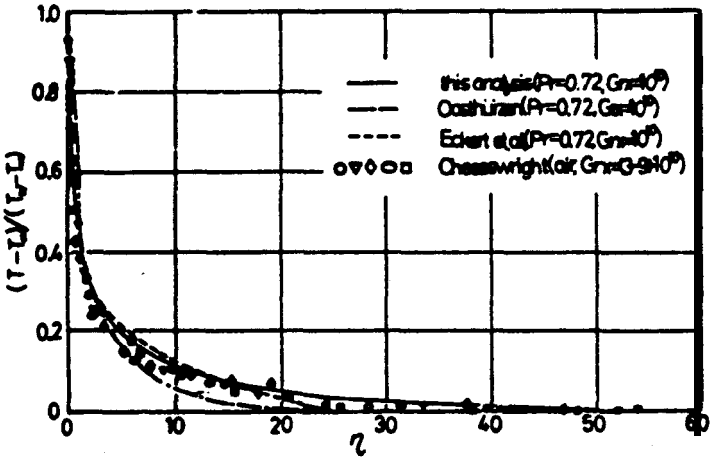

Figure 19b. Noto and Matsumoto (1975) temperature data-model comparison (Noto and Matsumoto (1975)).
temperature units = θ
distance units = y/x $Gr_x^{1/4}$.

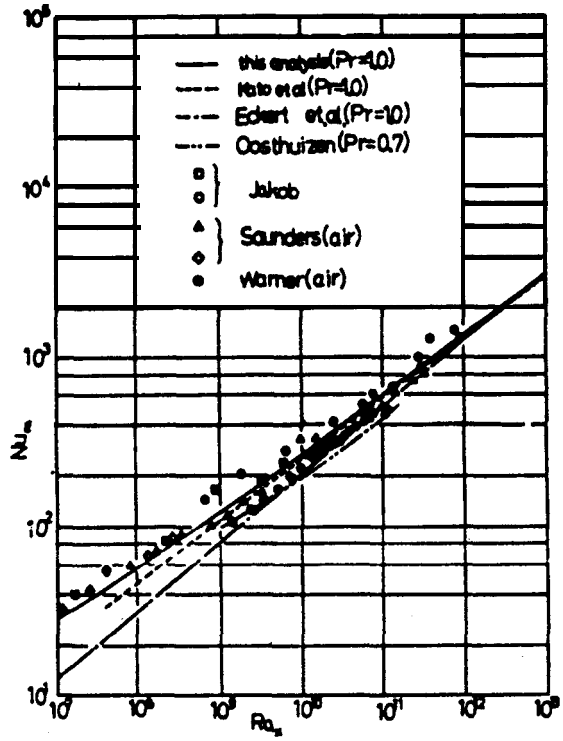

Figure 20a. Noto and Matsumoto (1975) Nusselt number data-model comparison for air (Noto and Matsumoto (1975)).

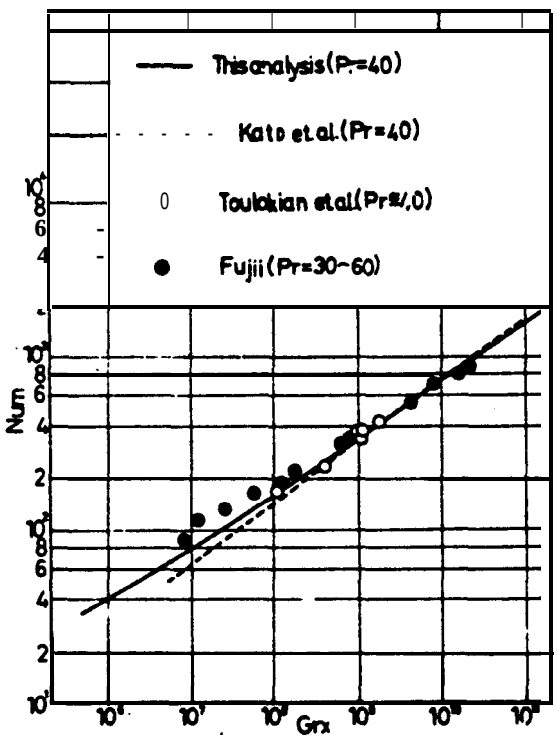

Figure 20b. Noto and Matsumoto (1975) Nusselt number data-model comparison for oil (Noto and Matsumoto (1975)).

$$\mu_{eff} = 1 + \frac{\left[\left(\frac{\partial u}{\partial y}\right)^2 + \left(\frac{\partial v}{\partial x}\right)^2\right]^{1/2} \left[\frac{l}{H}\right]^2}{2 + \frac{Ri_g}{Pr_t}} \tag{51}$$

The turbulent Prandtl number is assumed equal to 1. The effective viscosity includes laminar and turbulent contributions and is presumably normalized to the laminar value. The mixing length expression is

$$\frac{1}{H} = \kappa \left[\frac{(u^2 + v^2)^{1/2}}{\left[\left(\frac{\partial u}{\partial x}\right)^2 + \left(\frac{\partial u}{\partial y}\right)^2 + \left(\frac{\partial v}{\partial x}\right)^2 + \left(\frac{\partial v}{\partial y}\right)^2\right]^{1/2}} + \frac{\left[\left(\frac{\partial u}{\partial x}\right)^2 + \left(\frac{\partial u}{\partial y}\right)^2 + \left(\frac{\partial v}{\partial x}\right)^2 + \left(\frac{\partial v}{\partial y}\right)^2\right]^{1/2}}{\left[\left(\frac{\partial^2 u}{\partial x^2}\right)^2 + \left(\frac{\partial^2 u}{\partial y^2}\right)^2 + \left(\frac{\partial^2 v}{\partial x^2}\right)^2 + \left(\frac{\partial^2 v}{\partial y^2}\right)^2\right]^{1/2}} \right] \tag{52}$$

where κ is an adjustable constant equal to 0.2 based on comparison of the model to data. The gradient Richardson number, Ri_g, is equal to

$$Ri_g = \frac{H g}{\tilde{U}_o^2} \frac{\frac{\partial T}{\partial y}}{\left(\frac{\partial u}{\partial y}\right)^2}. \tag{53}$$

where T, u, and y are normalized values and $\tilde{U}_o$ is a reference velocity.

The model has some desirable features in that it is symmetrical with respect to x and y, and buoyancy is included through the gradient Richardson number. The model is discussed further by Yang and Lloyd (1985). However, while the approach seems reasonable, the only data-model comparisons presented are for the entire enclosure model, such as the temperature distribution in an outlet doorway; no comparison to boundary layer data is given. Since these data-model comparisons are not presented, modifications to the model needed for use in this study cannot be evaluated, and this model is not discussed further in this report.

d. Popov and Yan'kov

Popov and Yan'kov (1985) present a model for natural convection that is based on forced convection eddy viscosity formulae. The buoyancy effect is included through a Richardson number and through inclusion of the enthalpy gradient on the shear stress. The shear stress and heat flux equations are

$$\tau = (\mu + \rho \nu_t) \frac{\partial u}{\partial y} + \frac{\beta g l^2 \rho}{c_p Pr_t} \frac{\partial h}{\partial y} \tag{54}$$

$$q = - \left(\frac{k}{c_p} + \rho \alpha_t\right) \frac{\partial h}{\partial y}. \tag{55}$$

The expressions given above are equivalent to those derived in Appendix A except for the second term on the RHS of the shear equation. In this model, the effect of the temperature (or enthalpy) gradient is included in the shear stress. The turbulent eddy viscosity expression is

$$\nu_t^2 = \frac{\nu_{t0}^2}{2} + \left[\left(\frac{\nu_{t0}^2}{2} \right)^2 + \nu_{t\infty}^4 \mp \gamma \nu_{t0} \nu_{t\infty}^2 \nu_t \right]^{1/2} \tag{56}$$

where the subscripts 0 and ∞ refer to values as Ri → 0 and ∞ which are

$$\nu_{t0} = l^2 \sqrt{\left(\frac{\partial u}{\partial y}\right)^2 + l_1 \left(\frac{d^2 u}{\partial y^2}\right)^2} \tag{57}$$

$$\nu_{t\infty} = m\, l^2 \left(\frac{\beta g}{c_p Pr_t} \left| \frac{\partial h}{\partial y} \right| \right)^{1/2} \tag{58}$$

and the Richardson number is

$$Ri = \frac{- \beta g \frac{\partial T}{\partial y}}{\frac{\partial u}{\partial y} \left| \frac{\partial u}{\partial y} \right|}. \tag{59}$$

The - and + sign in the last term of the eddy viscosity expression is applicable for Ri > 0 and < 0, respectively. The expression for ν_{t0} uses a modification to the Prandtl mixing length which is discussed in Appendix B.

The value of the mixing length is based on expressions derived from forced convection data. The mixing length equation is

$$\frac{1}{\nu}\frac{u^+}{} = \left[\frac{\left(\frac{\nu_t}{\nu}\right)_{b.l.} \left(1 + \left(\frac{\nu_t}{\nu}\right)_{b.l.} \right)}{\left(\frac{\tau}{\tau_w}\right)_{b.l.}} \right]^{1/2} \tag{60}$$

where u^+ is given by

$$\left(\frac{u^+}{u_*}\right)^2 = 0.5 + \left[0.25 + \left(m^2 \frac{Ri}{Pr_t}\right)^2 - \gamma\, m^2 \frac{Ri}{Pr_t} \frac{u^+}{u_*} \right]^{1/2} \tag{61}$$

$$u_* = (\tau_w/\rho)^{1/2} \tag{62}$$

and

$$\left(\frac{\nu_t}{\nu}\right)_{b.l.} = \begin{cases} \kappa\, y^+ \left[1 - \dfrac{\tanh\,(y^+/\eta_1)}{(y^+/\eta_1)} \right] & 0 \le y+ \le 20 \\ \kappa\, y^+\, \Psi(Y) & 20 < y+ \end{cases} \tag{63}$$

$$\Psi(Y) = \begin{cases} \dfrac{\left(\frac{\tau}{\tau_w}\right)_{b.l.}}{1 + \pi n Y \sin(\pi Y)} & 0 \le Y \le 0.5 \\ \Psi(0.5)\, \exp\left[- \left(\dfrac{Y-0.5}{0.4}\right)^2 \right] & Y > 0.5 \end{cases} \tag{64}$$

$$Y = y/\delta \tag{65}$$

and equations for Q(Y) and $(\tau/\tau_w)_{b.l.}$ are given by Popov (1970). The expression for $(\nu/\nu_t)_{b.l.}$ is the Reichardt formula for near wall eddy viscosity in forced convection. The $\Psi(Y)$ and $(\tau/\tau_w)_{b.l.}$ equations are based on Coles' wake law, which is also for forced convection, Details on

the original models of Reichardt and Coles can be found in Hinze (1975). Values of γ, m, n, κ, and η_1 are discussed by Popov and Yan'kov.

In the above model, the boundary layer thickness, δ, is defined by

$$\tilde{y} = \frac{\delta - y_m}{\delta_{1/2}} = 2.5 \tag{66}$$

where $\delta_{1/2}$ is the distance where $u = 0.5\ u_{max}$ and y_m is the location of the maximum velocity. Figure 21 indicates the usefulness of this relationship as the outer region velocity profiles collapse onto a single curve shape for a number of different fluids.

Results from this model including comparison to data are shown in Figure 22a for air. Curve 1 and 1' are with and without the buoyancy modifications, respectively. The velocity data are from Cheesewright (1968), while the temperature data are from Cheesewright (1968) and from Warner and Arpaci (1968); Nusselt number data are also included. The predictions from a number of other investigators including Noto and Matsumoto (1975) and Mason and Seban (1974) are shown in the figure. Results for the Popov and Yan'kov model without buoyancy effects will be evaluated; buoyancy effects will not be addressed in the present investigation. In this manner, all the mixing length models can be assessed on an equal basis. Without the buoyancy modifications, the Popov and Yan'kov model velocity profile results are poorer than those of Noto and Matsumoto. These results are very similar to those of Cebeci and Khattab (1975) for the same data as shown later.

Figure 22b shows the velocity profile predictions for the Vliet and Liu (1969) water data and for ethyl alcohol data of Kutateladze, et al. (1972). Comparisons for the water data look good although, as discussed later, the predictions of Mason and Seban (1974) are similar. The model overpredicts the ethyl alcohol velocity data by about 10 percent; this model is the only known comparison to these data.

Without buoyancy, the basic Popov and Yan'kov model gives results similar or not as good as other zero-equation models. The Popov and Yan'kov approach offers no significant advantage compared to other approaches and has the disadvantage of a complicated form. Therefore, the Popov and Yan'kov model has not been investigated further in this study.

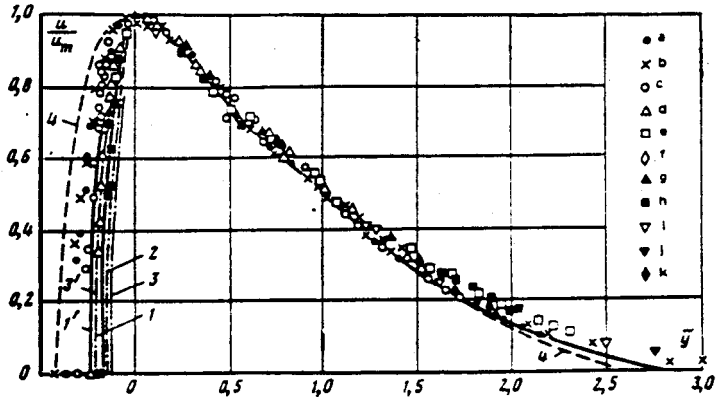

Data
a-h **Kutateladze, et al** (1972) for ethyl alcohol.
i-k **Cheesewright (1968)** for air.
Predictions
Popov and **Yan'kov** Model **for**
1,1' ethyl alcohol
2 **air**
3,3' rater
4 **mercury**

Figure 21. Natural convection velocity profile normalization (Popov and Yan'kov (1985)).

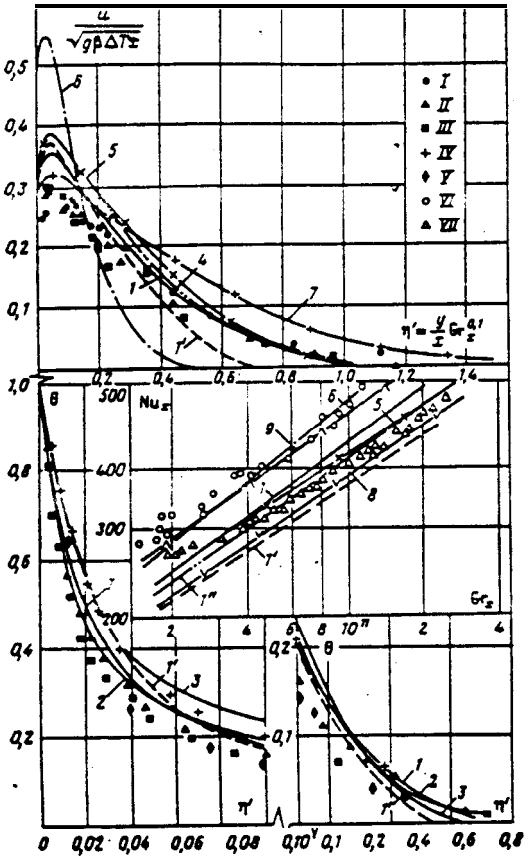

Data

I-IV	Cheesewright (1968)
V	Warner and Arpaci (1968)
VI,VII	Cheesewright (1968) and Pirovano et al. (1970)

Predictions

1,1',1",-33	Popov and Yan'kov Model
4	Noto and Matsumoto (1975)
5	Mason and Seban (1974)
6	Eckert Integral Method (Cheesewright (1968))
7	Plumb and Kennedy (1977)
8	Cebeci and Khattab (1975)
9	Kato, et al. (1968)

Figure 22a. Popov and Yan'kov Data-Model Comparison for Air (Popov and Yan'kov (1985)).

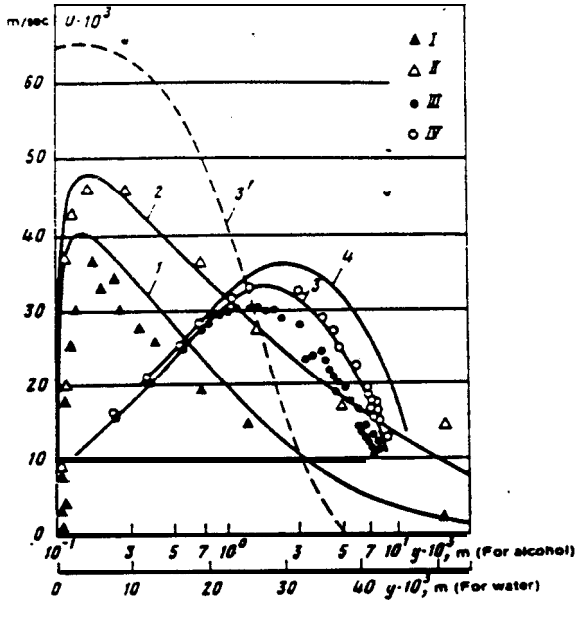

Data

I,II	Vliet and Liu (1969) for water
III,IV	Kutateladze, et al. (1972) for ethyl alcohol

Predictions

1,2	Popov and Yan'kov Model for water
3,4	Popov and Yan'kov Model for ethyl alcohol
3'	Eckert Integral Method for ethyl alcohol (Kutateladze, et al. (1972))

Figure 22b. Popov and Yan'kov data-model comparison for water and ethyl alcohol (Popov and Yan'kov (1985)).

2. One- and Two-Equation Models

As discussed briefly earlier in this section and in Appendix A, one- and two-equation eddy viscosity models are much more complicated than zero-equation models since additional PDEs are added to the equation set. For example, the turbulent shear stress for an eddy viscosity model is

$$-\overline{u'v'} = \nu_t \frac{\partial u}{\partial y}. \tag{67}$$

The value of ν_t for a two-equation k~ε model is (Yang and Aung (1985))

$$\nu_t = C_\mu \frac{k^2}{\varepsilon} \tag{68}$$

where k and ε are determined from the solution of appropriate PDEs for k and ε, and C_μ is a constant.

Numerical studies using the more complex one- and two-equation models have been conducted by Mason and Seban (1974), Plumb and Kennedy (1977), Lin and Churchill (1978), To and Humphrey (1986), and Heiss, Straub, and Catton (1988). In addition, To and Humphrey (1986) have used an algebraic stress turbulence model for their studies, while Heiss, et al. (1988) investigated algebraic and Reynolds stress models. Henkes and Hoogendoorn (1989b) compared the Cebeci and Khattab (1975) model (referred to as the Cebeci and Smith (1974) model) and a number of two-equation k~ε models to "generic" turbulent data. The results from some of these investigations are summarized in the next section.

C. Data-Model Comparisons

Data-model comparisons for the zero-, one-, and two-equation eddy viscosity turbulence models are presented in this section to indicate the predictive differences in the various approaches. All of the one- and two-equation studies, with the exception of Mason and Seban (1974), only present data-model profile comparisons for turbulent conditions in air. Mason and Seban (1974) present air and water data-model comparisons for their one-equation model. In addition, only the Popov and Yan'kov (1985) model has been compared with the ethyl alcohol data of Kutateladze, et al.

(1972). Thus, the data-model comparisons are very limited in scope with respect to the fluid involved and are primarily concerned with air.

Results from the zero-equation models were not compared to the Cheesewright and Ierokiopitis (1982) data by the original authors. Heiss, et al. (1988) did a partial comparison for the Cebeci and Khattab (1975) and Noto and Matsumoto (1975) approaches for the velocity and Nusselt number data. However, for both models, Heiss, et al. (1988) used a constant turbulent Prandtl number of 0.9 which is not in agreement with either original model. The net effect is probably small, but it precludes an exact comparison of the original models to the data. In their comparison, Heiss, et al. (1988) numerically integrated the boundary layer equations up the plate.

Figure 23 compares the mean velocity profiles predicted by a number of methods with the Cheesewright and Ierokiopitis data as presented by To and Humphrey (1986). Figure 23a shows the zero-equation velocity profile results given by Heiss, et al. (1988). The Cebeci and Khattab model overpredicts the velocity peak and underpredicts the velocity further out. The Noto and Matsumoto model results agree well with the peak value, while the velocity further out is only slightly underpredicted. Additional discussion of the Noto and Matsumoto (1975) model is given in the next section. Also shown are the results from an early forced convection zero-equation model by Escudier (see Heiss, et al. (1988)) which is very similar to the Cebeci and Khattab (1975) approach. Figure 23b from Heiss, et al. (1988) and Figure 23c from To and Humphrey (1986) compare one- and two-equation results and those for a k~ε model and an algebraic stress model (ASM) with the same data. All of these models predict the peak velocity well, and most of the models slightly underpredict the velocity further out.

Comparisons were also performed by Henkes and Hoogendoorn (1989b) using the Cebeci and Khattab (1975) model and nine different two-equation k~ε models. The predictions were compared to "generic" turbulent velocity and temperature profiles for air for a Grashof number of about 10^{11} (see Henkes and Hoogendoorn (1989b) for the exact range). Figure 24 shows the velocity profile data-model comparison. The Cebeci and Khattab (1975) model overpredicts the velocity maximum and underpredicts the velocity further out. In contrast, most of the k~ε models perform much better than the Cebeci and Khattab (1975) model and are in reasonable agreement with the data. Overall, these results are similar to those presented by Heiss, et al. (1988). Note that Henkes and Hoogendoorn (1989b) were not able to duplicate the k~ε model results reported by To and Humphrey (1986).

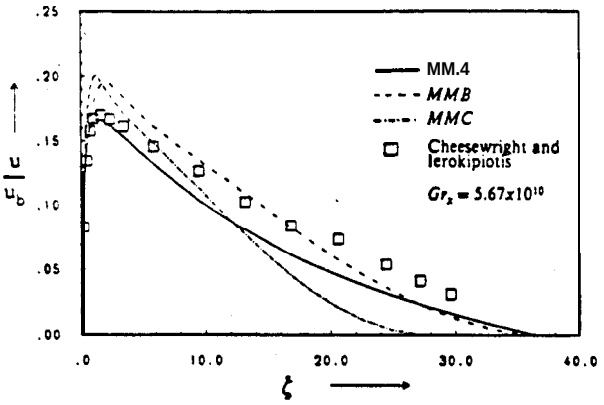

MMA - Noto and Matsumoto (1975)
MMB - Escudier (1966)
MMC - Cebeci and Khattab (1975)

Figure 23a. Zero-equation model comparison with velocity data (Heiss, et al. (1988)).
velocity units = f'

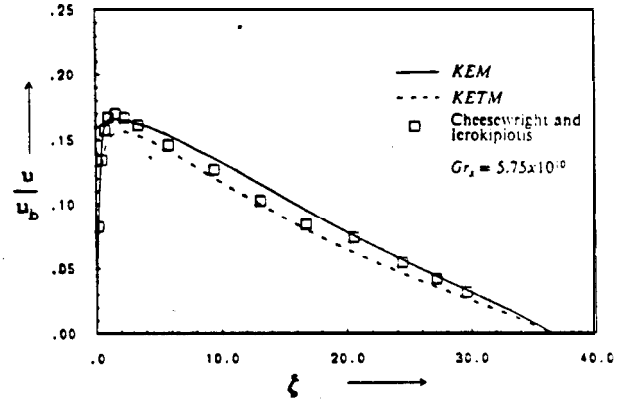

KEM - k ~ ε model
KETM - k~ ε - T'^2 model

Figure 23b. Two-equation model comparison with velocity data (Heiss, et al. (1988).
velocity units = f'

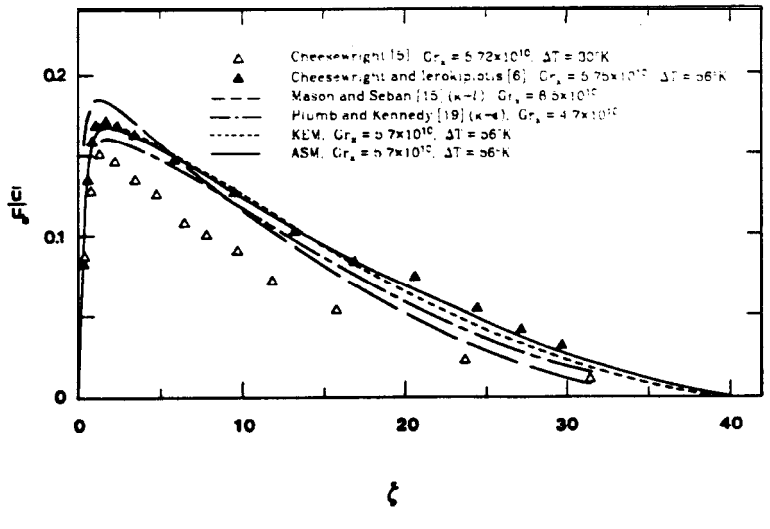

Figure 23c. Data-model comparison for velocity including stress models (To and Humphrey (1986)).
velocity units = f'

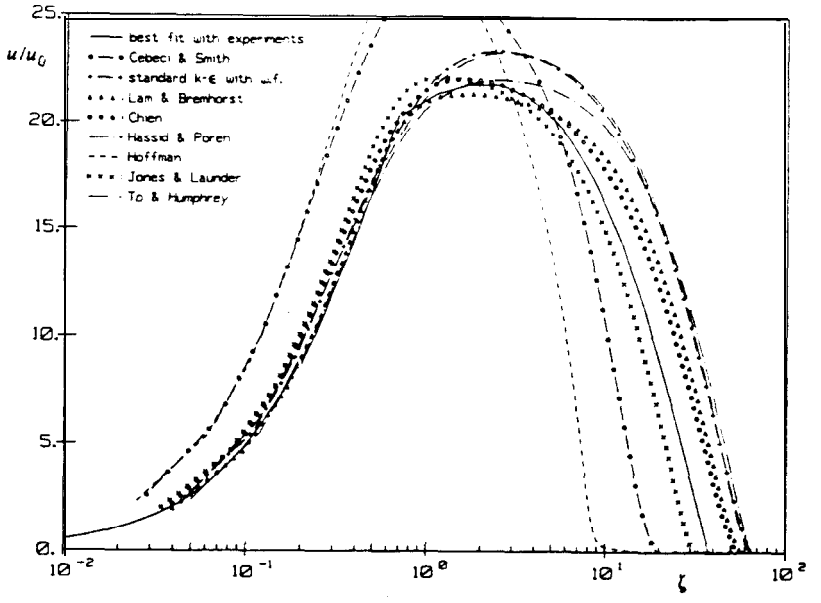

Figure 24. Air velocity profile data-model comparison (Henkes and Hoogendoorn (1989b)).

velocity units = $\frac{u}{(g\beta\Delta T\nu)^{1/3}}$

Mean temperature profile comparisons have been given by To and Humphrey (1986) for air as shown in Figure 25 based on the early Cheesewright (1968) data and on the Miyamoto, et al. (1982) data. All the models overpredict the temperature at moderate distances from the wall. Comparison of the zero-equation results was presented earlier in Figures 17 and 19 with similar results. The results of Henkes and Hoogendoorn (1989b) are given in Figure 26. This comparison indicates that most of the models slightly underpredict the temperature near the wall but overpredict it further out. The Cebeci and Khattab (1975) model, however, does just the opposite as it overpredicts near the wall and underpredicts further out. One interesting comment should be made about the Cebeci and Khattab (1975) temperature profile which has also been seen in the present investigation. The temperature profile has a "kink" in it at a ζ value of about 1. This "kink" occurs at the velocity maximum and is related to the mixing length definition which is proportional to the mean velocity gradient. This "kink" is also seen in the results predicted by the present model as shown later. Problems with the mixing length methodology at velocity maximums or minimums are discussed in more detail in Appendix B.

Nusselt number results are presented in Figures 27a and 27b from Heiss, et al. (1988) and Figure 27c from To and Humphrey (1986). All the predictions are in reasonable agreement with the data. The Nusselt number comparison presented by Henkes and Hoogendoorn (1989b) is shown in Figure 28. The Cebeci and Khattab (1975) model gives a low value of the Nusselt number. The largest discrepancy between the models is related to the location of the start of turbulence.

All of the above data-model comparisons are for air. The water data-model comparison for the mean velocity is given in Figure 29 for the Mason and Seban (1974) one-equation model, and the predictions agree well with the data. Note that the same Mason and Seban (1974) model did not agree as well with the air data as shown in Figure 23c. The Mason and Seban (1974) model also agrees well with water temperature profile data as shown earlier in Figure 17b. In contrast with the numerous data-model comparisons for air, the results of Mason and Seban (1974) and of Popov and Yan'kov (1985) in Figure 22b are the only comparisons available for water. For ethyl alcohol, the Popov and Yan'kov (1985) model compares reasonably well to the data as shown previously in Figure 22b and is the only known comparison to those data.

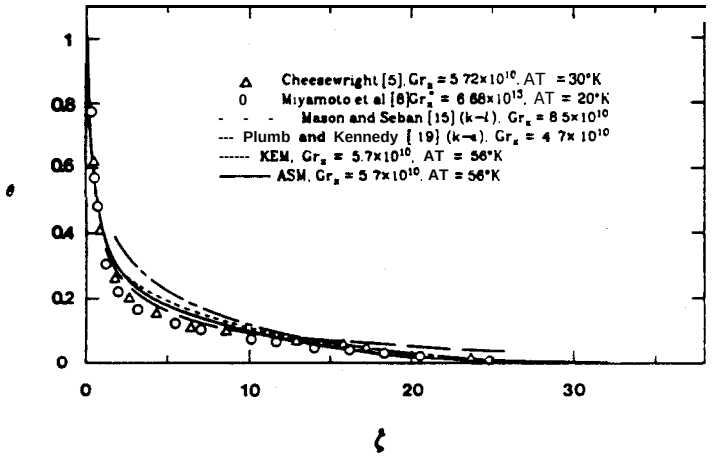

Figure 25. Temperature profile data-model (To and Humphrey (1986)).

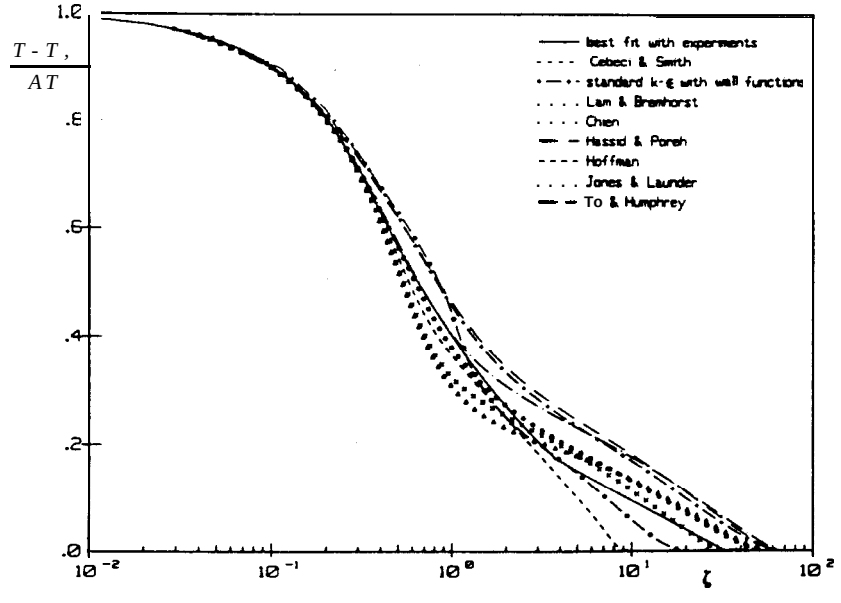

Figure 26. Comparison of model predictions to generic air temperature data (Henkes and Hoogendoorn (1989b)).

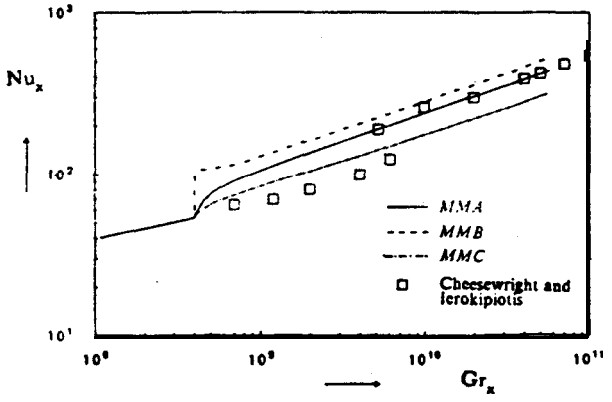

MMA - Noto and Matsumoto (1975)
MMB - Escudier (1966)
MMC - Cebeci end Khattab (1975)

Figure 27a. Zero-equation model comparison with Nusselt number data (Heiss, et al. (1989)).

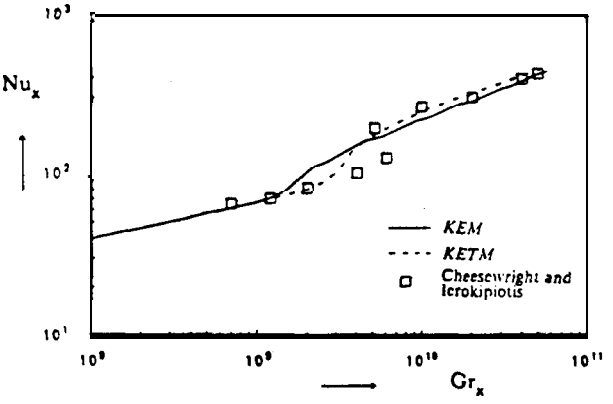

KEM - $k \sim \varepsilon$ model
KETM - $k \sim \varepsilon - T'^2$ model

Figure 27b. Two-equation model comparison with Nusselt number data (Heiss, et al. (1988)).

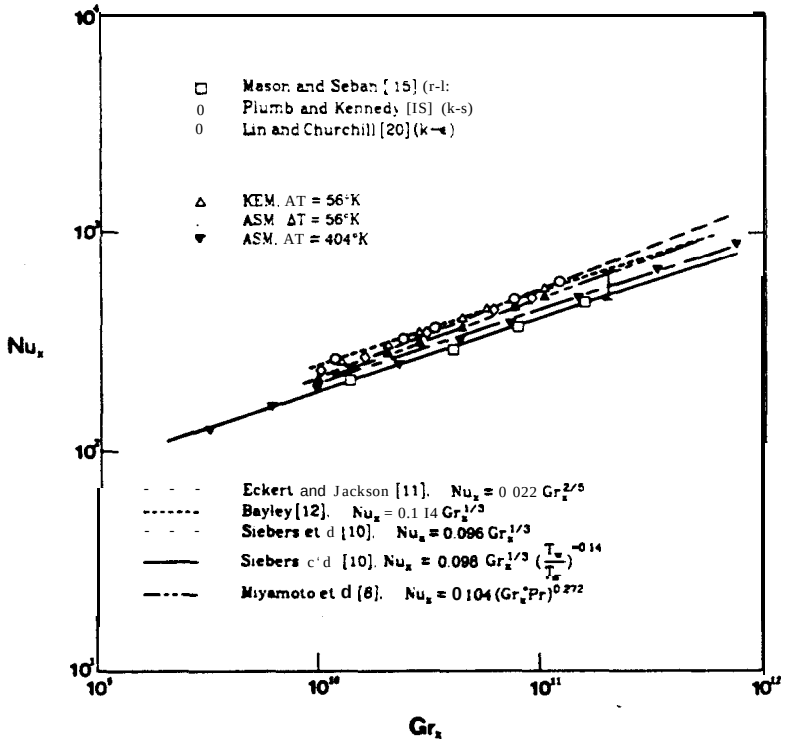

Figure 27c. Data-model comparison for Nusselt number including stress models (To and Humphrey (1986)).

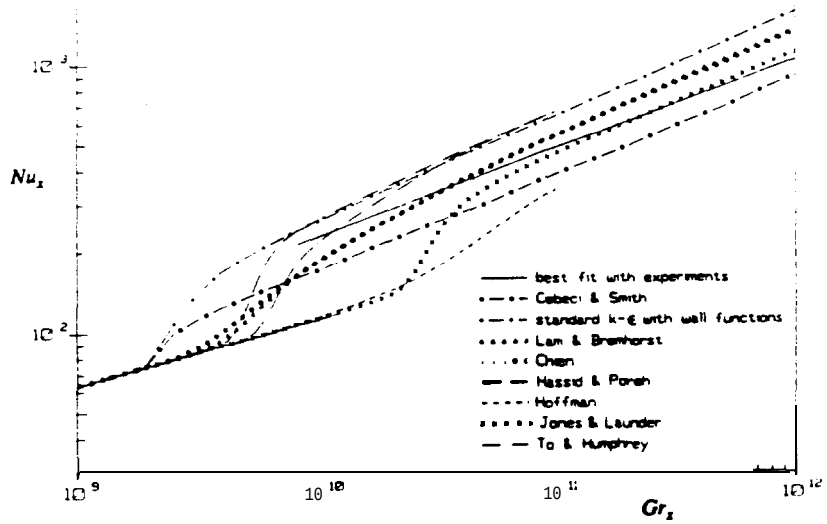

Figure 28. Nusselt number model comparison to generic air data (Henkes and Hoogendoorn (1989b)).

Points experiment	x (m)	q_w (W m^{-2})	T_i (K)	Curves theory
circle	0·76	6810	295	(a)
square	1·07	6810	295	(b)

o, □ } Vliet and Liu data (1968)

(a), (b) } Mason and Seban (1974)

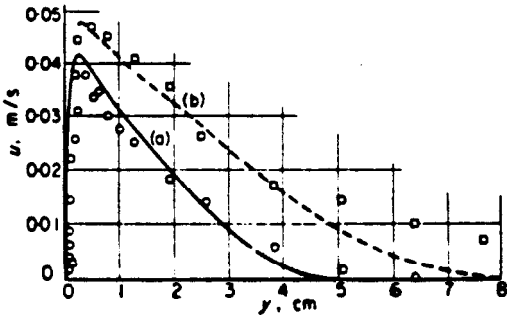

Figure 29. Velocity and data-model comparison for water (Mason and Seban (1974)).

D. Overall

Based on the above data-model comparisons, the zero-equation eddy viscosity models should provide a reasonable picture of the effect of turbulence on the velocity and temperature profiles as well as the Nusselt number. The agreement, while only fair for air and ethyl alcohol, is good for water. No data-model comparison is available for higher Prandtl number fluids such as oil. Some improvement could be gained from one-equation or two-equation models, but the added complexity and computer time and the question of applicability to a new fluid are not indicated for use in the SPR fluid velocity model.

The Noto and Matsumoto (1975) model looks good when compared to air data, but Gominho and White (1984) have noted some problems with the approach, especially in the outer region of the boundary layer. The Cebeci and Khattab (1975) approach, while not predicting the data as well as the Noto and Matsumoto (1975) model, is based on a well-established forced convection model and gives reasonable predictions. Other zero-equation models have been discussed earlier, and only the Cebeci and Khattab (1975) and Noto and Matsumoto (1975) models will be considered further.

While the Noto and Matsumoto (1975) model has been applied to the local similarity equations, the Cebeci and Khattab (1975) approach has not been and will have to be modified as developed in the next section. Both models as applied to the local similarity equation set will be compared to the available data discussed earlier to allow for a more complete evaluation of the two models under the conditions that they will be used.

C. Local Similarity Turbulence Model

1. Model Modification

The Noto and Matsumoto (1975) model does not need to be modified for application to the local similarity approach since the eddy viscosity is simply a function of y^+, or distance from the wall. However, the Cebeci and Khattab (1975) method needs some revision. As summarized earlier, the eddy viscosity is divided into two regions. The eddy viscosity in the inner region is simply a function of y and the local velocity gradient, so no changes have to be made in this region. In the outer region, the eddy viscosity is proportional to the boundary layer thickness and the velocity

gradient. Based on the local similarity requirement, the boundary layer thickness is based on the velocity profile at that location only; no feedback from the thickness at other locations can be used.

A straightforward application of the Cebeci and Khattab (1975) model would be to calculate the boundary layer thickness from the calculated velocity profile. However, this procedure is divergent. If the boundary layer thickness is overestimated, the outer region viscosity will also be too high. In turn, this behavior will increase the boundary layer thickness, and the process will diverge. Similarly, underestimation of the boundary layer thickness will result in too small a viscosity, and the same divergent cycle occurs. Thus, the present form of the Cebeci and Khattab (1975) model is incompatible with the local similarity requirement.

The Popov and Yan'kov (1985) velocity profile shape discussed earlier was also briefly considered. However, the relationship (Equation 66) only gives the boundary layer thickness in terms of the value where $u = 0.5\ u_{max}$. This expression would lead to the same divergent cycle as discussed above.

In order to apply the Cebeci and Khattab (1975) model to local similarity, an expression for the boundary layer thickness is needed which will cause the iterative procedure to converge. George and Capp (1979) developed a theory for natural convection turbulent boundary layers on a heated vertical surface which indicates that the thickness of the velocity boundary layer scales with the velocity or displacement boundary layer thickness, δ^*, which is defined as

$$\delta^* = \int_0^\infty \frac{u}{u_{max}}\, dy \tag{69}$$

where u_{max} is the maximum boundary layer velocity. Support for this scaling concept is from the velocity profile air data of Cheesewright (1968) and the water data of Vliet and Liu (1969) as shown earlier in Figure 10. Based on these data, a preliminary relationship is developed for the boundary layer thickness as

$$y(u\sim 0) = \delta \sim 2.5\ \delta^*. \tag{70}$$

This relationship provides a feedback mechanism on the boundary layer thickness used in the eddy viscosity model which allows for convergent iteration in the similarity method. The boundary layer thickness from the velocity profile and the displacement thickness, δ^*, have different functional relationships, and the iteration on the boundary layer velocity profile converges.

To further support this relationship, some of the Miyamoto, et al. (1982) data has been used. The displacement thickness correlated in their study is given by the equation

$$\delta^* = 0.743 \, Gr_x^{*-0.104} \, x. \tag{71}$$

The velocity data are given as velocity as a function of ζ, which is

$$\zeta = \frac{y}{x} \, Nu_x. \tag{72}$$

Using the appropriate Nusselt number correlation given in the paper, and estimating the boundary layer thickness from the velocity plots, the boundary layer thicknesses for the two turbulent velocity profiles reported are in the range

$$\delta \sim 2.4 \text{ to } 2.8 \, \delta^* \tag{73}$$

which is consistent with the value of 2.5 estimated earlier. Therefore, this preliminary relationship will be used to close the Cebeci and Khattab (1975) model for use in the local similarity approach. Since the constant of 2.5 is uncertain, the value will be treated as a parameter in the data-model comparison.

2. Comparison to Data

The predictions of the local similarity Cebeci and Khattab and the Noto and Matsumoto (1975) models will be compared to the natural convection velocity profile data discussed earlier. Three curves are shown for the modified Cebeci and Khattab model corresponding to δ values equal to 2.0, 2.5, and 3.0 times δ^*. Table 2 summarizes the investigators, fluid, wall conditions, and Grashof numbers involved. All the data have been transformed into the local similarity coordinates for consistent evaluation. The conversion process is summarized in Appendix C for each data set. Uniform environmental conditions have been assumed. The predictions for the local similarity Cebeci and Khattab model will be presented first for all the fluids followed by the Noto and Matsumoto results.

Figure 30 gives the results for the modified Cebeci and Khattab model for the air data listed in Table 2. A systematic overprediction of the peak velocity peak by about 20-40% is noted. Of course, the peak velocity overprediction is higher for the early Cheesewright (1968) data which are known to be low. For the most recent data (Tsuji and Nagano (1988)), the peak velocity is overpredicted by about 20%. The slope in the outer edge of the boundary layer can be reasonably approximated by a constant equal to about 2.5 in the boundary layer thickness relationship, although this number varies between 2.5 and 3.0 for the various data sets.

Figure 31 shows the local similarity Cebeci and Khattab model results for the water data in Table 2. In contrast to the air data, the model predictions using the Cebeci and Khattab approach agree well with the Vliet and Liu (1969) data including the value of the peak velocity for both Grashof numbers. Again, a constant equal to 2.5 in the boundary layer thickness relationship looks adequate.

The Lock and Trotter (1968) results are also shown in Figure 31. The model predictions are inconsistent with the data. Upon closer examination of the data, some problems are apparent. The data are inconsistent with that of Vliet and Liu (1969). According to information given by Vliet and Liu (1969) and by Jaluria (1980), the flow is probably laminar. In addition, the dimensionless velocity results indicate a velocity peak at f' of 0.32. For laminar conditions, the peak f' value for the Prandtl number of 10.25 is about 0.11 from Table 1. Therefore, the data of Lock and Trotter (1968) are questionable and this data-model comparison will not be used in the final evaluation of the turbulence model.

Table 2

Data for Data-Model Comparison

Author	Wall Conditions*	Gr_x Range
Air Data (Pr ~ 0.72)		
Cheesewright (1968)	UWT	3.0×10^{10}
		5.7×10^{10}
		8.65×10^{10}
Hoogendoorn and Euser (1978)	UWT	9.5×10^{9}
Cheesewright and Ierokiopitis (1982)	UWT	4.83×10^{10}
Miyamoto, et al. (1982)	UHF	1.2×10^{11}
		1.7×10^{11}
Tsuji and Nagano (1988)	UWT	1.55×10^{10}
		1.8×10^{11}
Water Data (Pr ~ 6.7 - 10.25)		
Vliet and Liu (1969)	UHF	1.9×10^{10}
		6.0×10^{10}
Lock and Trotter (1968)	UHF	6.7×10^{8}
Ethyl Alcohol (Pr ~ 13.2)		
Kutateladze, et al. (1972)	UWT	1.63×10^{9}
		3.66×10^{9}

* - UWT - Uniform Wall Temperature
UHF - Uniform Heat Flux

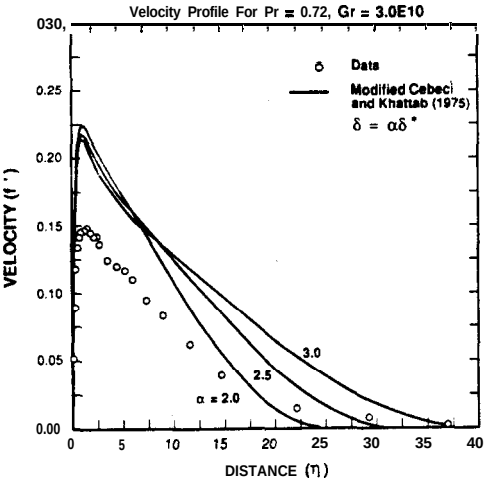

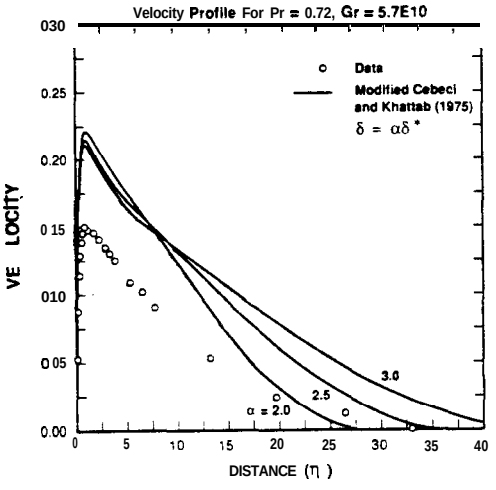

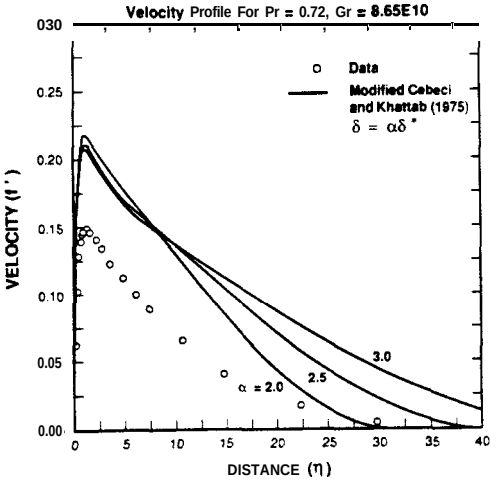

a) Cheesewright (1968) data.

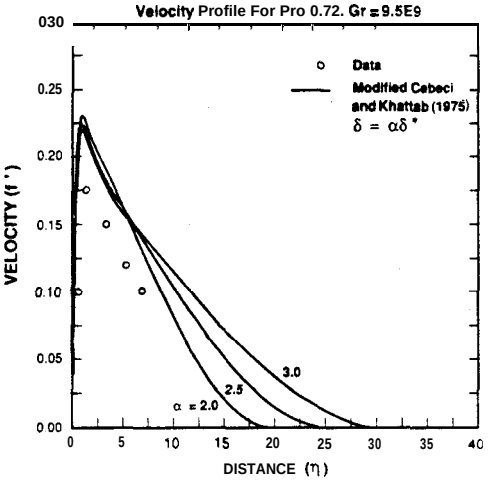

b) Hoogendoorn and Euser (1978) data.

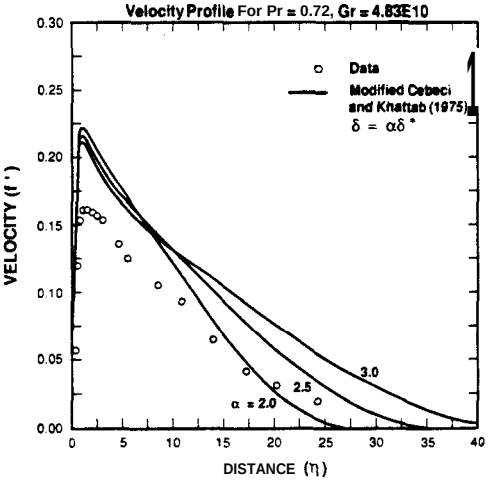

c) Cheesewright and Ierokiopitis (1982) data.

Figure 30. Local similarity model comparison to data for air.

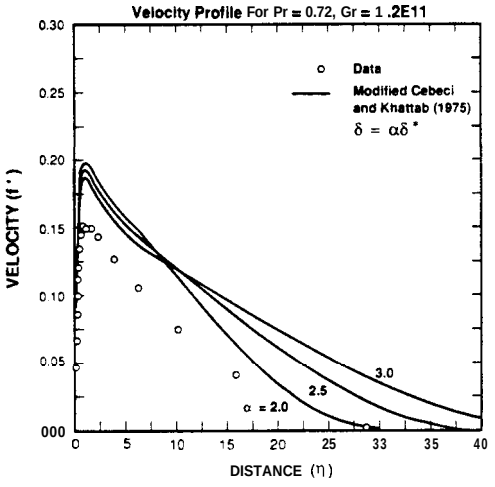

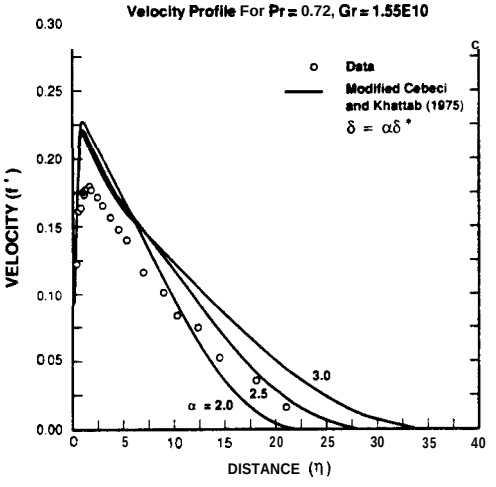

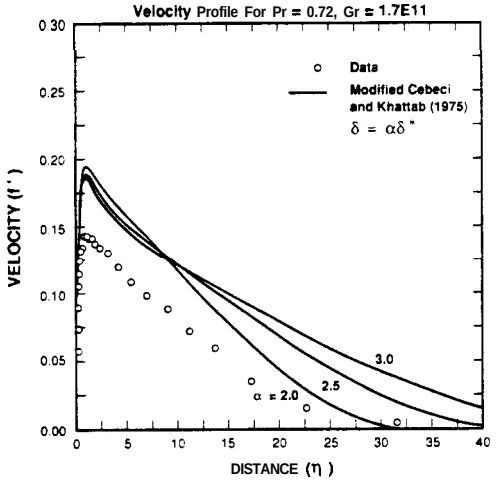

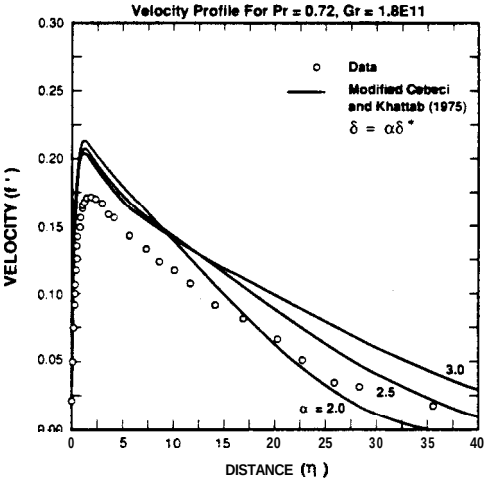

d) Miyamoto, et al. (1982) data

e) Tsuji and **Nagano (1988)** data

Figure 30 (continued).

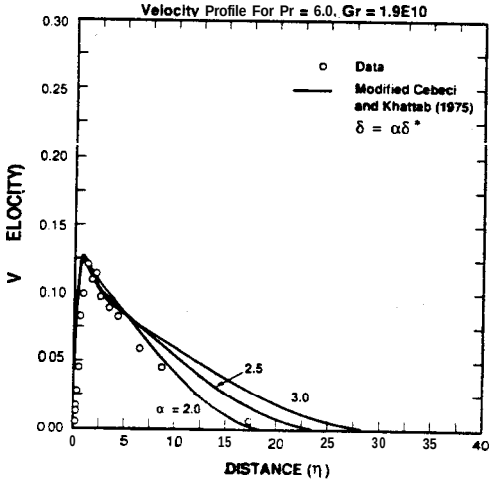

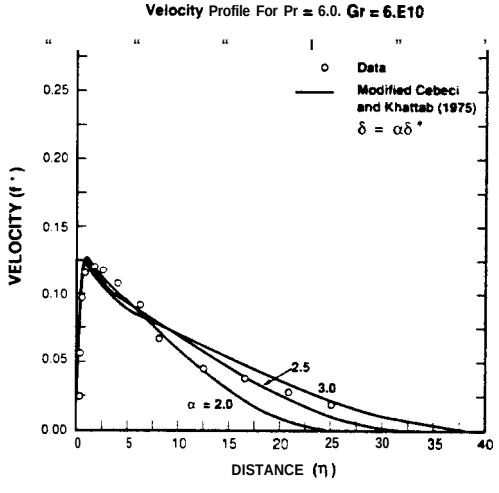

a) Vliet and Liu (1968) data.

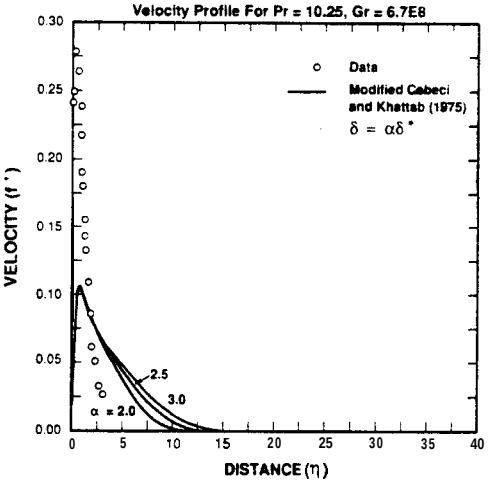

b) Lock and Trotter (1968) data.

Figure 31. Local similarity model comparison to data for water.

The data-model comparisons for the ethyl alcohol data from Kutateladze, et al. (1972) are shown in Figure 32. The peak velocity is overpredicted by the modified Cebeci and Khattab model by about 40%. A constant of 2.0 in the boundary layer thickness equation looks reasonable. The velocity data are more like the laminar profile as shown in Figure 32a than the turbulent predictions. This result is surprising in light of the excellent data-model agreement for water which has a similar Prandtl number and the fact that the overprediction by Popov and Yan'kov (1985) was only about 10%. This discrepancy has not been fully resolved at the present time.

Figures 33, 34, and 35 show the data-model comparison for the Noto and Matsumoto model and the data for air, water, and ethyl alcohol, respectively. In general, the predicted peak velocity is slightly lower than for the modified Cebeci and Khattab model and more in line with the data, especially for air and ethyl alcohol. However, the outer region of the boundary layer including the boundary layer thickness is greatly overpredicted by the Noto and Matsumoto (1975) model for all the data. The large difference between the present results and the data is due to the eddy viscosity formula. The eddy viscosity and effective mixing length increase continuously in contrast to data shown earlier in Figure 15. The present results have been calculated by requiring conservation of momentum and energy in the boundary layer within 1% or less as discussed in Section II. In order to conserve momentum locally, which is consistent with the local similarity assumption, the boundary layer must have negligible shear at η_∞. The slope at η_∞ has to be very small with the large viscosity inherent in the model, so the boundary layer thickness will be too large.

In contrast, the Noto and Matsumoto (1975) model seems to compare reasonably well to data as shown earlier in Figure 19a and in Figure 23. The velocity profile results given by Noto and Matsumoto in Figure 19a have been recalculated in Figure 36. Based on the local similarity assumption imposed by Noto and Matsumoto, momentum and energy should be conserved in the profiles. For η_∞ equal to 29.5, the velocity profile predictions are reasonably consistent with those in Figure 19a. However, as shown in Table 3, momentum is not conserved within a factor of 2., and the error in energy is 45%. Thus, significant conservation problems may exist with the earlier results of Noto and Matsumoto. Note that the Heiss, et al. (1988) results given earlier in Figure 23 may not have the same problem since the conservation equation were integrated along the plate and local similarity was not imposed.

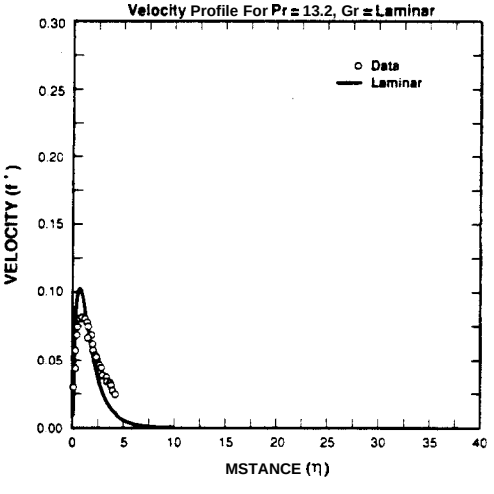

a) Laminar profile comparison.

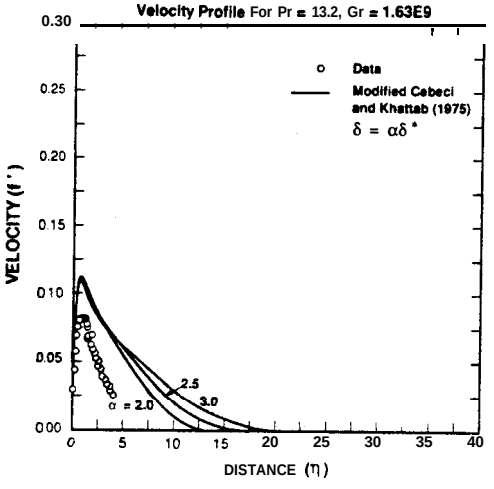

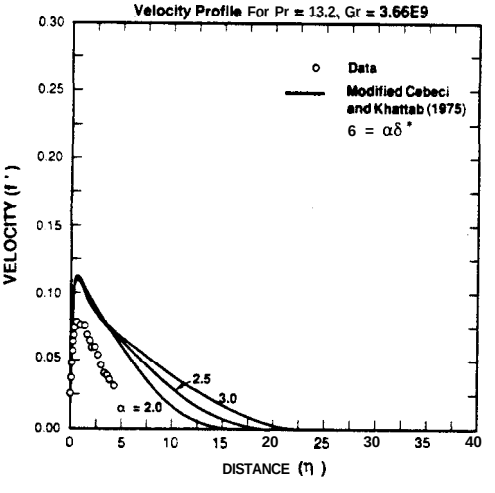

b) Turbulent prodictions.

Figure 32. Local similarity model comparison to data for ethyl alcohol.

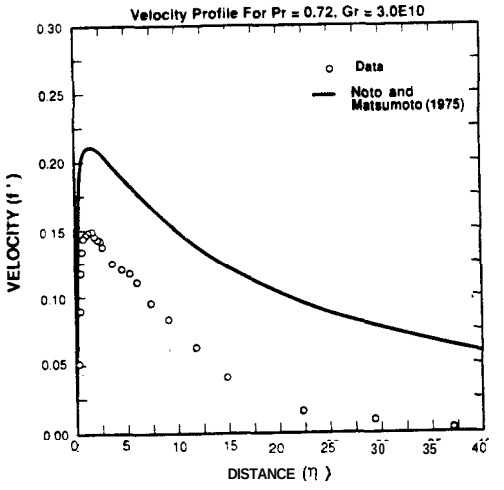

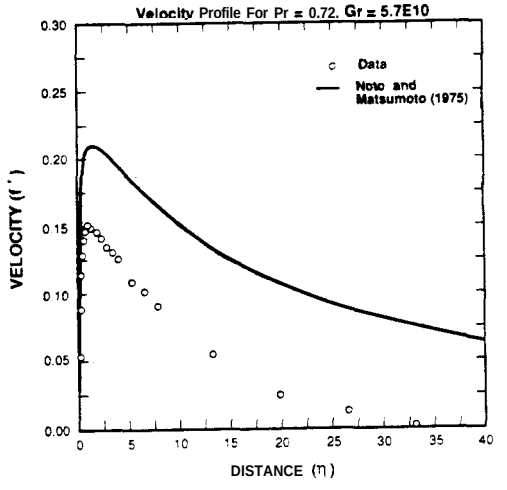

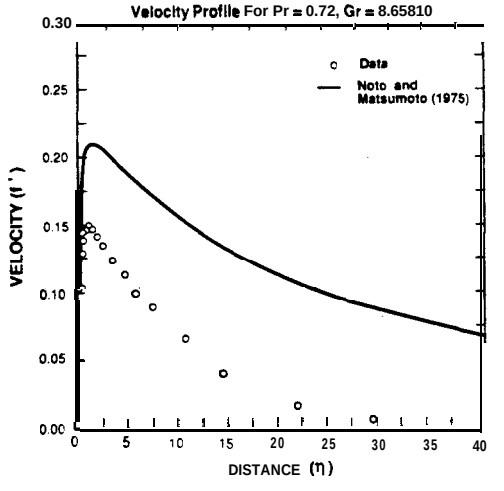

a) **Cheesewright (1968)** data.

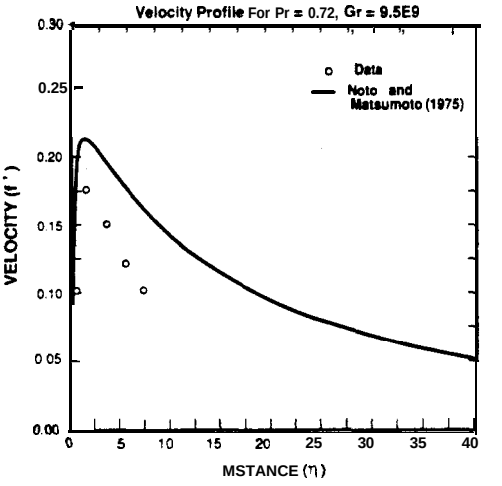

b) Haogendoorn and **Euser (1978)** data.

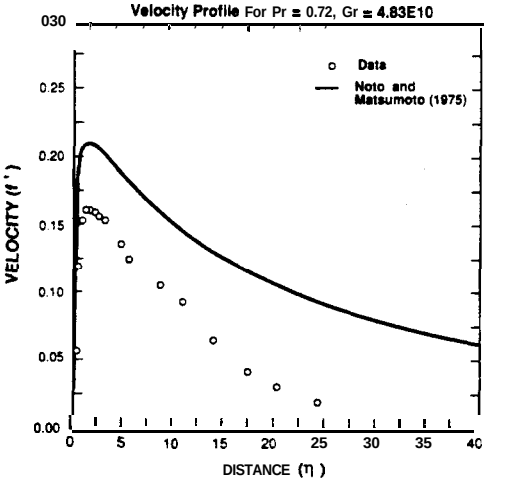

c) **Cheesewright** and **Ierokiopitis (1982)** data.

Figure 33. Noto and Matsumoto (1975) data-model comparison for air.

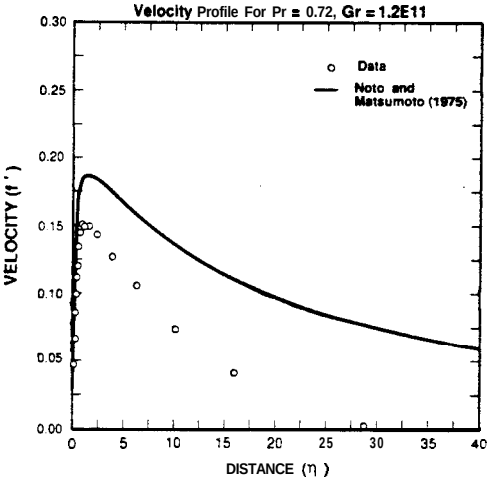

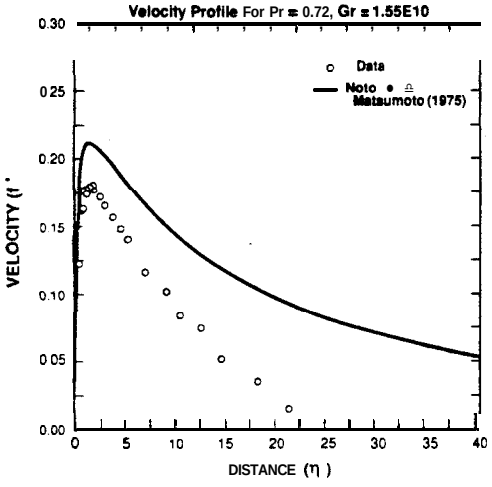

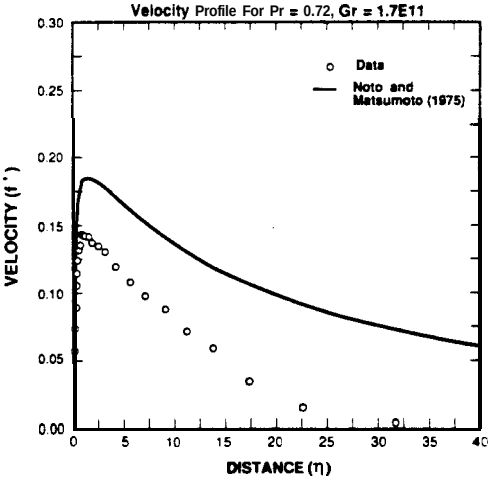

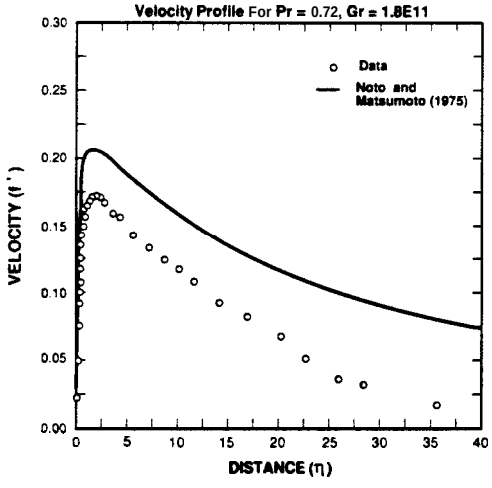

d) Miyamoto, et al. (1982) data.

e) Tsuji and Nagano (1988) data.

Figure 33 (continued).

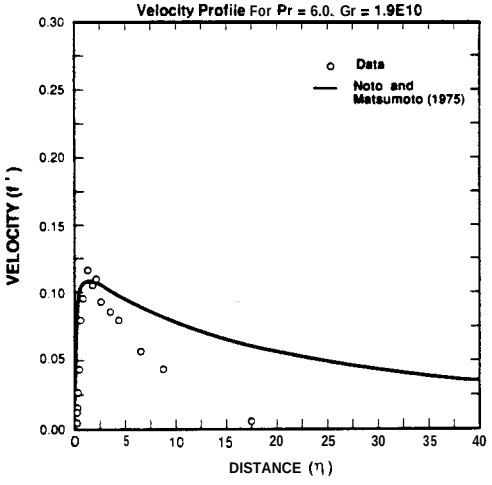

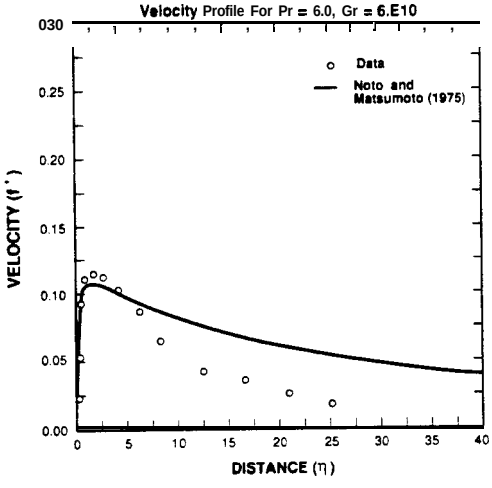

a) **Vliet** and Liu **(1968)** data.

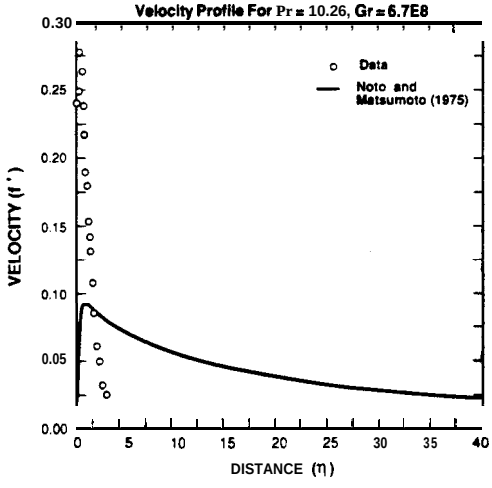

b) Lock and Trotter **(1968)** data.

Figure 34. **Noto** and Matsumoto (1975) data-model comparison for water.

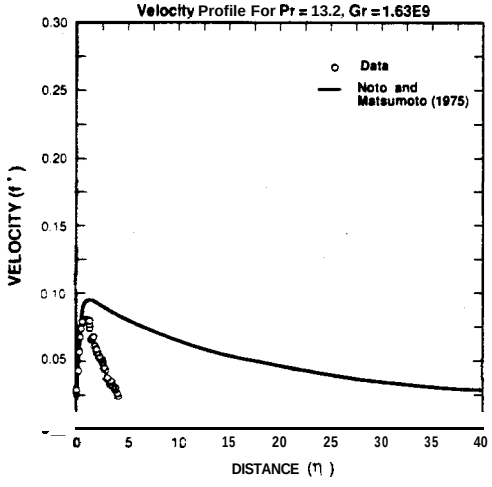

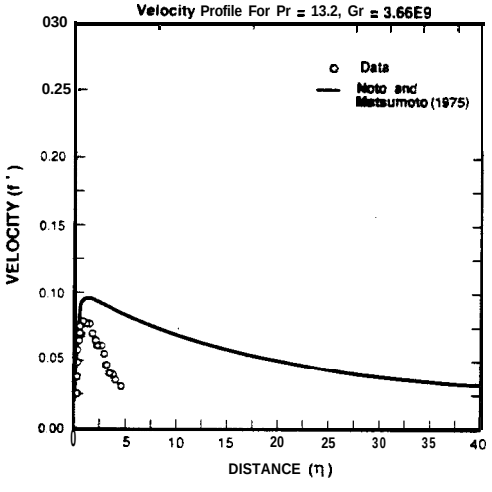

Kutateladze, et al. **(1972)** data.

Figure 35. **Noto** and Matsumoto Data-Model Comparison for Ethyl Alcohol.

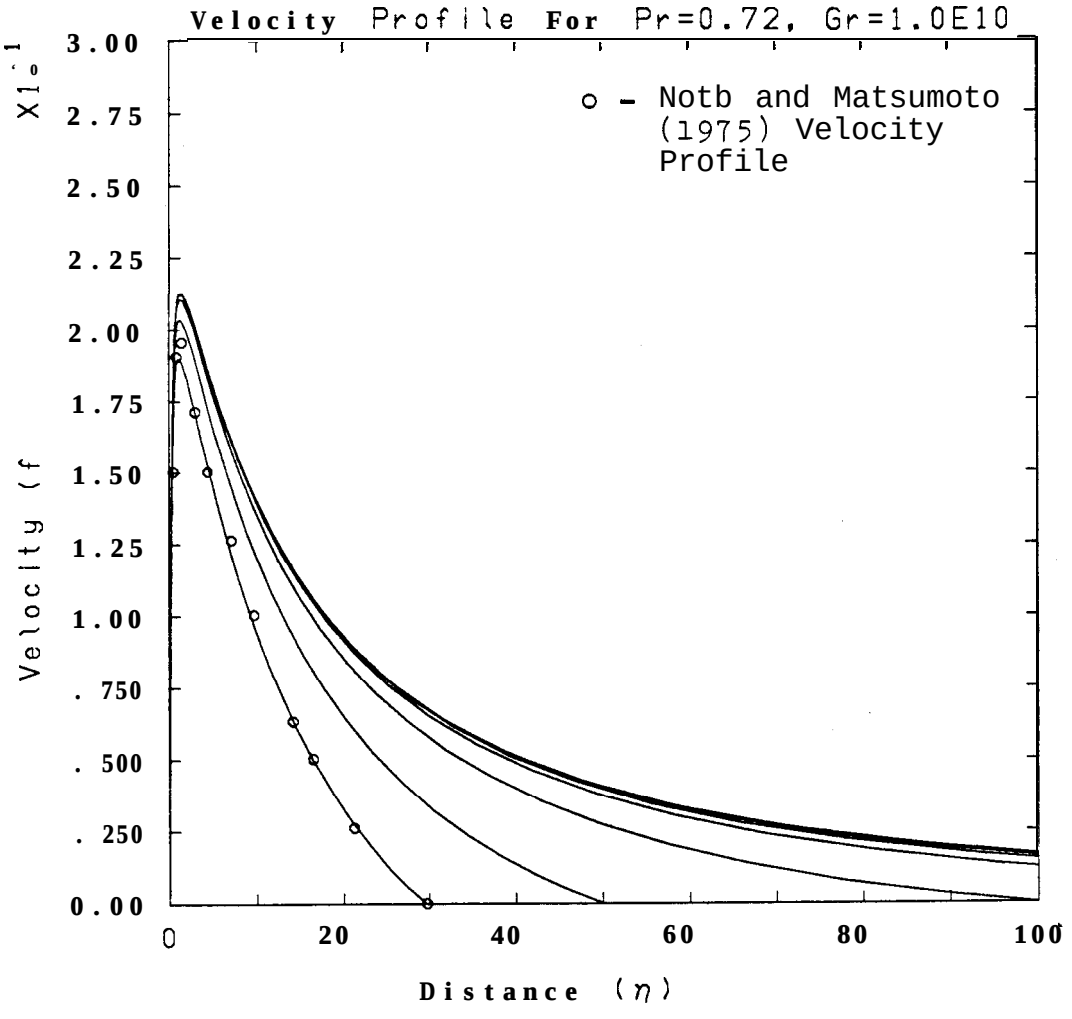

Figure 36. Velocity profile variation with η_∞.

Table 3

Noto and Matsumoto Conservation Results
for Pr-0.72

η_∞	Conservation of Momentum[1]	Conservation of Energy[2]	Error
Laminar			
10.	1.004	0.9998	6.2×10^{-11}
Turbulent ($Gr_x=10^{10}$)			
29.5	0.46	1.45	9.3×10^{-6}
50.	0.55	1.18	1.4×10^{-6}
100.	0.73	1.05	7.1×10^{-8}
200.	0.89	1.012	2.4×10^{-9}
300.	0.947	1.006	3.0×10^{-10}
400.	0.976	1.005	6.2×10^{-11}
500.	0.993	1.004	1.8×10^{-11}
600.	1.003	1.004	6.6×10^{-12}

[1] - Conservation of Momentum =

$$f_w'' \Big/ \left(\int \theta \, d\eta - (5 + 3n) \int f'^2 \, d\eta \right). \tag{74}$$

[2] - Conservation of Energy =

$$-\frac{\theta_w'}{Pr} \Big/ \left((5n + 3) \int f' \theta \, d\eta + J \int f' \, d\eta \right). \tag{75}$$

Based on the above results, the local similarity Cebeci and Khattab model performs better than the Noto and Matsumoto (1975) approach and will be used in this investigation. The constant in the boundary layer thickness relationship will be equal to 2.5, or

$$\delta = 2.5\,\delta^{*}. \tag{76}$$

While the data-model comparisons for air and ethyl alcohol do not look particularly good, the water results are encouraging. The discrepancy in the ethyl alcohol data-model comparison is unresolved at the present time. Other questions such as inclusion of buoyancy terms are currently under investigation. Neglecting the ethyl alcohol data, the current model seems to work better for higher Prandtl number fluids. This trend is also the case for the one-equation model of Mason and Seban (1974) as shown earlier in Figures 23c and 29. Whether the local similarity Cebeci and Khattab model works well for oil is not known and will not be until data becomes available.

The velocity predictions compared to the data have already been presented earlier in Figures 30 to 32. Temperature profile and Nusselt number comparisons to data will now be presented for the final similarity model discussed above. Figure 37 compares the calculated temperature profiles to data and to the results presented by Cebeci and Khattab (1975). The data are from Cheesewright (1968) for air (Pr-0.72) and from Fujii, et al. (1970) for water (Pr-5.9) and oil (Pr-58.7). The profiles compare reasonably well, although a "kink" is noted in each curve which corresponds to the location of the velocity maximum and zero turbulent transport as discussed earlier. Note that the "kink" is more severe for the local similarity method than for the finite difference solution of Cebeci and Khattab (1975). The reason for this difference is that the local similarity approach assumes negligible transport in the x-direction along the plate. Transport in this direction is included in any finite difference calculation such as that of Cebeci and Khattab (1975).

Nusselt number predictions are shown in Figure 38 along with the Cebeci and Khattab (1975) predictions and some data. Figure 38a shows the comparison for air which indicates that the local similarity modification has not significantly altered the Nusselt number predictions of the original Cebeci and Khattab (1975) approach. Figure 38b gives the same results for oil

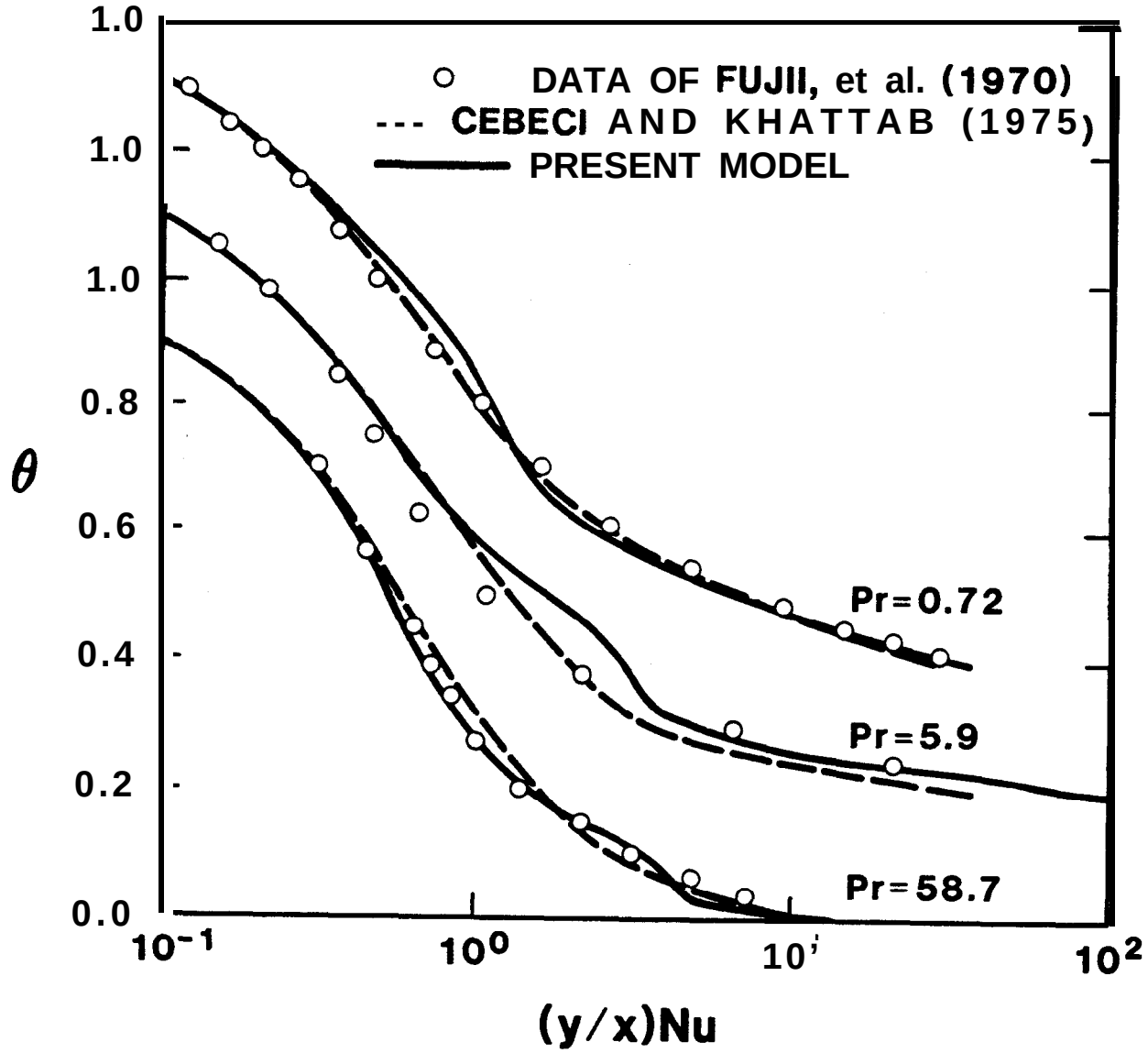

Figure 37. Comparison of local similarity model temperature profile with data and Cebeci and Khattab (1975) results.

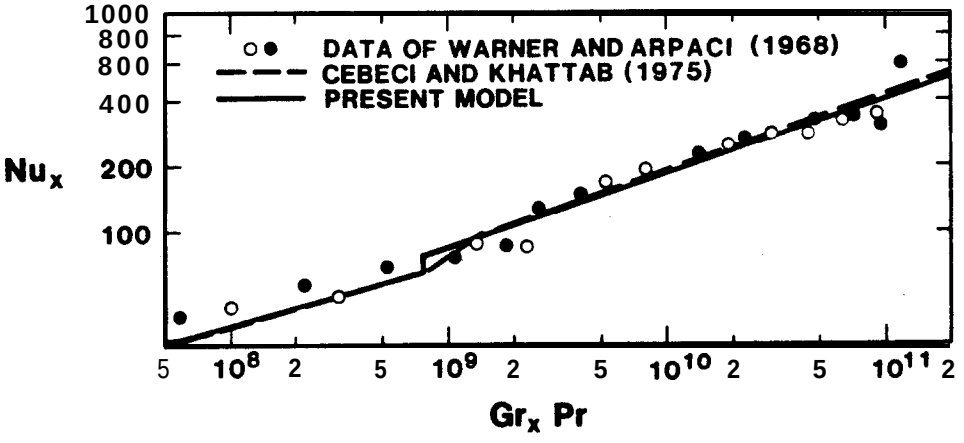

(a) sir

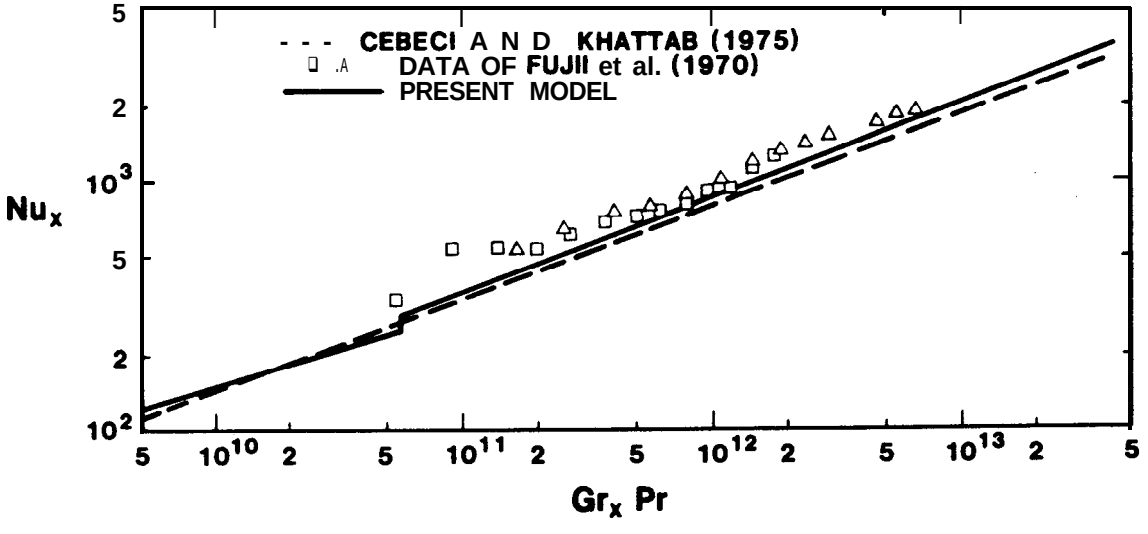

(b) spindle oil

Figure 38. Comparison of local similarity model Nusselt number results with data and Cebeci and Khattab (1975) predictions.

where the unmodified Cebeci and Khattab predictions as given by Cebeci and Bradshaw (1984) are used. Again, the differences due to the local similarity modification are small. No Nusselt number comparison for water has been presented since unaltered Cebeci and Khattab results are not available.

Comparison of the similarity modified Cebeci and Khattab model to the original model and to data indicates that the velocity predictions are reasonable, although the predictions of the original and modified models are probably too high by up to 30% compared to the data. The reason for this overprediction is currently being investigated. Temperature and Nusselt number predictions compare well to the original Cebeci and Khattab (1975) predictions and to the data. Therefore, the local similarity modification gives good results compared to the original model and has not significantly altered the behavior of the original model.

IV. Mixed Convection

Mixed convection occurs when buoyancy (natural convection) and forced convection forces act simultaneously. Depending on the direction of the buoyancy force and the forced convection flow direction, mixed convection can be classified as buoyancy assisted or buoyancy opposed. A recent review of mixed convection is given by Jackson, Cotton, and **Axcell** (1989).

Buoyancy assisted mixed convection occurs if the buoyancy force and the forced convection flow are in the same direction. For example, for a heated plate, the buoyancy force is upward, and buoyancy assisted mixed convection occurs if the forced convection flow is upward. Downward forced flow over a cooled wall would also result in assisted mixed convection. Buoyancy opposed mixed convection occurs when the two forces act opposite each other, as in downward forced convection over a heated vertical wall or upward forced flow over a cooled wall.

For buoyancy opposed conditions, the buoyancy force counteracts the forced convection velocity, and two situations occur depending on which force dominates in the near-wall region. If the buoyancy force is relatively weak, the net effect will be a slight modification of the forced convection velocity profile, but the velocity will be unidirectional in the direction of the forced flow. However, if the buoyancy force is relatively strong, "flow reversal" occurs in which the flow direction is different in the inner and outer portions of the boundary layer. For example, the flow may be upward near the wall due to the buoyancy force but downward far away from the wall due to the forced convection. The various mixed convection flow regimes are schematically depicted in Figure 39 for a heated wall.

The relative strength of the buoyancy to forced convection contribution is measured by the ratio of the Grashof number to the Reynolds number squared. This ratio can be expressed in terms of the natural convection similarity variable f'_∞ as

$$\xi = \frac{Gr_x}{Re_x^2} = Gr_x \frac{\nu^2}{u_\infty^2 x^2} \frac{1}{4 f'^2_\infty}. \qquad (77)$$

For laminar buoyancy opposed mixed convection, flow reversal has been observed in air for ξ values above 0.20 (Ramachandran, Armaly, and Chen (1985)).

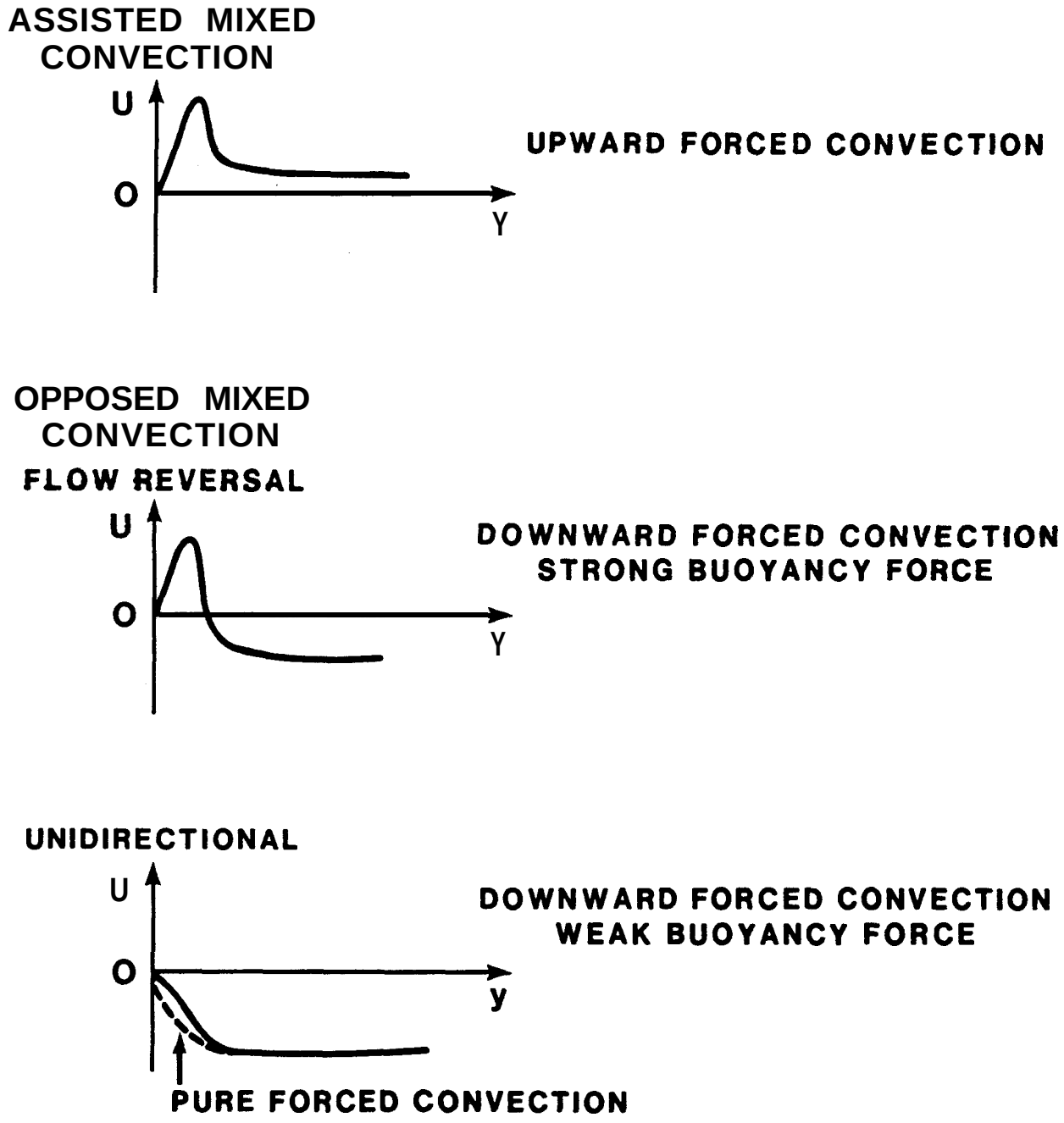

Figure 39. Mixed convection regimes for a heated wall.

For application to SPR and the enclosure problem, the forced convection effect on the profiles should be small since the free stream, or central core, velocity is much smaller than the peak boundary layer value as shown in Webb (1988a). The SPR flow pattern is clearly in the flow reversal mode since the boundary layer flow is upward while the central core region velocity is downward. For the example shown in Webb (1988a), the fluid is water, and the central core velocity is approximately 10 percent or less of the peak boundary layer velocity. From Table 1, the peak velocity for pure natural convection for water is approximately 0.13. Assuming that this value does not change significantly for the small central core region velocity encountered, the central region value of f'_∞ is about 0.013 which gives $\xi \sim 1500$. Figure 40 gives some mixed convection heat transfer results for various Prandtl numbers. Clearly, this large value of ξ indicates that this flow is controlled by natural convection and that the present application is buoyancy dominated.

Experimental and analytical efforts in the mixed convection regime have been predominantly occupied with the effect of buoyancy on forced convection. In this case, the value of ξ is typically 1 or less, buoyancy effects are small, and forced convection approaches are appropriate. The opposite case of forced convection effects on buoyancy flows with ξ much larger than 1 where buoyancy effects dominate, such as in the present application, has received much less attention. This lack of information in the buoyancy dominated opposed mixed convection regime for laminar and turbulent flow will be obvious in the following sections.

A. Laminar Conditions

1. Mixed Convection Data

Data for laminar mixed convection generally consist of heat transfer coefficients or Nusselt numbers as a function of ξ. Velocity and temperature data are only available from a few investigations. According to Ramachandran, Armaly, and Chen (1985), Kliegel (1959) reported the first mixed convection measurements for heat transfer in the assisted and opposed mixed convection regimes not including the flow reversal region. Heat transfer data were reported, but velocity and temperature profiles were not measured. Gryzagoridis (1975) reported some additional assisted mixed convection data which included velocity and temperature data. However, significant differences exist between his data and various analyses. Hishida, et al. (1983) reported some opposed mixed convection data for velocities

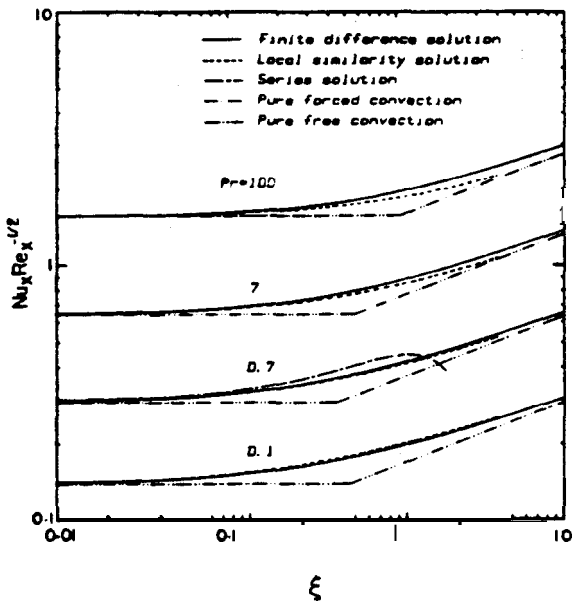

Figure 40. Mixed convection heat transfer results (Chen, Armaly, and Aung (1985)).

and temperatures, again confined to the unidirectional regime. Some inconsistent results are noted between the data and their numerical results. Finally, Ramachandran, Armaly, and Chen (1985) report some assisting and opposing velocity and temperature information. The flow reversal region was not investigated. Comparison of their data with numerical predictions indicates good agreement. As expected, heat transfer is increased for assisted mixed convection while it is impaired for opposed conditions.

The data taken by Ramachandran, et al. (1985) are shown in Figure 41 along with results from the finite difference analysis. The similarity variables used, $F'(\xi,\eta)$ and η, are the forced convection form, or

$$F'(\xi,\eta) = \frac{u}{u_\infty} \tag{78}$$

$$\eta = \left(\frac{u_\infty}{\nu\, x}\right)^{1/2} y. \tag{79}$$

For assisted mixed convection, the value of ξ is up to 16. which indicates a reasonable buoyancy contribution to the velocity and temperature profiles as can be inferred from the velocity profile data. For opposing flow, the maximum value of ξ is 0.208, and the profiles are dominated by forced convection. No data were reported for the flow reversal region in opposed mixed convection.

2. Mixed Convection Models

A number of different techniques have been used to analyze laminar mixed convection conditions, ranging from series solutions (Merkin (1969)) to local similarity based on the forced convection similarity variables (Lloyd and Sparrow (1970)) to finite difference methods (Ramachandran, et al. (1985)). The local similarity technique will be used for the present application as required by the MLS approach. However, since natural convection phenomena are dominant in the present application, the similarity technique will be based on the natural convection equations, not on the forced convection set.

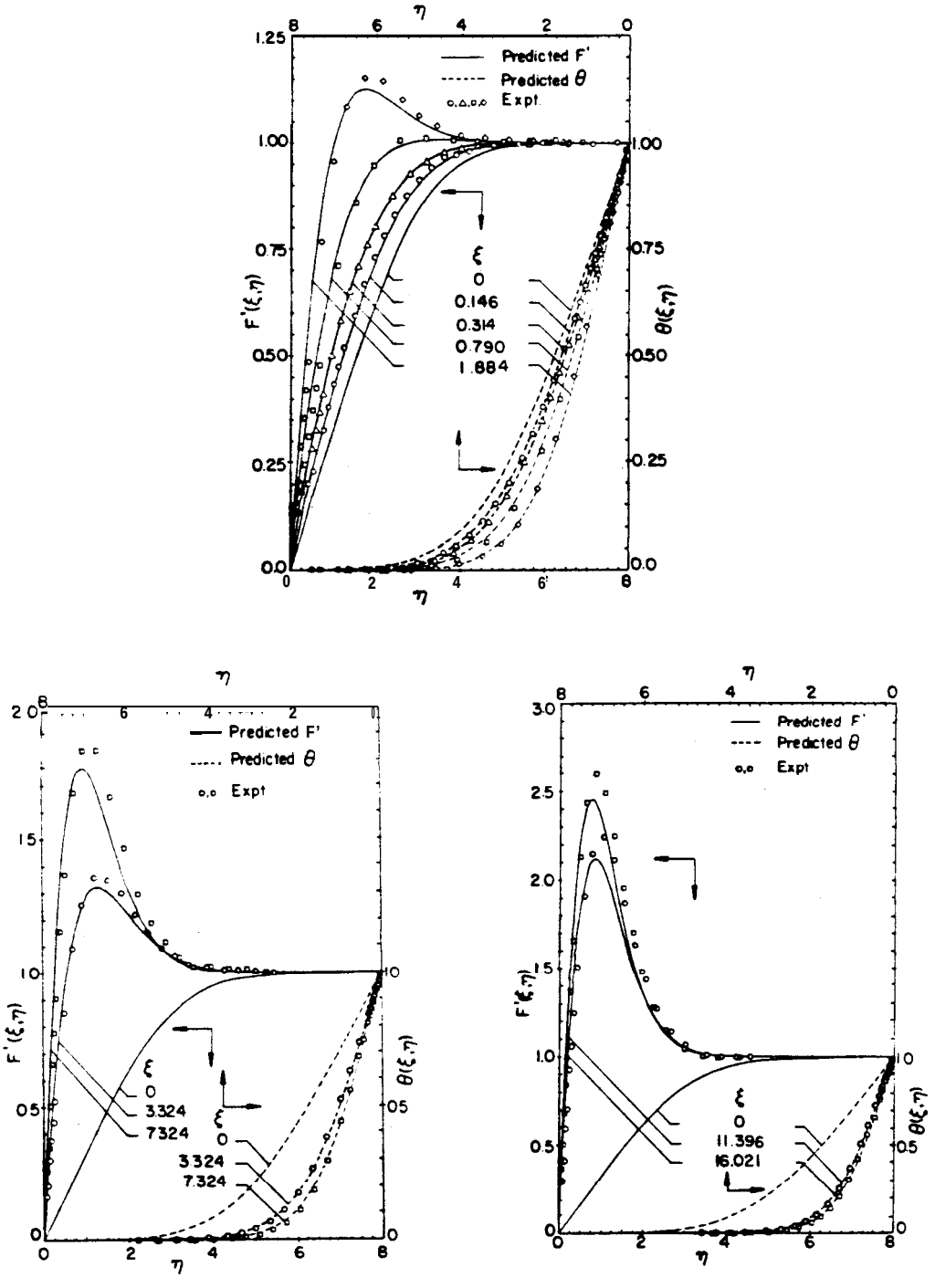

Figure 41. Mixed convection data and model predictions (Ramachandran, Armaly, and Chen (1985)). $F', \eta \rightarrow$ forced convection similarity variables.

Local similarity techniques have been applied to mixed convection problems by Lloyd and Sparrow (1970) among others. However, these analyses studied the effect of natural convection on forced convection and were based on the forced convection local similarity equations. According to Lloyd and Sparrow (1970), the natural convection local similarity equations are not applicable to mixed convection. The reason for this statement can be seen by inspecting the local similarity equations

$$f''' + (n+3)\, f\, f'' - 2\,(n+1)\, f'^{2} + \theta = 0 \tag{80}$$

$$\frac{\theta''}{Pr} + (n+3)\, f\, \theta' - 4\, n\, f'\, \theta = 0. \tag{81}$$

In the limit as $\eta \to \infty$, $f'''(\infty) = f''(\infty) = \theta(\infty) = 0$. For these conditions, $f'(\infty)$ must equal 0. from the above local similarity equations, and the nonzero $f'(\infty)$ boundary condition in mixed convection cannot be satisfied. Therefore, the standard local similarity natural convection form is not applicable to mixed convection conditions. Note that this limit is easily satisfied by the forced convection similarity equations since the free stream (∞) condition is nonzero in the general forced convection case.

For a small buoyant effect on the forced convection equations, local similarity based on forced convection gives reasonable results when compared to local nonsimilarity and finite difference solutions according to Ramachandran, Armaly, and Chen (1985). However, for $\xi=1$, differences of 12.6 and 15.7 percent are noted in the f"(O) values for the local similarity technique compared to local nonsimilarity and finite difference results, respectively, for the case of assisted mixed convection in air. Clearly, for more dominant natural convective conditions such as encountered in the present case, differences would be even greater, and the local similarity approach based on the forced convection equations is not appropriate.

Currently, no local similarity mixed convection model exists based on the natural convection similarity variables as needed for application of the current model to SPR caverns. The present study is the first application of the natural convection local similarity equations to mixed convection. The required model is developed in the next subsection.

3. Local Similarity Model

The natural convection local similarity equations are

$$f''' + (n+3)\, f\, f'' - 2\,(n+1)\, f'^{2} + \theta = 0 \tag{82}$$

$$\frac{\theta''}{Pr} + (n+3)\, f\, \theta' - 4\, n\, f'\, B - J\, f' = 0 \tag{83}$$

where, for generality, the fluid temperature stratification variable, J, has been included in the energy equation.

As mentioned earlier, in the limit as $\eta \to \infty$, the above momentum and energy equations are not able to accommodate a nonzero velocity boundary condition. In order to handle this boundary condition, some ad hoc modifications have been made to the above similarity equations, and the resulting equations are

$$f''' + (n+3)\, f\, f'' - 2\,(n+1)\left[f'^{2} - \Lambda\, f_{\infty}'^{2}\right] + \theta = 0 \tag{84}$$

$$\frac{\theta''}{Pr} + (n+3)\, f\, \theta' - 4\, n\, f'\, \theta - J\,(f' - f_{\infty}') = 0. \tag{85}$$

where Λ is the sign of the local value of $f' f_{\infty}'$. Thus, the sign Λ depends on whether the local velocity and the far-field velocity are in the same direction or not. While these modifications are ad hoc, the form had to satisfy certain requirements. The Λ term is needed to differentiate between buoyancy assisted and opposed conditions. In addition, the behavior of the expression is consistent with intuition. For opposed mixed convection, an increase in f_{∞}' (larger opposing velocity) decreases the maximum boundary layer velocity and the buoyancy mass flow rate. The opposite trend occurs for assisted mixed convection. Finally, of course, the term vanishes in the limit of pure natural convection ($f_{\infty}'=0$).

The usefulness of the above model can be established by comparison to appropriate experimental data. Ideally, the comparison should be made to opposed mixed convection velocity and temperature profiles with flow reversal. However, as discussed in the previous section, such data are not

available. Therefore, the data of Ramachandran, et al. (1985) for assisted mixed convection have been employed. The data consist of some forced convection dominated data (typically $\xi < 1$) and some buoyancy dominated data (typically $\xi > 1$). The present model will be compared against the detailed velocity and temperature profile information for the three ξ values of 1.884, 7.324, and 16.021 as well as to the results of numerical analysis.

The data-model comparison for the present model is shown in Figure 42 in terms of the natural convection similarity variables, not the forced convection ones. For the ξ value of 1.884, reasonable agreement between the present simplified model and the numerical predictions is noted. The peak velocity is slightly overpredicted as is the wall temperature gradient, but the ad hoc model seems reasonable. For the higher ξ numbers, the agreement is much better. The velocity and temperature profiles are surprisingly well predicted for all three cases considering the simple ad hoc modifications made to the local similarity equations. The changes seem more than adequate for natural convection dominated mixed convection, at least for the buoyancy assisted case. Since the buoyancy opposed case of interest in the present study is buoyancy dominated even more so than the above data, the present method is expected to be adequate for these conditions. However, until applicable data become available to adequately test the present model, full evaluation is impossible.

B. Turbulent Conditions

1. Mixed Convection Data

Turbulent mixed convection data have generally been obtained for the forced convection dominated case. For this condition, the effect of buoyancy on forced convection heat transfer is unexpected (Jackson and Hall (1978)). Contrary to laminar flow behavior, for assisted mixed convection, heat transfer can be lower under certain conditions than for pure forced convection. For opposed mixed convection, heat transfer can be enhanced over the forced convection value. Some velocity and temperature profile data have been obtained for the forced convection dominated case (Carr, et al. (1973), Nakajima, et al. (1980)) with a maximum value of ξ of 0.002. Axcell and Hall (1970) present some velocity and profile data for air with a maximum ξ value of about 4.0. However, the data are clearly dominated by forced convection and are not in the flow reversal regime.

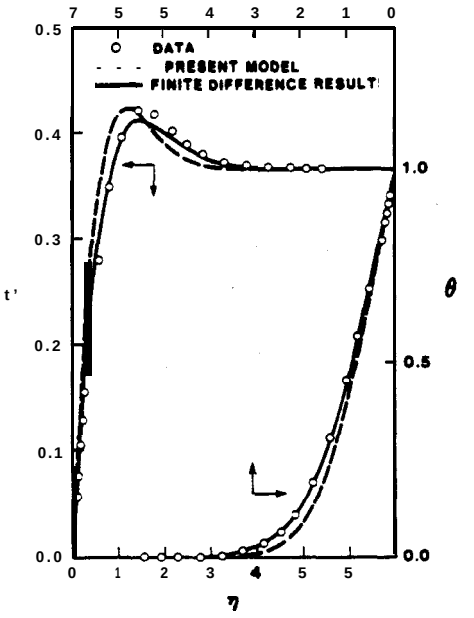

(a) ξ = 1.884

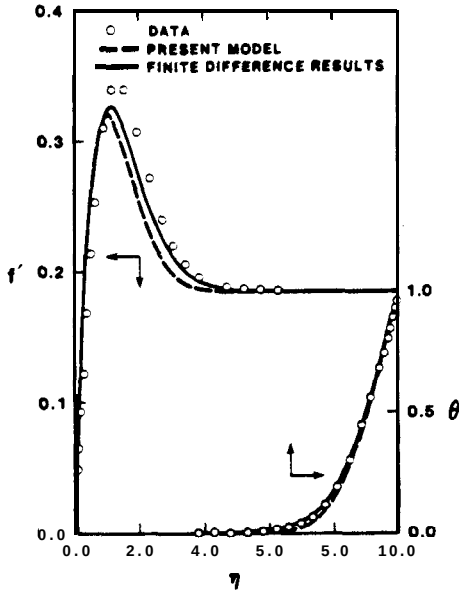

(b) ξ = 7.324

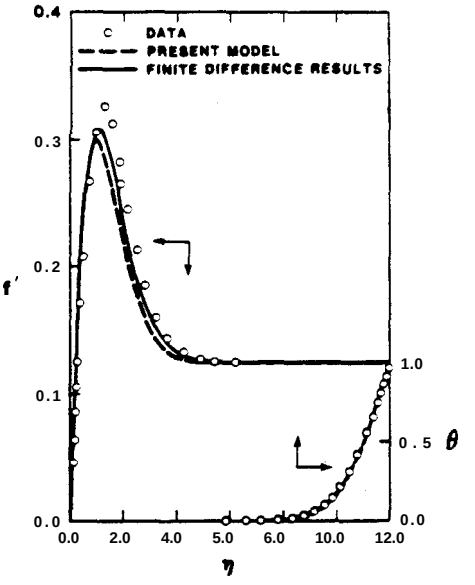

(c) ξ = 16.021

Figure 42. Comparison of local similarity model with data and finite difference results.

For the natural convection dominated case, only one experimental investigation has been performed. Hall and Price (1970) obtained some assisted mixed convection heat transfer data for a vertical heated plate in air with a maximum ξ value of about 50. Again, turbulent mixed convection yielded some surprises since the heat transfer was lower for assisted mixed convection under certain conditions than for pure natural convection. Only qualitative velocity and temperature profile information was obtained in this study; no quantitative profile data are presented.

2. Mixed Convection Models

A number of models for turbulent mixed convection flow have been developed. However, similar to laminar mixed convection, most of the models proposed and evaluated deal with the effect of buoyancy or natural convection on forced flow conditions. The effect of forced convection on a predominantly buoyancy driven problem has not been as extensively studied.

Models for the turbulent effects in mixed convection are generally in the eddy viscosity class, although Swanson and Catton (1987) applied the surface renewal theory to turbulent mixed convection including the flow reversal regime. Their model gave good results for the heat transfer variation for opposed mixed convection dominated by forced convection. For the eddy viscosity approaches, a few zero-equation and two-equation models have been used as discussed below.

Oosthuizen (1974) proposed the only known model for turbulent mixed convection flow for buoyancy dominated conditions. His model is based on a mixing length eddy viscosity approach modified for buoyancy effects. The mixing length model employed is similar to that used by Cebeci and Khattab (1975) for pure natural convection. The one adjustable constant in the model accounting for buoyancy was estimated from the experimental heat transfer data of Hall and Price (1970) discussed above. The initial decrease in heat transfer for assisting conditions as the forced convection velocity is increased is predicted by the model if the adjustable constant is correctly chosen. However, due to the sparsity of data, no systematic attempt to determine the behavior of the constant has been performed, and mean velocity and temperature profile comparisons were not performed.

A number of other investigators have used the mixing length eddy viscosity approach for mixed convection for forced convection dominated situations. Models developed include those by Chen, Armaly, and Ali (1987), Plumb and Evans (1983), and Nakajima, et al. (1980). The mixing length used in these models is very similar to that developed by Cebeci and Smith (1974) which was used by Cebeci and Rhattab (1975) for pure natural convection flow.

Recently, a number of investigators have used two-equation eddy viscosity (k-c) models to analyze mixed convection. For example, Pietrzyk and Crawford (1985), Armaly, Ramachandran, and Chen (1986), and Cotton and Jackson (1987) used this model to investigate turbulent mixed convection predominantly for the effect of buoyancy assisting conditions on forced convection dominated problems.

3. Local Similarity Model

Velocity and temperature profile data for mixed convection conditions dominated by natural convection are not available at the present time. In addition, most of the turbulent mixed convection models are for forced convection dominated mixed convection. No model has been fully developed for buoyancy dominated turbulent mixed convection, although the approach proposed by Oosthuiien (1974) is encouraging. In the absence of applicable data and models, the current turbulence model discussed earlier with the ad hoc mixed convection modifications for laminar flow will be employed.

For application to mixed convection, the displacement boundary layer thickness, δ^*, has to be redefined. The original definition,

$$\delta^* = \int_0^\infty \frac{u}{u_{max}} \, dy \tag{51}$$

is not adequate since the value of δ^* will continue to change since u does not go to zero at infinity. For assisted mixed convection, a reasonable definition would be the integral of

$$\delta^* = \int_0^\infty \frac{(u - u_\infty)}{u_{max}} dy. \tag{86}$$

This definition is also reasonable for opposed mixed convection with unidirectional flow, although this definition has not been used in the present study since application to SPR is only concerned with opposed mixed convection conditions with flow reversal. For flow reversal conditions, the following definition is used

$$\delta^* = \int_0^{y(u=0.)} \frac{u}{u_{max}} dy. \tag{87}$$

Thus, only the portion of the boundary layer with positive velocity values is considered for evaluation of the displacement thickness.

A number of questions remain to be answered about the applicability of the turbulent natural convection boundary layer thickness model to mixed convection. The scaling used as well as the constant of 2.5 may not be appropriate for mixed convection conditions. However, since the application of the present model is to natural convection dominated conditions, the boundary layer thickness model should be reasonable. At the present time, no data are available to evaluate this question.

C. Overall

Mixed convection conditions dominated by natural convection or buoyancy forces have generally not been investigated for laminar or turbulent flow conditions. While some velocity profile data for laminar flow are available for assisted mixed convection, no flow reversal opposed mixed convection data in the buoyancy dominated regime are available. For turbulent conditions, no buoyancy dominated velocity profile data are available under any conditions.

For laminar mixed convection, a local similarity model based on the natural convection similarity equations has been developed and compared to

the limited available data. The data-model comparison was surprisingly good in light of the ad hoc modifications. For turbulent conditions, no data are available, and modifications to the turbulence model proposed earlier were developed but could not be tested due to the lack of data.

In calculating the velocity profiles for mixed convection, the end point, η_∞, was often large. In the numerical calculations, the results for large values of the end point are sensitive to the initial guesses. Sometimes two different solutions were produced as depicted in Figure 43 depending on the initial assumed profile. However, after considering the converged solutions, only one is appropriate based on satisfaction of all the desired boundary conditions. In Figure 43, the top curve is obviously the preferred solution since the bottom curve does not have a negligible slope at the end point, η_∞.

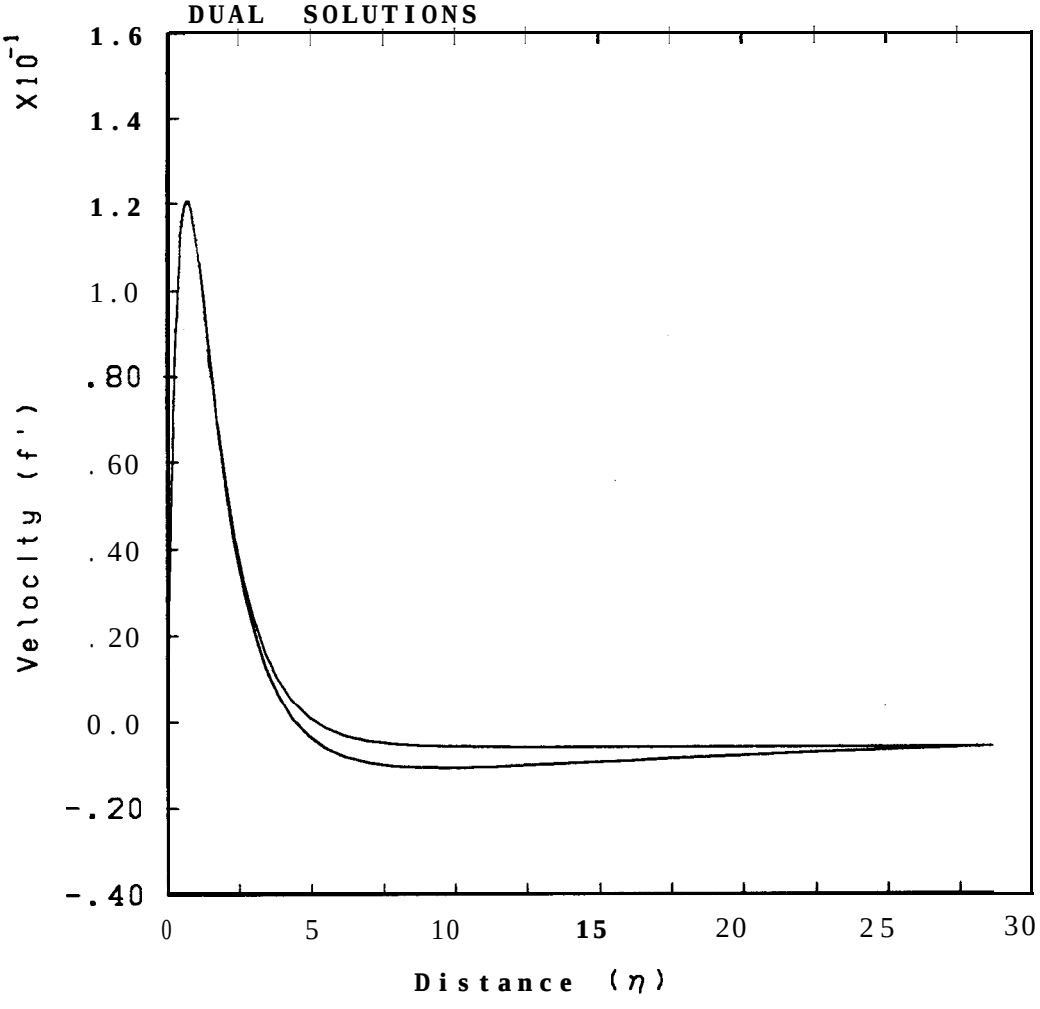

Figure 43. Dual solutions.

V. Summary and Conclusions

The SPR cavern fluid velocity model for natural convection (Webb (1988a)) is based on the local similarity approach as implemented in the Modified Local Similarity (MLS) method (Webb (1988b)). In this application, the local similarity equations are based on the natural convection similarity variables. Provisions for turbulent flow and mixed convection conditions must be included in the local similarity formulation for application to the conditions encountered in SPR caverns.

In the development of these models, the traditional shooting method employed to solve the local similarity equations was unreliable. Therefore, a finite difference method based on the Box scheme was developed to solve the equations. This new approach was found to be reliable and robust in this application.

In order to satisfy the local similarity requirement, an appropriate turbulence model had to be developed. The one existing turbulence model that is applicable to the local similarity approach gave unsatisfactory results. Therefore, another turbulence model was modified to conform to the local similarity requirements. Comparison of this model to turbulent velocity profile data gave reasonable to good results.

Application of the natural convection local similarity equations to mixed convection conditions, which is required in the present case, had not previously been done. Ad hoc modifications were made to the local similarity equations in order to satisfy the required boundary conditions. Data-model comparisons for the velocity and temperature profiles in laminar flow show surprisingly good results, especially for buoyancy dominated conditions. Turbulent data-model comparisons could not be performed due to the lack of experimental data.

The full local similarity equation set including turbulence and mixed convection effects is

$$(1 + \frac{\nu_t}{\nu} f'')' + (n+3)ff'' - 2(n+1)\left[f'^2 - \Lambda f_{\infty_1}'^2\right] + \theta = 0 \qquad (88)$$

$$((\frac{1}{Pr} + \frac{\nu_t}{\nu}\frac{1}{Pr_t})\theta')' + (n+3)f\theta' - 4n f'\theta - J(f' - f_\infty') = 0 \qquad (89)$$

where the turbulence model is the local similarity modified Cebeci and Khattab model developed in this report, or

$$\nu_t = l^2 \left| \frac{\partial u}{\partial y} \right| \tag{36}$$

$$l_i = 0.4y\,(1 - \exp(-y/A)) \qquad \text{(inner region)} \tag{38}$$

$$l_o = 0.075\,\delta \qquad \text{(outer region)} \tag{39}$$

$$l = \min(l_i, l_o) \tag{40}$$

$$A = 26\,\nu\,(\tau_w/\rho)^{-1/2} \tag{41}$$

$$\delta = 2.5\,\delta^*. \tag{76}$$

$$\delta^* = \int_0^{y(u=0.)} \frac{u}{u_{max}}\,dy \tag{87}$$

The integrated conservation equations, which are necessary for the evaluation of momentum and energy conservation in the calculated profiles as discussed in Section II, are

Momentum

$$(5+3n)\int_0^{\eta_\infty} f'^2\,d\eta = \int_0^{\eta_\infty} \theta\,d\eta - f_w'' - 2(n+1)\,f^* + (n+3)\,f_\infty' \int_0^{\eta_\infty} f'\,d\eta \tag{90}$$

Energy

$$(5n+3)\int_0^{\eta_\infty} f'\,\theta\,d\eta = -\frac{\theta_w'}{Pr} - J\left[\int_0^{\eta_\infty} f'\,d\eta - f_\infty'\,\eta_\infty\right] \tag{91}$$

where

$$f^* = f_\infty'^2 \left[\eta(u=0.) - \left[\eta_\infty - \eta(u=0.) \right] \right]. \qquad (92)$$

The first term in f^* is the portion of η that f' and f_∞' are opposite each other, while the second term is when they are in the same direction. Note that the above momentum conservation equation is only applicable to opposed mixed convection with flow reversal or to pure natural convection.

The models developed in this report allow the application of the natural convection local similarity approach to SPR caverns. Comparison of the results of each of these models to the available data show reasonable to good results, although development and full testing of these models has been hampered by the lack of applicable data. The use of these models in the SPR fluid velocity model has been shown by Webb (1988a) to provide good results for the limited available data for velocity and temperature profiles is enclosures.

In conclusion, the applicability of the local similarity approach to turbulent and mixed convection conditions has been extended by the present investigation. Further development and evaluation of these models is continuing such as the inclusion of buoyancy in the eddy viscosity expression. However, verification of the models for conditions encountered in an SPR cavern must await the availability of additional applicable experimental data.

VI. Nomenclature

A, B	coefficients in Cebeci and Khattab model
C_μ	k-c model coefficient
E	error
f	stream function natural convection similarity variable
F	stream function forced convection similarity variable
g	gravitational constant
Gr	Grashof number
J	fluid temperature stratification similarity variable
k	turbulent kinetic energy
1	mixing length
l_1	additional Prandtl mixing length
q''	heat flux
N	temperature difference constant
Nu	Nusselt number
Pr	Prandtl number
Ra	Rayleigh number
Re_t	effective Reynolds number
Ri	Richardson number
Ri_x	gradient Richardson number
T	temperature
AT	temperature difference
u	x-direction velocity
u^+	dimensionless velocity in Popov and Yan'kov model
u^*	characteristic velocity, $= 2(g \beta \times \Delta T)^{1/2}$
u_*	friction velocity, $= (\tau_w/\rho)^{1/2}$
$\tilde{U}_o$	reference velocity
U^+	dimensionless velocity, $= u/u_*$
v	y-direction velocity
x	distance along plate surface
Y	distance normal to plate surface
y^+	dimensionless distance, $= u_* y/\nu$

Greek

α	thermal diffusivity
β	coefficient of thermal expansion
δ	boundary layer thickness
$\delta_{1/2}$	value of 6 where u = 0.5 u_{max}
ε	turbulent energy dissipation parameter
ζ	dimensionless coordinate, = (y/x) Nu
η	similarity dimensionless coordinate
η_1	constant in Popov and Yan'kov model
θ	similarity dimensionless temperature
κ	mixing length constant
Λ	mixed convection variable
ν	kinematic viscosity
ξ	dimensionless parameter for mixed convection
ρ	density
τ	shear stress
τ_w	shear stress, = $\mu(\partial u/\partial y)_w$
ψ	stream function
Ψ	variable in Popov and Yan'kov model

Subscripts

f	fluid
i	inner
max	maximum
o	outer
t	turbulent
w	wall
x	value at x
0	as Ri → 0
∞	value at edge of boundary layer; as Ri → ∞

Superscripts

n	mesh point indice
'	derivative with respect to η
*	constant heat flux value
—	average value

VII. References

Armaly, B. F., N. Ramachandran, and T. S. Chen (1986), "Prediction of Turbulent Mixed Convection Along a Vertical Plate," Proc. 8th IHTC, Vol. 3, pp. 1445-1450, San Francisco, 1986.

Axcell, B. P., and W. B. Hall (1978), "Mixed Convection to Air in a Vertical Pipe," Proc. 6th IHTC, Paper MC-7, Toronto, 1978.

Bejan, A. (1984), Convection Heat Transfer, John Wiley & Sons, New York, 1984.

Blottner, F. G. (1975), "Computational Techniques for Boundary Layers," SAND74-5821, 1974; also AGARD Lect. Ser. No. 73, pp. l-51, 1975.

Carr, A. D., M. A. Conner, and H. 0. Buhr (1973), "Velocity, Temperature, and Turbulence Measurements in Air for Pipe Flow With Combined Free and Forced Convection," Trans. ASME, J. Heat Transfer, pp. 445-452, November 1973.

Cebeci, T. (1973), "A Model for Eddy Conductivity and Turbulent Prandtl Number," Trans. ASME, J. Heat Transfer, pp. 227-234, 1973.

Cebeci, T., and P. Bradshaw (1977), Momentum Transfer in Boundary Layers, Hemisphere Publishing Corp, Washington, 1977.

Cebeci, T., and P. Bradshaw (1984), Physical and Computational Aspects of Convective Heat Transfer, Springer-Verlag, New York, 1984.

Cebeci, T., and A. Khattab (1975), "Prediction of Turbulent-Free-Convective-Heat Transfer From a Vertical Flat Plate," Trans. ASME, J. Heat Transfer, pp. 469-471, August 1975.

Cebeci, T. and A. M. 0. Smith (1974), Analysis of Turbulent Boundary Layers, Academic Press, Inc., New York, 1974.

Cheesewright, R. (1968), "Turbulent Natural Convection From a Vertical Plane Surface," Trans. ASME, J. Heat Transfer, pp. 1-8, February 1968.

Cheesewright, R., and E. Ierokiopitis (1982), "Velocity Measurements in a Turbulent Natural Convection Boundary Layer," Proc. 7th IHTC, Vol. 2, pp. 305-309, Munich, 1982.

Chen, T. S., B. F. Armaly, and M. M. Ali (1987), "Turbulent Mixed Convection Along a Vertical Plate," Trans. ASME, J. Heat Transfer, Vol. 109, pp. 251-253, February 1987.

Chen, T. S., B. F. Armaly, and W. Aung (1985), "Mixed Convection in Laminar Boundary-Layer Flow," Natural Convection - Fundamentals and Applications, edited by S. Kakac, W. Aung, and R. Viskanta, pp. 699-725, Hemisphere Publishing Corporation, Washington, 1985.

Cotton, M. A., and J. D. Jackson (1987), "Comparison Between Theory and Experiment for Turbulent Flow of Air in a Vertical Tube With Interaction Between Free and Forced Convection," Mixed Convection Heat Transfer - 1987, ASME HTD-Vol. 84, pp. 43-50, ASME WAM, Boston, December 13-17, 1987.

Doshi, M. R., and W. N. Gill (1970), "A Note on the Mixing Length Theory of Turbulent Flow," AIChE J., Vol. 16, No. 5, pp. 885-888, September 1970.

Doshi, M. R., and W. N. Gill (1971), "An Improved Mixing Length Theory of Turbulent Heat and Mass Transfer," Int. J. Heat Mass Transfer, Vol. 14, pp. 1355-1362, 1971.

Eckert, E. R. G., and T. W. Jackson (1951), "Analysis of Turbulent Free-Convection Boundary Layer on a Flat Plate," NACA-TR-1015, 1951.

Fujii, T., M. Takeuchi, M. Fujii, K. Suzaki, and H. Uehara (1970), "Experiments on Natural-Convection Heat Transfer From the Outer Surface of a Vertical Cylinder to Liquids," Int. J. Heat Mass Transfer, Vol. 13, pp. 753-787, 1970.

Gebhart, B. (1985), "Similarity Solutions for Laminar External Boundary Region Flows," Natural Convection - Fundamentals and Applications, edited by S. Kakac, W. Aung, and R. Viskanta, pp. 3-35, Hemisphere Publishing Corporation, Washington, 1985.

Gebhart, B., and J. Mollendorf (1969), "Viscous dissipation in external natural convection flows," J. Fluid Mech., Vol. 38, Part 1, pp. 97- 107, 1969.

George, W. K., Jr., and S. P. Capp (1979), "A Theory for Natural Convection Turbulent Boundary Layers Next to Heated Vertical Surfaces," Int. J. Heat Mass Transfer, Vol. 22, pp. 813-826, 1979.

Gominho, L. C., and F. M. White (1984), "Turbulent Free Convection on a Large Vertical Icewall in Seawater," ASME Paper 84-WA/HT-15, 1984.

Griffiths, E., and A. H. Davis (1922), "The Transmission of Heat by Radiation and Convection," DSIR Special Report No. 9, British Food Investigation Report, London, see Cheesewright (1968).

Gryzagoridis, J. (1975), "Combined Free and Forced Convection From an Isothermal Vertical Plate," Int. J. Heat Mass Transfer, Vol. 18, pp. 911-916, 1975.

Hall, W. B., and P. H. Price (1970), "Mixed Forced and Free Convection From a Vertical Heated Plate to Air," Proc. 4th IHTC, Vol. IV, Paper NC 3.3, pp. l-10, Paris, 1970.

Heiss, A., J. Straub, and I. Catton (1988), "Application of Turbulence Models to Natural Convection From a Vertical Isothermal Plate," Proc. 1988 NHTC, Vol. 2, pp. 181-190, Houston, 1988.

Henkes, R. A. W. M., and C. J. Hoogendoorn (1989a), "Laminar natural convection boundary-layer flow along a heated vertical plate in a stratified environment," Int. J. Heat Mass Transfer, Vol. 32, No. 1, pp. 147-155, 1989.

Henkes, R. A. W. M., and C. J. Hoogendoorn (1989b), "Comparison of turbulence models for the natural convection boundary layer along a heated vertical plate," Int. J. Heat Mass Transfer, Vol. 32, No. 1, pp. 157-169, 1989.

Hinze, J. O., (1975), Turbulence, Second Edition, McGraw-Hill Book Company, Inc., New York, 1975.

Hishida, K., A. Yoshida, and M. Maeda (1983), "Buoyancy Effects on Boundary Layer Flow and Forced Convective Heat Transfer Over a Vertical Isothermally Heated Plate," ASME-JSME Thermal Engineering Joint Conference, Vol. 3, pp. 163-168, March 20-24, 1983, Hawaii.

Hoogendoorn, C. J., and H. Euser (1978), "Velocity Profiles in the Turbulent Free Convection Boundary Layer," Proc. 6th IHTC, Vol. 2, pp. 193-197, Toronto, 1978.

Jackson, J. D., M.A. Cotton, and B. P. Axcell (1989), "Studies of mixed convection in vertical tubes," Int. J. Heat and Fluid Flow, Vol. 10, No. 1, pp. 2-15, March 1989.

Jackson, J. D., and W. B. Hall (1978), "Influences of Buoyancy on Heat Transfer to Fluids Flowing in Vertical Tubes under Turbulent Conditions," -in Turbulent Forced Convection in Channels and Bundles - Theory and Application to Heat Exchangers and Nuclear Reactors, edited by S, Kakac and D. B. Spalding, pp. 613-640, Hemisphere Publishing Corp., New York, 1978.

Jaluria, Y. (1980), Natural Convection Heat and Mass Transfer, Permagon Press, Oxford, 1980.

Jaluria, Y., and B. Gebhart (1974), "On transition mechanisms in vertical natural convection flow," J. Fluid Mech., Vol. 66, Part 2, pp. 309-337, 1974.

Kato, H., N. Nishiwaki, and M. Hirata (1968), "On the Turbulent Heat Transfer by Free Convection From a Vertical Plate," Int. J. Heat Mass Transfer, Vol. 11, pp. 1117-1125, 1968.

Keller, H. B. (1971), "A New Difference Scheme for Parabolic Problems," pp. 327-350, Numerical Solution of Partial Differential Eauations-II, SYNSPADE 1970, B. Hubbard, ed., Academic Press, New York, 1971.

Keller, H. B. (1978), "Numerical Methods in Boundary-Layer Theory," Ann. Rev. Fluid Mech., Vol. 10, pp. 417-433, 1978.

Keller, H. B., and T. Cebeci (1972), "An Inverse Problem in Boundary-Layer Flows: Numerical Determination of Pressure Gradient for a Given Wall Shear," J. Comp. Physics, Vol. 10, pp. 151-161, 1972.

Khattab, A. A. (1975), "Prediction of Turbulent-Free-Convective-Heat Transfer From a Vertical Flat Plate," M.S. Thesis, Cal. State University, Long Beach, CA, January 1975.

Kliegel, J. R. (1959), "Laminar Free and Forced Convection Heat Transfer from a Vertical Flat Plate," Ph. D. Thesis, Department of Mechanical Engineering, University of California, Berkeley, 1959.

Kreith, F. (1965), Principles of Heat Transfer, Second Edition, International textbook Company, Scranton, PA, 1965.

Kutateladze, S. S., A. G. Kirdyashkin, and V. P. Ivakin (1972), "Turbulent Natural Convection on a Vertical Plate and in a Vertical Layer," Int. J, Heat Mass Transfer, Vol. 15, pp. 193-202, 1972.

Lin, S., and S. W. Churchill (1978), "Turbulent Free Convection From a Vertical, Isothermal Plate," Numerical Heat Transfer, Vol. 1, pp. 129-145, 1978.

Lloyd, J. R., and E. M. Sparrow (1970), "Combined Forced and Free Convection Flow on Vertical Surfaces," Int. J. Heat Mass Transfer, Vol. 13, pp. 434- 438, 1970.

Lock, G. S. H., and J. J. deB. Trotter (1968), "Observations on the Structure of a Turbulent Free Convection Boundary Layer," Int. J. Heat Mass Transfer, Vol. 11, pp. 1225-1232, 1968.

Mason, H. B., and R. A. Seban (1974), "Numerical Predictions for Turbulent Free Convection from Vertical Surfaces," Int. J. Heat Mass Transfer, Vol. 17, pp. 1329-1336, 1974.

Merkin, J. H. (1969), "The effect of buoyancy forces on the boundary-layer flow over a semi-infinite vertical flat plate in a uniform free stream," J. Fluid Mech., Vol. 35, Part 3, pp. 439-450, 1969.

Minkowycz, W. J., and E. M. Sparrow (1974), "Local Nonsimilar Solutions for Natural Convection on a Vertical Cylinder," Trans. ASME, J. Heat Transfer, pp. 178-183, May 1974.

Miyamoto, M., H. Kajino, J. Kimura, and I. Takanami (1982), "Development of Turbulence Characteristics in a Vertical Free Convection Boundary Layer," Proc. 7th IHTC, Vol. 2, pp. 323-328, Munich, 1982.

Nachtsheim, P. R., and P. Swigert (1965), "Satisfaction of Asymptotic Boundary Conditions in the Numerical Solution of Boundary-Layer Equations,,, Proc. Ninth Midwestern Mechanics Conference, Developments in Mechanics, Vol. 3, Part 2: Dynamics and Fluid Mechanics, pp. 361-371, University of Wisconsin, Madison, 1965.

Nakajima, M., K. Fukui, H. Ueda, and T. Mizushina (1980), "Buoyancy Effects on Turbulent Transport in Combined Free and Forced Convection Between Vertical Parallel Plates,,, Int. J. Heat Mass Transfer, Vol. 23, pp. 1325-1336, 1980.

Noto, K., and R. Matsumoto (1975), "Turbulent Heat Transfer by Natural Convection Along an Isothermal Vertical Flat Surface,,, Trans. ASME, J. Heat Transfer, pp. 621-624, November 1975.

Oosthuizen, P. H. (1974), "Turbulent Combined Convective Flow Over a Vertical Plane Surface,,' 5th IHTC, Vol. III, pp. 129-133, Tokyo, 1974.

Ostrach, S. (1953), "An Analysis of Laminar Free-Convection Flow and Heat Transfer About a Flat Plate Parallel to the Direction of the Generating Body Force,,, NACA TR 1111, 1953, also NACA TN 2635, February 1952, superceded by NACA TR 1111.

Pietrzyk, J. R., and M. E. Crawford (1985), "A Numerical Investigation of Turbulent Mixed Convection in Vertical Annular Channels,,, Fundamentals of Forced and Mixed Convection, ASME HTD-Vol. 42, pp. 149-158, 23rd NHTC, Denver, August 4-7, 1985.

Plumb, 0. A., and G. H. Evans (1983), "Turbulent Mixed Convection From a Vertical Heated Surface In a Crossflow,,, Proc. ASME-JSME Thermal Eng. Joint Conf., Vol. 3, pp. 47-53, 1983.

Plumb, 0. A., and L. A. Kennedy (1977), "Application of a $k-\varepsilon$ Turbulence Model to Natural Convection From a Vertical Isothermal Surface,,, Trans. ASME, J. Heat Transfer, pp. 79-85, February 1977.

Popov, V. N. (1970), "Heat Transfer and Frictional Drag in the Longitudinal Flow of a Gas With Variable Physical Properties Past a Plate,,, High Temperature, Vol. 8, No. 1-6, pp. 311-321, 1970.

Popov, V. N., and G. G. Yan'kov (1985), "Free Turbulent Convection Near a Vertical Plate,,, Power Engineering (USSR Academy of Sciences), Vol. 23, No. 3, pp. 114-124, 1985.

Ramachanandran, N., B. F. Armaly, and T. S. Chen (1985), "Measurements and Predictions of Laminar Mixed Convection Flow Adjacent to a Vertical Surface,,, Trans. ASME, J. Heat Transfer, pp. 636-641, August 1985.

Reynolds, A. J. (1975), "The Prediction of Turbulent Prandtl and Schmidt Numbers,,, Int. J. Heat Mass Transfer, Vol. 18, pp. 1055-1069, 1975.

Schmidt, E., and W. Beckmann (1930), Tech. Mech. Thermodyn., Vol. 1, pp. 341 and 391, 1930 (see Jaluria (1980)).

Schlichting, H. (1968), Boundary-Laver Theory, Sixth Edition, McGraw-Hill Book Company, New York, 1968.

Sparrow, E. M., and J. L. Gregg (1958), "Similar Solutions for Free Convection From a Nonisothermal Vertical Plate,,, Trans. ASME, pp. 379-386, January 1958.

Sparrow, E. M., H. Quack, and C. J. Boerner (1970), "Local Non-similarity Boundary-Layer Solutions,,, AIAA J., Vol. 8, No. 11, pp. 1936-1942, November 1970.

Sparrow, E. M., and H. S. Yu (1971) "Local Non-Similarity Thermal Boundary-Layer Solutions,,, Trans. ASME, J. Heat Transfer, pp. 328-334, November 1971.

Swanson, L. W., and I. Catton (1987), "Surface renewal theory for turbulent mixed convection in vertical ducts,,, Int. J. Heat Mass Transfer, Vol. 30, No. 11, pp. 2271-2279, 1987.

To, W. M., and J. A. C. Humphrey (1986), "Numerical simulation of buoyant, turbulent flow - I. Free convection along a heated, vertical, flat plate,,, Int. J. Heat Mass Transfer, Vol. 29, pp. 573-592, 1986.

Tsuji, T., and Y. Nagano (1988), "Characteristics of a turbulent natural convection boundary layer along a vertical flat plate,,, Int. J. Heat Mass Transfer, Vol. 31, No. 8, pp. 1723-1734, 1988.

Vliet, G. C., and C. K. Liu (1969), "An Experimental Study of Turbulent Natural Convection Boundary Layers,,, Trans. ASME, J. Heat Transfer, pp. 517-531, November 1969.

Warner, C. Y., and V. S. Arpaci (1968), "An Experimental Investigation of Turbulent Natural Convection in Air at Low Pressure Along a Vertical Heated Flat Plate," Int. J. Heat Mass Transfer, Vol. 11, pp. 397-406, 1968.

Webb, S. W. (1988a), Development and Validation of the SPR Cavern Velocity Model, SAND88-2711, October 1988.

Webb, S. W. (1988b), Modified Local Similarity for Natural Convection Alone a Nonisothermal Vertical Flat Plate Including Stratification, SAND88-2710, November 1988.

White, F. M. (1988), personal communication, April 22, 1988.

Wilhoit, R. C., and B. J. Zwolinski (1973), Physical and Thermodynamic Pronerties of Alinhatic Alcohols, J. Phys. Chem. Ref. Data, Volume 2, Supplement No. 1, 1973.

Yang, K. T. (1960), "Possible Similarity Solutions for Laminar Free Convection on Vertical Plates and Cylinders,,, Trans. ASME, J. Appl. Mech., pp. 230-236, June 1960.

Yang, K. T., and J. R. Lloyd (1985), "Turbulent Buoyant Flow in Vented Simple and Complex Enclosures,,' Natural Convection - Fundamentals and Applications, edited by S. Kakac, W. Aung, and R. Viskanta, pp. 303-329, Hemisphere Publishing Corporation, Washington, 1985.

Yang, R. J., and W. Aung (1985), "Equations and Coefficients for Turbulence Modeling,,, Natural Convection - Fundamentals and Anolications, edited by S. Kakac, W. Aung, and R. Viskanta, pp. 259-300, Hemisphere Publishing Corporation, Washington, 1985.

Appendix A

Development of Eddy Viscosity Conservation Equations

The basic conservation equations for natural convection given in the Introduction are for laminar flow conditions. For turbulent flow, additional stresses are produced by turbulence that modify the behavior of the fluid. The velocity and temperature values can be written as the sum of mean and fluctuating values, or

$$u(t) = u + u' \tag{A-1}$$

$$v(t) = v + v' \tag{A-2}$$

$$T(t) = T + T' \tag{A-3}$$

where the fluctuations around the mean values are due to turbulence. Assuming small fluctuations, the steady-state turbulent natural convection equations can then be written as:

mass

$$\frac{\partial u}{\partial x} + \frac{\partial v}{\partial y} = 0 \tag{A-4}$$

x-momentum

$$u \frac{\partial u}{\partial x} + v \frac{\partial u}{\partial y} = g \beta (T - T_f(x)) + \frac{\partial}{\partial y} \left(\nu \frac{\partial u}{\partial y} - \overline{u' v'} \right) \tag{A-5}$$

energy

$$u \frac{\partial T}{\partial x} + v \frac{\partial T}{\partial y} = \frac{\partial}{\partial y} \left(\alpha \frac{\partial T}{\partial y} - \overline{u' T'} \right) \tag{A-6}$$

where the standard Boussinesq approximations for natural convection have been used. The influence of turbulence in the above equations is due to the fluctuating velocities and temperatures. If the fluctuations are zero, the above equations reduce to the laminar form given earlier.

In order to solve the above equations, closure relationships are needed for the average of the fluctuation terms to complete the equation set. Turbulent closure models are concerned with predicting the quantities

$$\overline{u'v'} \quad \text{and} \quad \overline{u'T'}.$$

According to Yang and Aung (1985), two approaches are generally used for the closure equations for the stress - the Boussinesq eddy viscosity approach and the stress model.

The Boussinesq eddy viscosity approach assumes that the eddy viscosity parameter is a scalar, implying an isotropic eddy viscosity, and the closure relationship for the velocity fluctuation term is

$$-\overline{u'v'} = \nu_t \left(\frac{\partial u}{\partial y} + \frac{\partial v}{\partial x}\right). \tag{A-7}$$

Making use of the boundary layer behavior that $\partial u/\partial y >> \partial v/\partial x$, the equation reduces to

$$-\overline{u'v'} = \nu_t \frac{\partial u}{\partial y}. \tag{A-8}$$

For the velocity-temperature relationship, the turbulent heat flux is assumed to vary like Fourier's law, or

$$-\overline{u'T'} = \alpha_t \frac{\partial T}{\partial y}. \tag{A-9}$$

The ratio of the two turbulence parameters is the turbulent Prandtl number, Pr_t, or

$$Pr_t = \frac{\nu_t}{\alpha_t} \tag{A-10}$$

in line with the definition of the molecular Prandtl number

$$Pr = \frac{\nu}{\alpha} \tag{A-11}$$

The conservation equations for an eddy viscosity turbulence model are:

mass

$$\frac{\partial u}{\partial x} + \frac{\partial v}{\partial y} = 0 \tag{A-12}$$

x-momentum

$$u \frac{\partial u}{\partial x} + v \frac{\partial u}{\partial y} = g \beta (T - T_f(x)) + \frac{\partial}{\partial y} \left[(\nu + \nu_t) \frac{\partial u}{\partial y} \right] \tag{A-13}$$

energy

$$u \frac{\partial T}{\partial x} + v \frac{\partial T}{\partial y} = \frac{\partial}{\partial y} \left[(\alpha + \alpha_t) \frac{\partial T}{\partial y} \right] \tag{A-14}$$

where the closure equations for ν_t and α_t have to be defined. Models for ν_t and Pr_t $(=\nu_t/\alpha_t)$ are discussed in the main report.

In contrast to the eddy viscosity approach, the stress models for closure solve transport PDEs for the fluctuation products instead of the algebraic equations discussed above in the Boussinesq eddy viscosity method. The turbulent stress is calculated as a tensor instead of as a scalar thereby relaxing the isotropic assumption made in the Bnussinesq eddy viscosity model. Note that some results from stress models are presented in the main report. More'advanced models such as large eddy simulation and the vortex model are also being developed. These more advanced techniques, as well as the stress models, are not within the scope of the present study due to their prohibitive computational requirements. Information on these other approaches is given by Yang and Aung (1985) and is not included here.

Appendix B

Problems of the Mixing Length Approach

A problem with the eddy viscosity model is that the turbulent transport of momentum and energy, as characterized by ν_t and Pr,, is zero at a velocity maximum or minimum since $\partial u/\partial y = 0$ as shown by the general expression

$$- \overline{u'v'} = \nu_t \frac{\partial u}{\partial y}. \qquad \text{(B-1)}$$

This problem occurs for the zero-, one-, and two-equation models. However, the problem is further compounded for the zero-equation models since the eddy viscosity is also proportional to $\partial u/\partial y$, or

$$- \overline{u'v'} = \nu_t \frac{\partial u}{\partial y} = l^2 \left| \frac{\partial u}{\partial y} \right| \frac{\partial u}{\partial y}. \qquad \text{(B-2)}$$

In many cases, the velocity maximum or minimum is located in a region of symmetry where net momentum or energy transfer is minimum, such as in the center of a pipe or the center of a symmetrical wake or jet. In these cases, this problem with the mixing length formulation should not significantly effect the mean velocity or temperature profiles for symmetrical boundary conditions. Work in this area has been reported by Schlichting (1968) for free turbulent jets and wakes. Differences between results using the conventional expression and those modified to account for the $\partial u/\partial y = 0$. problem differ little from each other for the above cases.

The mixing length eddy viscosity drawback, however, may be significant for asymmetrical cases, such as flow in a channel with the walls at two different temperatures. In this case, the turbulent transport predicted by a mixing length model across the channel will be minimal due to the velocity maximum in the middle of the channel. Prandtl recognized this drawback of his mixing length formulation and proposed the following modification (see Doshi and Gill (1970))

$$\nu_t = l^2 \sqrt{\left(\frac{du}{dy}\right)^2 + l_1\left(\frac{d^2u}{dy^2}\right)^2} \qquad \text{(B-3)}$$

where the mixing length l_1 is an additional variable that is determined by data. By the nature of this modification, two separate mixing lengths have to be determined, and this form has not often been used. Note, however, that since the turbulent stress term is still proportional to the mean velocity gradient, the problem of zero turbulent transport at a velocity minimum or maximum still exists.

In order to overcome this problem of two mixing lengths and the zero turbulent transport at velocity minimums and- maximums, Doshi and Gill (1970,1971) reformulated the mixing length and resultant turbulent transport expressions in terms of the first and second velocity derivatives with a single mixing length, 1, equal to the standard value. Thus, they eliminated the extra mixing length variable, l_1, so standard expressions are still applicable, and the mixing length and turbulent transport are nonzero at or near velocity maximums and minimums.

The Doshi and Gill expressions are

$$-\overline{u'v'} \sim \begin{cases} l^2\left(\frac{du}{dy}\right)^2 & , \left|l\frac{du}{dy}\right| > \left|\frac{l^2}{2}\frac{d^2u}{dy^2}\right| \\ \frac{l^4}{4}\left|\frac{d^2u}{dy^2}\right|^2 & , \left|\frac{l^2}{2}\frac{d^2u}{dy^2}\right| > \left|l\frac{du}{dy}\right| \end{cases} \qquad \text{(B-4)}$$

This formulation overcomes a significant problem with the application of the standard mixing length eddy viscosity approach. The results from the standard mixing length model and the Doshi and Gill modification are shown in Figure B-l for a channel with two different wall temperatures. For the standard mixing length model, the temperature predictions are poor in the middle of the channel since the velocity gradient is small. The Doshi and Gill predictions agree much better with the experimental data in this low velocity gradient region.

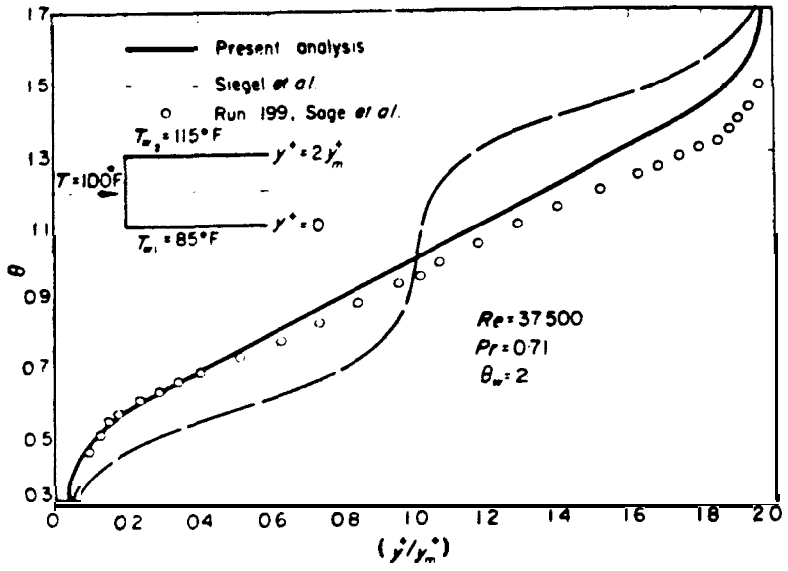

Figure B-l. Effect of Doshi and Gill (1970,1971) model on temperature distribution in a two temperature channel (Doshi and Gill (1971)).

The importance of the zero slope problem in zero-equation models for natural convection can be assessed from information presented in Figure B-2 from Henkes and Hoogendoorn (1989b) . The eddy viscosity for the zero-equation model of Cebeci and Khattab (called Cebeci and Smith in the figure) and for the two-equation models studied are not significantly different around the velocity peak, which occurs around $\zeta = 1$ as shown in Figure 24 of the main report. The eddy viscosity at the velocity peak is also significantly below the values in the outer region of the boundary layer, so the velocity profile will be controlled by the outer region value. The major difference between the zero- and two-equation models is in the outer region of the boundary layer. Therefore, the mixing length problem at the velocity peak is not expected to be significant for natural convection conditions, and the mixing length modifications discussed above have not been employed.

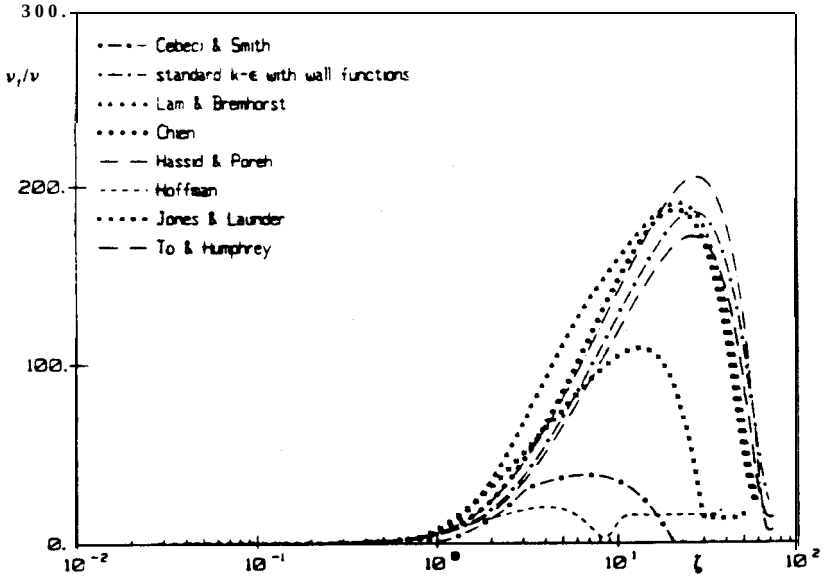

Figure B-2. Variation of eddy viscosity with distance from the wall (Henkes and Hoogendoorn (1989b)).

Appendix C

Turbulent Data Reduction Procedure

In the data-model comparisons presented in the main report for turbulence, the existing data often had to be modified from the original presentation. All the data-model comparisons are presented in this report in terms of the laminar similarity velocity and distance coordinates for simplicity and to allow direct comparison with laminar results. The laminar similarity variables are

$$f' \quad \text{vs.} \quad \eta$$

where

$$f' = \frac{x}{2\nu\ Gr_x^{1/2}} u = \frac{u}{2\ (g\ \beta\ x\ \Delta T)^{1/2}} \tag{C-1}$$

$$\eta = \frac{y}{x} \left[\frac{Gr_x}{4}\right]^{1/4} \tag{C-2}$$

The data reduction procedure to allow this comparison, including any assumptions, is given in this appendix. Each data set is treated independently since the technique is dependent on the form of the original data presentation as well as any additional available information.

The method for the following data sets will be presented in order.

1. Cheesewright (1968).
2. Lock and Trotter (1968).
3. Vliet and Liu (1969).
4. Kutateladze, et al. (1972).
5. Hoogendoorn and Euser (1978).
6. Cheesewright and Ierokiopitis (1982).
7. Miyamoto, et al. (1982).
8. Tsuji and Nagano (1988).

Cheesewright

As shown in Figure 4 in the main report, the Cheesewright (1968) velocity data are presented in terms of

$$\frac{u}{u^*} \text{ vs. } \frac{y}{x} Gr^{0.1}.$$

The velocity variable is simply equal to 2f' since the u^* value used by Cheesewright is the present definition divided by 2. The distance variable is the laminar variable with a different power on the Grashof number. The Grashof number is given in Figure 5, and the conversion is easily made. The Prandtl number was assumed to be 0.72 in the data-model comparisons.

Lock and Trotter

The Lock and Trotter (1968) data shown in Figure 9 of the main report are in terms of

$$U \text{ vs. } y$$

where U is equal to f' and y is in the unusual units of 0.1 inches. Thus, a y value of 2.0 corresponds to a physical distance of 0.2 inches. The highest Grashof number data presented with sufficient information are used. The appropriate Grashof and Prandtl numbers as well as the x distance are 6.66×10^8, 10.25, and 10.8 inches, respectively. These data are sufficient for the data-model comparison results.

Vliet and Liu

Figure 10a in the main report shows the velocity data which are in terms of the variables

$$\frac{u}{u_{max}} \text{ vs. } \frac{y}{\delta^*}$$

and u_{max} and δ^* are defined in the figure as is the Rayleigh number Ra^*. Figure 10b for the temperature profile defines the Ra number for the data. Based on information in the text, the x distance for the two profiles is 30 and 42 inches with the lower distance corresponding to the lower Rayleigh number. These distances are the same as used by Mason and Seban (1974). The Prandtl number used in the similarity analysis is assumed to be equal to 6.0 in accordance with the Prandtl number range of 5-7. A viscosity (ν) of 0.945 x 10^{-5} ft^2/sec is used for consistency with the assumed Prandtl number based on data in Kreith (1965). The resulting Grashof numbers are 1.9 x 10^{10} and 6.0 x 10^{10} for the two velocity profiles.

Kutateladze

The ethyl alcohol (ethanol) velocity data of Kutateladze, et al. (1972) shown in Figure 12 of the main report are reported in terms of

u vs. y.

The Prandtl number is reported to be 13.2. Rayleigh number, x, AT, and T_∞ information is presented in the figure caption in the reference. The only unknown in transforming the data to the desired similarity coordinates is β, the volumetric expansion coefficient. This value has been calculated from information given by Wilhoit and Zwolinski (1973) as approximately 1.1 x 10^{-3} 1/°C (6.1 x 10^{-4} 1/°F) for the reported temperatures.

Hooeendoorn and Euser

The Hoogendoorn and Euser (1978) data were shown in Figure 6 of the main report in terms of

$$\frac{u}{u^*} \text{ vs. } \frac{y}{x} Gr^{0.1}$$

just like the original Cheesewright data presentation. The velocity coordinate is simply 2f', while conversion for the y coordinate is simply dependent on the Grashof number. Using an average Rayleigh number from the data given on the figure and an assumed Prandtl number of 0.72, the Grashof number is 9.5 x 10^9.

Cheesewrieht and Ierokiopitis

Cheesewright and Ierokiopitis (1982) give velocity data in terms of velocity and distance as shown in Figure 8 of the main report, or

u vs. y.

Information in the reference gives the x distance as 2.2 m and the Grashof number as 4.83 x 10^{10}, and the plate temperature is approximately 80°C (176°F). Based on the data reported by To and Humphrey (1986), the temperature difference between the plate and the environment was 56°C (101°F), so the environmental temperature is 24°C (75°F). These values allow the calculation of u^* assuming $\beta=1/T_\infty$ and the translation of y to η. The Prandtl number was assumed equal to 0.72.

Note that the data attributed to Cheesewright and Ierokiopitis (1982) by To and Humphrey (1986) are not in the original reference. To and Humphrey cite the Grashof number of 5.75 x 10^{10} which is not given in the reference. Perhaps these data are given in a more detailed report on the data. At the present time, the origin of these data is not known and the presentation made by To and Humphrey will not be used for data-model comparison purposes.

Miyamoto

Figure 13a shows the Miyamoto, et al. (1982) velocity data in terms of

$$\frac{u}{u_{max}} \text{ vs. } \frac{y}{x} \text{ Nu.}$$

The turbulent regime is quoted as being for Gr_x^*Pr values greater than 1.5 x 10^{13}. Assuming a Prandtl number of 0.72, only two velocity profiles are clearly in the turbulent regime with Gr_x^* values of 6.68 x 10^{13} and 1.06 x 10^{14}. To convert the Gr_x^* values to Gr,, the Nusselt number correlation presented by Miyamoto, et al. (1982) for turbulent flow

$$Nu_x = 0.104\ (Gr_x^* Pr)^{0.272} \qquad \text{(G-3)}$$

was used. The resulting Grashof numbers are 1.22 x 10^{11} and 1.71 x 10^{11}. This information was also used to convert the (y/x)Nu coordinate to η values.

To convert the velocity data to f' similarity values, the correlation plotted for the maximum velocity variation

$$\frac{u_{max}\ x}{\nu} = 10.9\ Gr_x^{*0.288} \qquad \text{(G-4)}$$

was used. Using the similarity relationship

$$f' = \frac{u\ x}{\nu}\ \frac{1}{2\ Gr_x^{1/2}} \qquad \text{(G-5)}$$

results in

$$f' = \frac{u}{u_{max}}\ \frac{10.9\ Gr_x^{*0.288}}{2\ Gr_x^{1/2}} \qquad \text{(C-6)}$$

which gives the value of f' directly since the Grashof numbers are known.

Tsuii and Nagano

The velocity data of Tsuji and Nagano (1988) in Figure 14b of the main report are in terms of

u+ vs. y+

where

$$U^+ = u / u_* \tag{C-7}$$

$$y^+ = u_* y / \nu \tag{C-8}$$

$$u_* = (\tau_w/\rho)^{1/2} \tag{C-9}$$

and, for the turbulent experimental data,

$$\tau_w/\rho = 0.684\ Gr_x^{1/11.9}\ U_b^2 \tag{C-10}$$

where

$$U_b = (g\ \beta\ AT\ \nu)^{1/3} \tag{C-11}$$

Since the fluid is air, β is evaluated from $1/T_\infty$, and the value of ν is equal to 1.60 x 10^{-4} ft^2/sec as given by Kreith (1965) for the reported environmental temperature 16°C (61°F). The temperature difference of 44°C (79°F) was also used to calculate U_b. The assumed Prandtl number is 0.72 for the data-model comparisons.

Distribution:

U.S. DOE SPR PMO (9)
900 Commerce Road East
New Orleans, LA 70123
Attn: D. R. Spence, PR-62
E. E. Chapple, PR-622 (5)
D. W. Whittington, PR-622
TDCS (2)

U.S. Department of Energy (1)
Strategic Petroleum Reserve
1000 Independence Avenue SW
Washington, D.C. 20585
Attn: R. Smith

U.S. Department of Energy (1)
Oak Ridge Operations Office
P.O. Box E
Oak Ridge, TN 37831
Attn: W. Manning

Boeing Petroleum Services (4)
850 South Clearview Parkway
New Orleans, LA 70123
Attn: K. Mills
T. Eyermann
J. Siemers
J. McHenry

Dr. Frank M. White
Department of Mechanical
Engineering & Applied Mechanics
University of Rhode Island
Kingston, RI 02881

3141	S. A. Landenberger (5)
3151	W. I. Klein (3)
3154-l	C. L. Ward (8)
	For: DOE/OSTI
8524	J. A. Wackerly
1511	A. J. Russo
1513	C. E. Hickox
1513	V. F. Nicolette
6000	D. L. Hartley
6200	V. L. Dugan-
6250	R. K. Traeger
6252	T. Y. Chu
6257	J. K. Linn (10)
6257	S. L. Chavez
6257	G. S. Heffelfinger
6257	J. T. Neal
6257	J. L. Todd, Jr.
6257	S. W. Webb (10)
6258	J. G. Castle